Nanoparticles based on natural, engineered or synthetic proteins and polypeptides for drug delivery applications

Evangelos Georgilis, Mona Abdelghani, Jan Pille, Esra Aydinlioglu, Jan C.M. van Hest, Sébastien Lecommandoux, Elisabeth Garanger

Author manuscript of article published in *International Journal of Pharmaceutics*, DOI: 10.1016/j.ijpharm.2020.119537

Nanoparticles based on natural, engineered or synthetic proteins and polypeptides for drug delivery applications

Evangelos Georgilis,[a] Mona Abdelghani,[b,§] Jan Pille,[b,§] Esra Aydinlioglu,[a,§] Jan C. M. van Hest,[*,b] Sébastien Lecommandoux,[*,a] and Elisabeth Garanger[*,a]

[a] *Univ. Bordeaux, CNRS, Bordeaux INP, LCPO, UMR 5629, F-33600, Pessac, France.*
[b] *Eindhoven University of Technology, Bio-organic Chemistry Lab, P.O. Box 513 (STO 3.31), 5600 MB Eindhoven, The Netherlands.*
[§] *Authors contributed equally to the work.*
Corresponding authors:
**Mailing address: Eindhoven University of Technology, Bio-organic Chemistry Lab, P.O. Box 513 (STO 3.31), 5600 MB Eindhoven, The Netherlands. E-mail: J.C.M.v.Hest@tue.nl*
** Mailing address: Université de Bordeaux, Bordeaux INP, ENSCBP, 16 avenue Pey-Berland, 33607 Pessac Cedex, France. E-mail: lecommandoux@enscbp.fr*
** Mailing address: Université de Bordeaux, Bordeaux INP, ENSCBP, 16 avenue Pey-Berland, 33607 Pessac Cedex, France. E-mail: garanger@enscbp.fr*

Abstract

Medicine formulations at the nanoscale, referred to as nanomedicines, have managed to overcome key challenges encountered during the development of new medical treatments and entered clinical practice, but considerable improvement in terms of local efficacy and reduced toxicity still need to be achieved. Currently, the fourth-generation of nanomedicines is being developed, employing biocompatible nanocarriers that are targeted, multifunctional, and stimuli-responsive. Proteins and polypeptides can fit the standards of an efficient nanovector because of their biodegradability, intrinsic bioactivity, chemical reactivity, stimuli-responsiveness, and ability to participate in complex supramolecular assemblies. These biomacromolecules can be obtained from natural resources, produced in heterologous hosts, or chemically synthesized, allowing for different designs to access suitable carriers for a variety of drugs. To enhance targeting or therapeutic functionality, additional chemical modifications can be applied. This review demonstrates the potential of polypeptide and protein materials for the design of drug delivery nanocarriers with a special focus on their preclinical evaluation *in vitro* and *in vivo*.

1. Introduction

The field of nanomedicine relates to the use of nanometer-sized objects for diagnostic and/or therapeutic purposes, primarily for human health applications. These include nanoparticles of various chemical compositions (organic or inorganic), sizes (in the 1-500 nm range) and morphologies (isotropic or anisotropic), which are used as diagnostic tools, imaging agents, drug-loaded carriers, or combinations thereof. In particular, the need for appropriate nanocarriers results from several issues encountered with different classes of bioactive compounds such as rapid degradation, lack of solubility in biological fluids, inappropriate pharmacokinetic parameters and biodistribution (*e.g.*, rapid clearance), high systemic toxicity and severe side effects. Therapeutic nanocarriers are therefore expected to protect and confine actives in a suitable chemical environment, increase their residence time, accumulation and delivery at the target organ/tissue. The development of drug-delivery systems has been an active field of multidisciplinary research for more than twenty years and has led to successful improvement of treatments for different pathologies. Organic nanocarriers range from antibody- and polymer-drug conjugates to micellar formulations, liposomes, and polymersomes (Beck et al., 2017; Boutros et al., 2016; Che and van Hest, 2016; Niu et al., 2016; Thambi et al., 2016; Yingchoncharoen et al., 2016). Doxil® and AmBisome® were the first liposomal formulations of Doxorubicin and Amphotericin B approved in the mid 90's for the treatment of cancers and fungal infections, respectively. Abraxane® and Genoxol-PM® are two distinct nanocarriers of Paclitaxel, a highly cytotoxic and poorly soluble anti-proliferative low molecular weight drug, based on different classes of materials, namely a human-derived protein (*i.e.*, albumin) and a block copolymer (PLA-*b*-PEG). Clinical practices count today approximately fifty nanotherapeutics, most of them being nanoformulations of previously approved drugs,

while a greater number of investigational drug nanocarriers are undergoing clinical investigation for a variety of indications (Caster et al., 2017).

Nanoparticle-based therapeutics have been sometimes considered slow to enter clinical practices. However, their development has required the concomitant implementation of analytical techniques and specific regulatory guidelines. An additional challenge comes from the complexity of certain pathological contexts (*e.g.*, cancers) and poor predictivity of pre-clinical animal models. The discrepancies between the knowledge and understanding of the physico-chemical characteristics of nanoparticles and how these affect their behavior and fate *in vivo* are also large. While some general guidelines about nanoparticle size, shape, surface charge or composition for instance have emerged, these are far too less predictive of the actual behavior *in vivo*. Although the comparison of *in vivo* results is difficult to achieve due to the broad variability of models used and data interpretation, we believe such an attempt is of significant importance for nanoparticle systems that share common features acknowledging their differences in materials properties and chemical adaptability. This is the main ambition of this review article focused on peptide- and protein-based nanoparticles. These have the major advantages of being biodegradable, potentially non-immunogenic, sometimes stimuli-responsive, intrinsically bioactive or easily post-modified through orthogonal bioconjugation reactions, and able to participate in complex supramolecular assemblies. With sizes ranging from 30 nm to 200 nm, peptide- and protein nanoparticles have optimal sizes, and are composed of a defined core and corona, which are able to display or integrate multiple additional functionalities. The present review does not attempt to be exhaustive, but rather highlights recent examples of protein and/or peptide-based nanoparticle systems, typically of micellar or vesicular structure, whose translation *in vivo* has been significantly investigated. (Fig. 1)

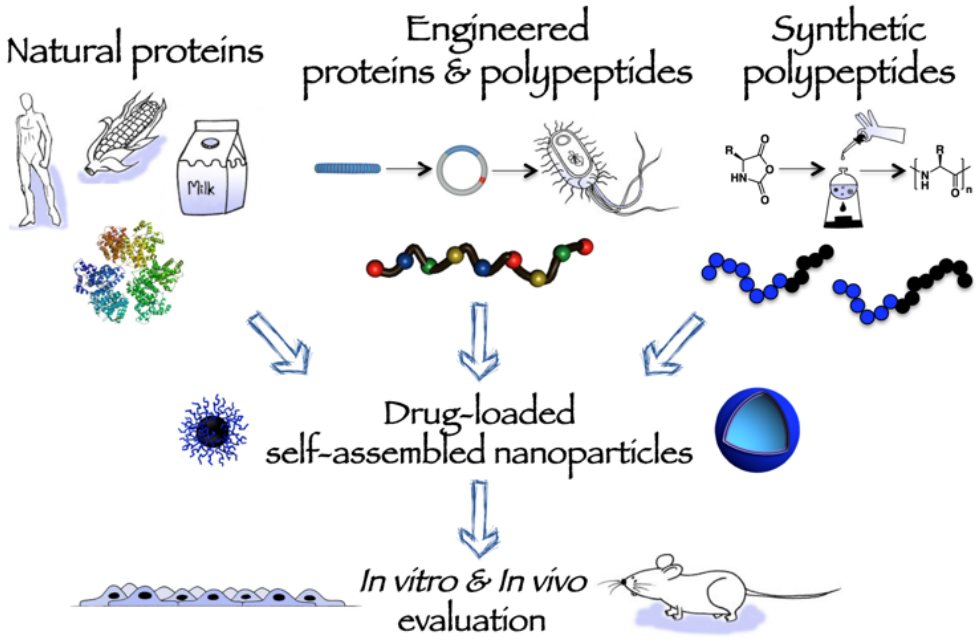

Figure 1. General overview of the present review article.

2. Nanoparticles based on natural proteins

Certain natural proteins have been systematically employed in drug formulations (Jao et al., 2017; Lohcharoenkal et al., 2014; MaHam et al., 2009). The key features that render natural proteins as potentially efficient nanocarrier candidates for nanomedicine are their availability from natural resources, inherent biocompatibility, biodegradability, and biological function (*e.g.*, entrapment of hydrophobic molecules, temperature and/or pH responsiveness). For this purpose, suitable proteins are commonly isolated from the human (or other mammalian) body or from food sources, provided that they fit the standards of a safe carrier in the case of proteins of exogenous origin. Furthermore, these biomolecules are amenable to chemical modifications, allowing the modulation of their physico-chemical and/or biological properties. In this section,

the main categories of natural proteins employed in nanomedicine will be discussed, as well as certain "hybrid" systems, resulting from chemical modification approaches of naturally-occurring proteins (Table 1).

2.1 Human-derived proteins

2.1.1 Albumin

Albumin has been extensively studied as solubilizing agent of hydrophobic drugs. It can be found in abundance in the egg white (ovalbumin, OVA), bovine plasma (bovine serum albumin, BSA), and human plasma (human serum albumin, HSA). One interesting characteristic of albumin for the development of drug formulations is that hydrophobic molecules can bind to certain sites within the protein (Elzoghby et al., 2012). The development of a nanoparticle albumin-bound (nab) paclitaxel formulation approved by the FDA, Abraxane, has been an important advancement to decrease the strong toxicity and improve the delivery of this cancer chemotherapeutic (Gradishar et al., 2005). Abraxane is regarded as one of the few commercially available and successful applications of nanomedicine in cancer. Abraxane is supplied as a powder which is dissolved in a sodium chloride solution for intravenous administration, but albumin-based nanoparticles are also potent candidates for local administration, such as in the inner ear or through the nasal route (Wong and Ho, 2018; Yu et al., 2014).

The albumin-bound technology, an emulsion-based technique used for Abraxane (Fu et al., 2009; Larsen et al., 2016), was shown to decrease drug toxicity but also replaced and avoided the use of toxic adjuvants. For this reason, this so-called nab® technology is currently applied for the formulation of other toxic drugs, such as docetaxel, thiocolchicine dimer, and rapamycin, which are currently under Phase I and II clinical trials. The same preparation technology can also be applied for more hydrophilic chemotherapeutics such as gemcitabine, since the protein-based vehicle can be more effective than the free drug in terms of tumor growth inhibition by overcoming drug resistance mechanisms (Z. Guo et al., 2018).

One method widely applied to form protein nanoparticles is desolvation, which involves the coacervation of a protein using a solvent or an agent (*e.g.* alcohol) that disrupts the protein structure and leads to nanometer-sized aggregates that are subsequently stabilized *via* crosslinking (Nicolas et al., 2013). This technique enables the loading of a wide variety of drugs in albumin particles. Desolvation was investigated by Zhang *et al.* for the preparation of HSA-gambogic acid nanoparticles (Fig. 2). The particles were developed as an alternative to the use of L-arginine, which is traditionally used for improving the solubilization of this insoluble phenolic natural compound. As compared to the arginine mix solution, nanoparticles showed increased efficiency in suppressing the tumor growth, less body weight loss, and increased survival rates in A549-bearing mice (Zhang et al., 2017). Dong *et al*. have prepared albumin nanoparticles loaded with Dasatinib *via* desolvation using methanol and studied their activity *in vitro* (Dong et al., 2016). Efficiently internalized in leukemia cells, the nanoparticles showed a similar anti-proliferative activity as the free drug. However, while the free drug caused a significant permeability increase on the endothelial barrier model, which can result in peripheral edema and pleural effusion *in vivo*, the albumin nanoparticles loaded with Dasatinib only slightly affected the barrier integrity. Following a similar particle preparation method, Casa *et al.* developed albumin nanoparticles loaded with Amphotericin B for the treatment of leishmaniasis (Casa et al., 2018). *In vitro*, the albumin-based formulation was less toxic to macrophages and remained effective against the internalized parasite *L. amazoniensis*, showing decreased CC_{50} and increased IC_{50} values compared to a liposomal formulation. Both formulations effectively reduced leishmaniasis lesions in mice, but the albumin-encapsulated drug showed reduced toxicity to lung and kidney tissue. Iwao *et al.* developed HSA nanoparticles loaded with 5-aminosalicylic acid to reduce inflammation in ulcerative colitis (UC) lesions (Iwao et al., 2018). The particles colocalized at the site of inflammation with the overexpressed myeloperoxidase in a UC mouse model, and the interaction was also verified by QCM experiments. For the treatment of membranous glomerulonephritis (MGN), a common cause of nephropathy, Gai *et al.* used the desolvation-crosslinking method to prepare BSA-bound methylprednisolone (Gai et al., 2018). The particles were administered to an MGN rat model, and successfully enhanced the reduction of serum creatinine and urinary protein, compared to a commercial product, in the course of 7 days.

Cross-linking of protein particles is important to prevent their aggregation, especially in preparation methods such as desolvation (Nicolas et al., 2013). Harmful cross-linkers such as glutaraldehyde are often employed, but alternative methods are being investigated. Vanillin for instance has been used as a non-toxic cross-linking agent of albumin nanoparticles resulting in stable particles with a pH- and glutathione-sensitive doxorubicin release profile *in vitro* (F. Li et al., 2016). Notably, the IC_{50} value of doxorubicin loaded in the particles was lower (3.693 µg/mL) compared to the free drug (4.007 µg/mL), and the release was faster close

to conditions of tumor microenvironment (pH 6.5, 20 mM glutathione). These results may explain the lower accumulation of doxorubicin in the heart and longer survival of Heps tumor-bearing mice. Self-cross-linking of free thiols present in albumin or crosslinking with bis(acryloyl)cystamine has also been used for the development of redox-responsive nanoparticles (Catanzaro et al., 2017; Thirupathi Kumara Raja et al., 2017). In these cases, *in vitro* drug release was dependent on the concentration of glutathione, an antioxidant whose levels increase in malignant tumors.

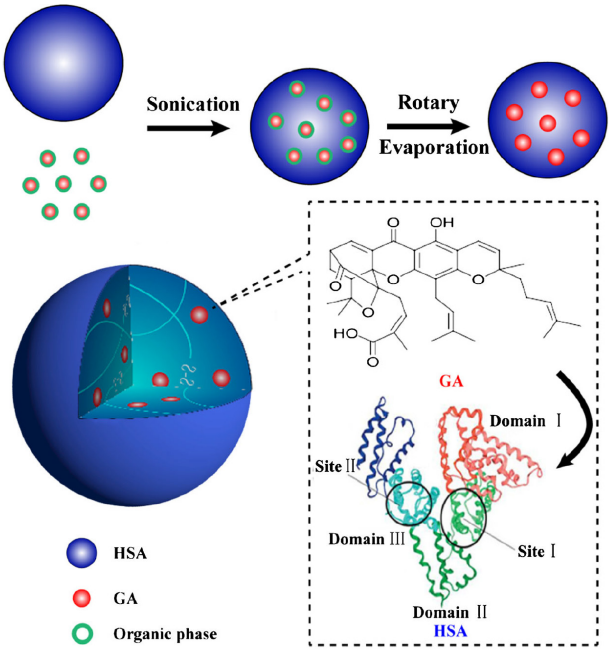

Figure 2. Schematic representation of the formation of albumin nanoparticles loaded with gambogic acid (GA) (Zhang et al., 2017). The chemical structure of GA and crystal structure of human serum albumin (HSA) are shown, indicating the protein sites where GA can bind. Reprinted with permission from Springer Nature: Springer, American Association of Pharmaceutical Scientists, Development of a More Efficient Albumin-Based Delivery System for Gambogic Acid with Low Toxicity for Lung Cancer Therapy, Y. Zhang et al. © 2016, 08 December 2016 (doi: 10.1038/sj.AAPSPharmSciTech.).

Albumin-based nanoparticles are usually employed as carriers with passive targeting properties, for example they accumulate in tumors due to defective vascular architecture or impaired lymphatic drainage. Active targeting may however be achieved by specific chemical modifications with targeting molecules. Zhao *et al.*, for instance, prepared BSA nanoparticles loaded with paclitaxel by a desolvation method and subsequently functionalized BSA with folic acid in order to increase the particle uptake by prostate cancer cells *in vitro* (Zhao et al., 2010).

Chemical modifications can also be used to provide additional properties to albumin. For instance, Du *et al.* introduced cationic polymers to permit the complexation of nucleic acids for transfection *in vitro* (Du et al., 2016). He *et al.* functionalized albumin with histamine as pH-responsive-chelating agent to enable the loading and acidic release of drug complexes with metal ions (He et al., 2017).

Nucleic acids with specific binding and recognition properties have also been introduced for enhanced targeting of albumin nanoparticles. For this purpose, Esfandyari-Manesh *et al*. have used a MUC1 aptamer coating to improve the targeting efficiency of paclitaxel-loaded nanoparticles to breast cancer cells (Esfandyari-Manesh et al., 2016). The aptamer was anchored on a chitosan coating, which proved to enhance nanoparticle uptake and reduce *in vitro* toxicity, with the IC_{50} of paclitaxel in the particles being 31% lower than the free drug in 24 h, and further decreasing in 48 h.

2.1.2 High-Density Lipoprotein (HDL)

HDL are a class of protein-lipid particles of 7-13 nm in size, with apolipoprotein A-I (ApoA-I) being the most abundant protein component, which encircles a load of lipids that include mainly cholesterol and phospholipids (Damiano et al., 2013; Michell and Vickers, 2016; Mo et al., 2016). The structure of HDL depends on the cholesterol content; the uptake of cholesterol remodels the architecture of HDL from discoidal to spherical. The natural source of apolipoproteins is mainly human plasma, but they can also be produced in *E.*

coli and be prepared as reconstituted HDL (rHDL). HDL promotes cholesterol efflux from tissues to the liver for excretion, thus it is often characterized as the "good" cholesterol. Cholesterol efflux involves the interaction of HDL with protein receptors including scavenger receptor class B type 1 (SR-BI), and lipid transporters including ATP-binding cassette (ABC) transporters ABCA1 and ABCG1; these proteins are primarily expressed in macrophages and hepatocytes. The biological role of HDL as well as its biocompatibility and biodegradability, render these particles as promising candidates for drug delivery and imaging, especially for cardiovascular diseases.

The lipid cargo of HDL enables the encapsulation of hydrophobic molecules in the core of the structure. Discoidal and spherical recombinant HDL loaded with a plant-derived quinone with anti-atherogenic potential - tanshinone IIA (TA) - prepared by thin-film dispersion and nanoprecipitation/solvent evaporation, were administered intravenously in atherosclerotic rabbits (Zhang et al., 2013). The particles showed increased localization in atherosclerotic lesions of the aortic tree. Compared to sulfotanshinone sodium injection, liposome and nanostructured lipid TA formulations, the discoidal rHDL particles achieved higher retention in the plasma and healthier serum lipid levels. The levels of total cholesterol, triglyceride and low-density lipoprotein (LDL) were lowered after administration of the particles, and the atherosclerotic burden decreased in a dose-dependent manner (Fig. 3).

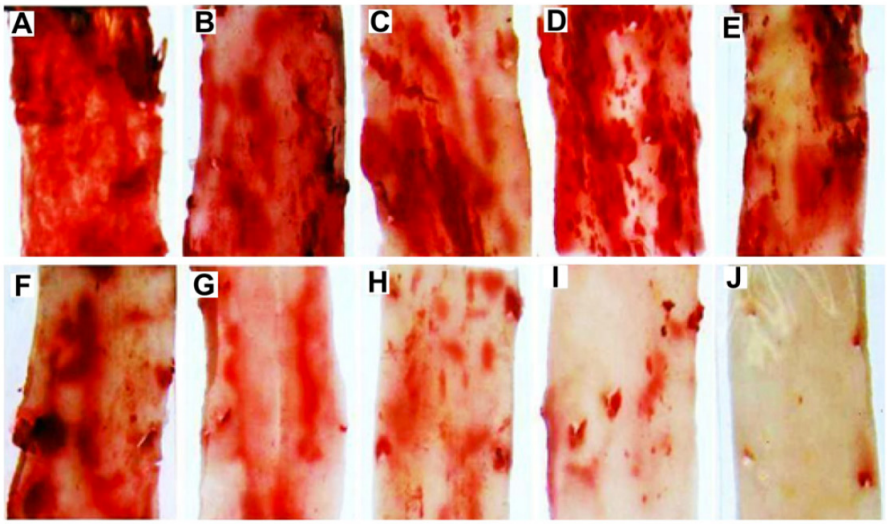

Figure 3. Lipid deposit of atherosclerotic rabbit aortas stained with Oil Red O (Zhang et al., 2013). Positive control (A), sulfotanshinone sodium injection (B), blank discoidal rHDL (C), blank spherical rHDL (D), liposome TA (E), nanostructured lipid TA (F), low dose discoidal TA-rHDL (G), low dose spherical TA-rHDL (H), high dose discoidal TA-rHDL (I) and high dose spherical TA-rHDL (J). Reprinted from Biomaterials, Vol 34, W. Zhang et al., Pharmacokinetics and atherosclerotic lesions targeting effects of tanshinone IIA discoidal and spherical biomimetic high-density lipoproteins, 306-319. © 2012, with permission from Elsevier.

Simvastatin-loaded rHDL nanoparticles (Fig. 4), prepared by film hydration, decreased the viability of macrophages and endothelial cells *in vitro*, and suppressed the inflammatory response of macrophages through inhibition of the mevalonate pathway (Duivenvoorden et al., 2014). The particles were effectively localized in atherosclerotic plaques of ApoE knock-out mice, where they were targeted to monocytes and macrophages, and reduced the plaque formation and anti-inflammatory effect. Reduction of atherosclerotic plaques had also been observed after the delivery of the liver X receptor (LXR) agonist T0901317 by a synthetic HDL (particle reconstitution using the ApoA-I mimetic peptide 22A) which activated the macrophage LXRs (Y. Guo et al., 2018). The particle treatment resulted in the upregulation of ABC transporters in the aorta of ApoE deficient mice, increasing the efflux of cholesterol.

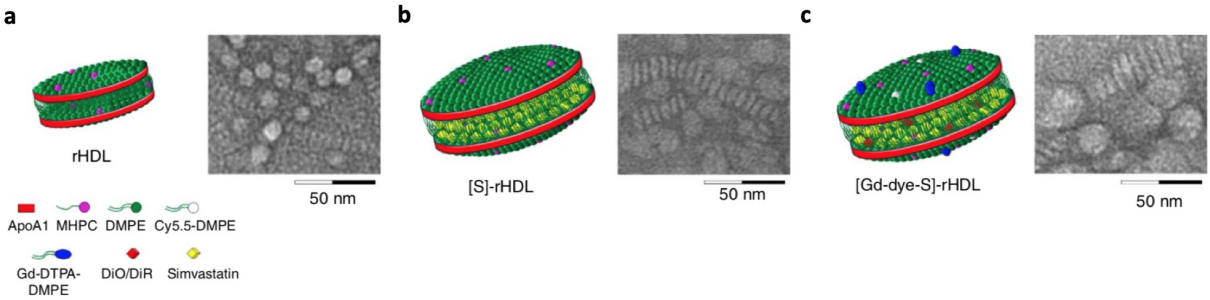

Figure 4. Schematic representation with the corresponding TEM images of rHDL particles before (a) and after loading of Simvastatin ([S]-rHDL, b). The particles could also be loaded with gadolinium and/or fluorescent probes for imaging purposes (c). Adapted from Nature communications, R. Duivenvoorden et al., A Statin-Loaded Reconstituted High-Density Lipoprotein Nanoparticle Inhibits Atherosclerotic Plaque Inflammation, 1-23. © 2014, with permission from Springer Nature.

HDL-inorganic hybrid structures are a promising tool for imaging and therapy. Particles encapsulating inorganic nanocrystals have been prepared by mixing the nanocrystals and lipids in an organic solvent mixture which was evaporated with warm water; ApoA-I was added after change of the buffer to phosphate buffered saline (PBS) (Cormode et al., 2008). *In vitro* results indicated that the properties of endogenous HDL were retained for the hybrid structures, since they could be internalized by macrophages more effectively compared to PEG analogues. *In vivo*, the hybrid system showed association with macrophages in ApoE knock-out mice aortas, with gold nanocrystals showing the best contrast in aortic plaques. In another work, HDL-gold hybrids developed for lymphoma targeting were prepared by mixing phospholipids in ethanol with an aqueous solution of ApoA-I and gold nanoparticles, followed by purification using tangential flow filtration (Yang et al., 2013). The nanoparticles reduced the viability of lymphoma cells *in vitro*, using a SR-B1 mediated uptake mechanism. The system was able to target and reduce the growth of tumors overexpressing SR-B1 in mice; however, repeated injections were needed to outcompete natural HDL. For imaging of atherosclerotic lesions, HDL nanoparticles were also labelled either at ApoA-I or phospholipids with ^{89}Zr for PET imaging (Pérez-Medina et al., 2016). Intravenous administration in rabbits showed higher radioactivity concentration in atherosclerotic rabbit aortas, as well as slower clearance for phospholipid-labelled particles in rabbits. The phospholipid-labelled particles were also tested in pigs, where they accumulated in lesions of femoral arteries.

Hybrid structures of HDL with synthetic polymers may be employed to combine biomimicry with controlled release. HDL with a PLGA core was formulated using a microfluidics system, with the occurring particles exhibiting a slow release of Nile red in PBS (60% in 24 h, 90% in 5 days) (Sanchez-Gaytan et al., 2015). The particles were localized along the aorta and the aortic root of ApoE knock-out mice, and mainly associated with macrophages in the plaques.

The lipid layer of HDL can be used in order to bind functional biomolecules to HDL, especially for gene silencing or expression. Cholesterol-functionalized ApoB1-siRNA bound in HDL and LDL particles showed accumulation in the liver after intravenous administration in mice. The accumulation of LDL particles was more specific for the liver, while HDL particles also accumulated in other tissues due to the uptake mechanism of the particles. The uptake mechanism involved the receptors of LDL (LDLr) for LDL-siRNA and SR-BI for HDL-siRNA (Wolfrum et al., 2007). *In vitro* results suggested that the uptake could also be mediated by the transmembrane protein Sid1. α-Tocopherol-conjugated siRNA was bound to HDL to knock-down the β-site amyloid precursor protein cleaving enzyme 1 (siBACE1) in the brain (Uno et al., 2011). After intracerebroventricular infusion in mice for 7 days, the particles were distributed in the brain and the uptake was evident in neuronal, rather than glial cells. In LDLr knock-out mice the uptake was less efficient, suggesting LDLr-mediated uptake of the particles. HDL was also used to deliver siRNA to the brain through the blood-brain barrier (BBB) (Kuwahara et al., 2011). For this purpose, cholesterol-conjugated siRNA targeting the organic anion transporter 3 (OAT3) mRNA (Chol-siOAT3) was bound to HDL. The particles localized in brain capillary endothelial cells after injection in mice, while no immune or inflammatory responses were observed in the brain. The uptake was found to be mediated by ApoE and LDLr in knock-out mice. In order to protect siRNA from degradation, HDL particles encapsulating siRNA were produced by adding an oligo-lysine mixture of signal transducer and activator of transcription 3 (STAT3) and focal adhesion kinase (FAK) siRNAs to dried lipids. The mixture was solubilized in DMSO, and diluted with aqueous buffer before adding ApoA-I (Shahzad et al., 2011). The organic solvent was removed by dialysis. The intravenous and intraperitoneal injection of the HDL-siRNA complex in mice facilitated silencing of STAT3 and FAK, which are important for the progression and

invasion of tumor cells, and the co-encapsulation of siRNA and chemotherapeutics reduced tumor cell proliferation in ovarian and colorectal cancer.

2.1.3 Collagen and Gelatin

Collagen is a major component of the extracellular matrix. Its main source is animal tissue, and thus production routes such as recombinant expression have been investigated in order to reduce the risk of host's immune response (Gorgieva and Kokol, 2011). The collagenous fragment of this protein is predominantly comprised of Gly-X-Y repeats, where Pro and Hyp (hydroxyproline) occur most often at the X and Y positions, respectively. Other residues that can be found in the sequence include Lys, Met, and Val. In addition, the cell-binding Arg-Gly-Asp (RGD) motif is naturally incorporated, which is the major reason why collagen been extensively investigated for the development of scaffolds for tissue engineering (Liu et al., 2019). Drug delivery systems based on collagen mainly consist in hydrogels and microcapsules, rather than nano-sized objects (Erokhina et al., 2013; Liu et al., 2019; Pastorino et al., 2011; Posadas et al., 2016). For that reason, the present review will be focused on nanoparticles based on the treated counterpart of collagen, gelatin.

Gelatin is a product derived from hydrolysis or degradation of collagen, and it is a material regarded as safe by the FDA (Sahoo et al., 2015). Because of its sequence resemblance with collagen and low antigenicity, it has been investigated for both tissue engineering and drug delivery applications (Foox and Zilberman, 2015; Sahoo et al., 2015).

As was mentioned for albumin particles, gelatin-based formulations designed for drug delivery are also often prepared by desolvation and crosslinking with glutaraldehyde. However, other methods such as spray-drying could be further adapted in order to create nanoparticle formulations (Manca et al., 2013).

The net charge of gelatin depends on the hydrolysis method of collagen. In physiological pH, the charge is positive after acid hydrolysis (gelatin type A) and negative after base hydrolysis (gelatin type B). The charge plays an important role for the drug delivery applications, where type A gelatin is usually used. Type A gelatin nanoparticles prepared by desolvation using ethanol, crosslinked with glutaraldehyde and loaded with indomethacin were orally administered for the treatment of formalin induced edema in rats (Kumar et al., 2011). The particles helped to increase the plasma concentration of the drug and enabled reduction of edema compared to the free drug. Tseng *et al*. developed type A gelatin nanoparticles that were found to be non-toxic to human corneal epithelial (HCE) cells and did not disrupt tight junctions of the cell layer barrier *in vitro*, an important feature in order to retain the integrity of the natural barrier of the anterior part of the eye against micro-organisms (Tseng et al., 2013). Type A gelatin-cryptolepine nanoparticles prepared by desolvation were administered for chemosuppression of *P. bergei* in rats (Kuntworbe et al., 2013). The intraperitoneal injection of the particles showed increased chemosuppressive activity compared to the free drug. However, intravenous injection was more controversial, as two rats died after rapid injection.

Positive charges can also be added to gelatin using chemical modifications. After their *in vitro* results, Tseng *et al.* further modified the cationic gelatin particles with tetramethylrhodamine succinyl ester to further increase the positive charge for improved cell uptake. This was demonstrated by administration of the modified particles to the rabbit cornea, where they were retained for 16h, without significant effect on tissue integrity (Tseng et al., 2013). Particles of gelatin cationized with spermine have also been loaded with pMUC5AC for transfection of IOBA-NHC cells; this process was efficient especially in presence of chondroitin sulfate; transfection was also efficient in rabbit eye conjunctiva (Contreras-Ruiz et al., 2013; Konat Zorzi et al., 2011). For vaccine delivery applications, gelatin cationized with ethylene diamine was used for the development of nanoparticles loaded with tetanus toxoid (Sudheesh et al., 2011). The particles were prepared by desolvation and crosslinked with glutaraldehyde. After subcutaneous injection in BALB/c mice, antibodies against the tetanus toxoid were expressed and the levels of interleukin-2 and interferon-γ increased.

PEGylation is a method employed to increase the biocompatibility and bioavailability of gelatin particles. Gelatin-PEG nanoparticles loaded with noscapine using a desolvation method were shown to have reduced IC_{50} values compared to either the free drug or gelatin particles without PEG in MCF-7 cells (Madan et al., 2011). Moreover, the recovery of noscapine in mouse plasma was higher using the PEGylated system. Aminized gelatin-PEG complexes with tissue-type plasminogen activator (t-PA) prepared in aqueous solution by agitation at 37 °C have been used for ultrasound mediated thrombolysis (Fig. 5) (Uesugi et al., 2010). The degree of amination was important for cytotoxicity in mouse fibroblasts. t-PA activity was suppressed in the complexes and activity was recovered with ultrasound, resulting in thrombolysis in rabbits. In later work by the same group, cationic gelatin-t-PA complexes were formed in presence of zinc ions, which suppressed t-PA activity (Uesugi et al., 2012). Again, the activity was recovered with ultrasound in a fibrin clot lysis assay, and a

longer t-PA half-life in the complexes was observed in mice blood. Chemical modification can also provide other functionalities to gelatin particles, such as binding with specific moieties. Biotinylated EGF was bound to NeutrAvidin-FITC-gelatin nanoparticles which were uptaken by the EGFr lung tumor model in mice after aerosol delivery (Tseng et al., 2008).

Coatings of gelatin particles have been mainly employed to guarantee the stability of the formulations in harsh environments in the organism, while the gelatin carrier increases the bioavailability of the drug and can penetrate in tissues such as the gastric mucosa. Shutava *et al.* studied gelatin nanoparticles prepared by desolvation and glutaraldehyde crosslinking, which were loaded with a green tea polyphenol and encapsulated in a layer-by-layer (LbL) polyelectrolyte shell. The shielded particles released epigallocatechin gallate, blocking HGF-induced intracellular signaling in MBA-MD-231 cells (Shutava et al., 2009). Bhavsar and Amiji fabricated complexes of gelatin with plasmid DNA through precipitation. The complexes were shielded in a polycaprolactone microsphere and orally administered in mice; the gene encoded in the plasmid was efficiently expressed mainly in the large intestine (Bhavsar and Amiji, 2008, 2007). Later on, a similar model was used in the work of Kriegel and Amiji for TNF-α si-RNA delivery to an acute colitis model in mice (Kriegel and Amiji, 2011). Mannan-coated didanosine-gelatin nanoparticles prepared *via* desolvation and crosslinking with glutaraldehyde, were used in the work of Kaur *et al.* (Kaur et al., 2008). After oral administration in rats, increased accumulation was observed in spleen, lymph nodes and brain as compared to the free drug. Moreover, the accumulation was lower in kidney and the particles could be internalized by macrophages in heparinized human blood.

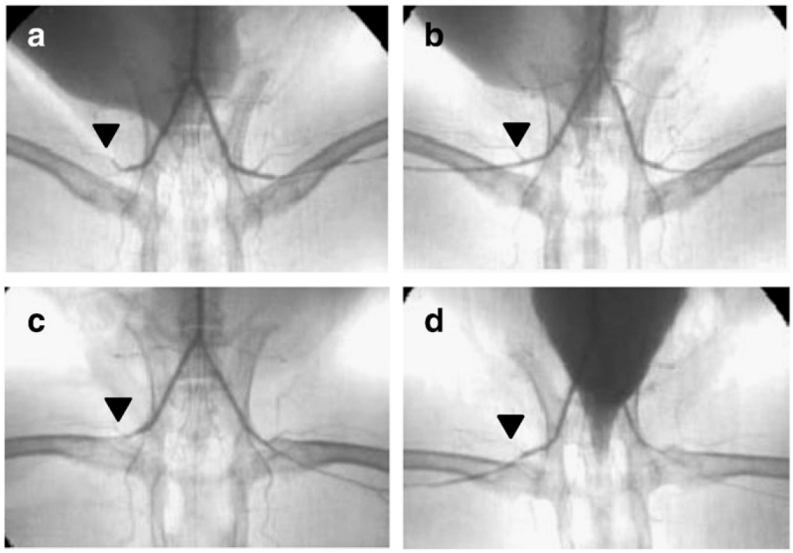

Figure 5. Angiographic images of the thrombolytic effect of t-PA complexed with cationic gelatin-PEG and free t-PA with or without ultrasound irradiation in a rabbit thrombosis model (Uesugi et al., 2010). Arrow heads show the infarction site at the right femoral artery 1 hr after intravenous administration of (a) t-PA, (b) t-PA with ultrasound, c) t-PA complexed with cationic gelatin-PEG, (d) t-PA complexed with cationic gelatin-PEG with ultrasound. Reprinted from Journal of Controlled Release, Vol 147, Y. Uesugi, An ultrasound-responsive nano delivery system of tissue-type plasminogen activator for thrombolytic therapy, 269-277. © 2010, with permission from Elsevier.

2.2 Proteins of non-human origin

Food is a valuable source for therapeutics, but also for carriers in drug delivery or scaffolds in tissue engineering (Elzoghby et al., 2011; MaHam et al., 2009; Yong Zhang et al., 2016). The abundance and wide variety of food proteins provide systems that can effectively suit desired biomedical applications. The basic consideration when using food protein carriers in the human body are the allergic reactions that may be caused, so the systems should be extensively investigated for their immunogenicity. Regarding food proteins, this review will be mainly focused on casein and zein carriers, as they have been most extensively investigated in the last years.

Proteins of exogenous origin other than food also come in a wide range, but immunogenicity remains an even more important limitation in their case. One of the most suitable proteins for drug delivery are fungal hydrophobins (Ren et al., 2013), which will be presented in this section too.

2.2.1 Casein

Casein is abundant in milk and dairy products, and is generally regarded as safe (GRAS) (Elzoghby et al., 2011). The amphiphilic nature and pH sensitivity of these proteins are parameters that facilitate the formation of particles, and crosslinking can be employed to increase the robustness of the structures and their application potential. Casein nanoparticles loaded with flutamide were prepared using an emulsion technique and electrostatically crosslinked with tripolyphosphate (Elzoghby et al., 2013). The drug half-life was extended in rat plasma when the nanoparticles were compared to a drug solution containing ethanol and PEG-200. Levonorgestrel-loaded casein microparticles were produced with an emulsion method and crosslinked with glutaraldehyde for pregnancy control in rabbits (Puthli and Vavia, 2008). The particles were injected into the muscle of fertile female rabbits and drug release was facilitated in blood for one month. During this period pregnancy did not occur, and fertility was reversed after 5-6 months.

2.2.2 Zein

Zein is abundant in maize, and like casein, it is also a GRAS material approved by the FDA (Luo and Wang, 2014; Yong Zhang et al., 2016). It is a protein with high content in hydrophobic amino acids and, due to its self-assembling properties, can be used to construct robust particles. It may be combined with other food proteins to modulate the properties of the final particles.

The hydrophobic nature of zein also renders it a good candidate to encapsulate hydrophobic drugs such as 5-fluorouracil (5-FU) (Lai and Guo, 2011). Drug-loaded particles were prepared with a phase-separation procedure, and using rhodamine-B, they showed higher accumulation in liver and blood after intravenous administration in mice compared to the free dye.

Since zein particles are robust, they are often investigated for delivery *via* the GI tract. Zein-curcumin particles stabilized with caseinate were fabricated *via* desolvation. When Caco-2 cells, which are surrounded by an additional mucin layer, were incubated with these particles, curcumin showed a better association with mucin comparing to a solution of the pure compound (Patel et al., 2010). In another study, soy protein isolate-zein nanoparticles loaded with riboflavin were fabricated with a cold gelation method (Chen et al., 2010). In a simulated GI tract, maximal absorption of riboflavin was observed in the jejunum after delivery of the particles. Except for drugs, functional enzymes can be protected in zein particles for delivery through the GI tract. Lee et al. employed zein to encapsulate catalase and superoxide dismutase *via* phase separation (Lee et al., 2013). The enzymes were protected in conditions resembling GI fluids and functionalization of the enzymes with folate facilitated targeting to macrophages *in vitro*. Zein particles can also protect nucleic acids. Particles loaded with plasmid DNA have been prepared by desolvation, and the complex was used to transfect Caco-2 cells (Regier et al., 2012).

Polymer conjugation to zein can confer additional stability to the particles in complex matrices. Zou and Gu demonstrated a bioconjugate of α-tocopherol-PEG-zein loaded with daidzin, prepared *via* phase-separation (Zou and Gu, 2013). When incubated with Caco-2 cells, the particles were internalized by the cells and could also penetrate through Caco-2 monolayers. After oral administration of the loaded particles in mice, the concentration of daidzin in plasma was higher compared to the free drug, with the area under the curve (AUC_{0-12h}) enhanced by 2.4-fold for the particle formulation.

Inorganic-zein hybrids can also be developed for a variety of applications. Silver nanoparticles encapsulated in acidified zein by desolvation and low pH showed low accumulation of antibodies *in vitro*, indicative of good hemocompatibility, while retaining bactericidal properties against *E. coli* and *S. aureus* (Zhang et al., 2010). In order to combine imaging and drug delivery, Aswathy et al. employed a system of zein particles encapsulating ZnS:Mn quantum dots that were loaded with 5-FU (Girija Aswathy et al., 2012). The self-assembly was done using a desolvation method. These structures were efficiently internalized by MCF-7 and L929 cells and decreased their viability. Wang *et al.* prepared zein-QD630 nanoparticles using phase-separation, which were internalized by NIH3T3 cells and localized in the perinuclear space, exhibiting cytotoxicity similar to the free quantum dot (Wang et al., 2013). However, the penetration of the nanoparticles was limited in nude mouse skin, showing the need for chemical modification of the particle surface.

2.2.3 Hydrophobins

Hydrophobins are proteins produced in fungi for the dispersal of hyphae (thread-like structures that serve for asexual reproduction) from water to air (Mitraki, 2010; Ren et al., 2013). They can be obtained from *T. reesei*, or heterologously produced in *P. pastoris* and *E. coli*. Their amphiphilic nature drives class I hydrophobins to assemble into rod-like structures at the water:air interface, while class II hydrophobins form monolayers. Thus, class II hydrophobins are more useful for particle formation.

Due to their physicochemical properties, hydrophobins can facilitate the solubilization of hydrophobic drugs, as well as encapsulate other proteins or inorganic particles. Hydrophobin-coated docetaxel nanoparticles, prepared *via* nanoprecipitation and ultrasonication, exhibited limited hemolysis and cytotoxicity *in vitro* and also improved pharmacokinetic parameters compared to the formulation of docetaxel in polysorbate 80 (Taxotere) in rats, with the AUC increasing by 1.3 fold for the particle formulation (Fang et al., 2014). Regarding protein encapsulation, glucagon-like peptide was encapsulated in a hydrophobin shell by sonication, and the particle formulation increased the peptide lifetime in rats, achieving efficient glucose regulation (L. Zhao et al., 2016). In order to increase the transit time of silicon nanoparticles in the GI tract, a hydrophobin coating was applied and these coated particles were retained in the stomach mucosa for up to 3 hrs (Sarparanta et al., 2012). Regarding composite assemblies, Au nanoparticle clusters confined in a hydrophobin shell were developed by drying a two-phase solution of the Au particles (in $CHCl_3$) and protein (in water) to a film that was rehydrated to form the supraparticle. Paclitaxel-loaded composite structures showed reduced IC_{50} values by two orders of magnitude compared to the free drug in different cancer cell lines, including Paclitaxel-resistant cells. The particles disassembled in the presence of glutathione, indicating a release mechanism linked to the intracellular levels of the antioxidant. When administered in mice, the composite particles were found to be stable within the course of 4 days, and accumulated in filter organs (Maiolo et al., 2017).

Table 1. Characteristics and applications of natural protein-based carriers.

Protein	Radius of NPs	Zeta potential*	Application	Targeting / active compound	Method of application / Main findings	Synthesis / Preparation	Reference
Albumin	68 nm	−22 mV (at pH 6)	Cancer	Gambogic acid	Delivery of gambogic acid to lung tumor xenograft	Albumin-bound preparation method	(Zhang et al., 2017)
Albumin	90 nm	-45 mV	Leishmaniasis	Amphotericin-B	Leishmaniasis treatment with reduced toxicity of Amphotericin-B	Albumin-bound preparation method	(Casa et al., 2018)
Albumin	95 nm	-12 mV	Ulcerative colitis	5-aminosalicylic acid	Inflammation treatment in ulcerative colitis with 5-aminosalicylic acid	Albumin-bound preparation method	(Iwao et al., 2018)
Albumin	66 nm	-19 mV	Membranous glomerulonephritis	Methylprednisolone	Treatment of membranous glomerulonephritis	Albumin-bound preparation method	(Gai et al., 2018)
Albumin	39 nm	-	Cancer	Doxorubicin	Doxorubicin delivery to breast tumor	Histamine-derivatized albumin chelating $Fe3^{+}$ with doxorubicin	(He et al., 2017)
HDL	15 nm	-	Atherosclerosis	Simvastatin	Simvastatin-loaded HDL nanoparticles prepared by film hydration	Targeted delivery of simvastatin to monocytes and macrophages located in atherosclerotic plaques to reduce inflammation	(Duivenvoorden et al., 2014)
HDL	12 nm	-	Atherosclerosis	Liver X receptor agonist	Liver X receptor agonist-loaded HDL nanoparticles prepared by mixing and reconstitution in aqueous solution	Upregulation of the ABC transporters for the reduction of atherosclerotic plaques	(Y. Guo et al., 2018)
HDL	44 nm	-7.1 mV (at pH 7.4)	Atherosclerosis	Dye	HDL nanoparticles with a PLGA core formulated using a microfluidics system	Combinatorial strategy for controlled release from PLGA core and HDL targeting of macrophages in atherosclerotic plaques	(Sanchez-Gaytan et al., 2015)

Gelatin	120 nm	+23 mV	Vaccine	Tetanus toxoid	Vaccine formulation of tetanus toxoid with gelatin as an immunoadjuvant	Cationic (ethylene diamine)gelatin nanoparticles loaded with tetanus toxoid prepared by desolvation, crosslinked with glutaraldehyde	(Sudheesh et al., 2011)
Gelatin	175 nm	+11 mV (at pH 7.4)	Thrombosis	Tissue-type plasminogen activator	Delivery of tissue-type plasminogen activator (t-PA) for thrombolysis	Cationized gelatin complexes with tissue-type plasminogen activator(t-PA) and PEG-gelatin formed in aqueous solution.	(Uesugi et al., 2010)
Gelatin	1.2 µm	-	Colitis	TNFα siRNA	Oral delivery of siRNA for colitis treatment	Gelatin-TNFα siRNA nanoparticles prepared by precipitation. Encapsulated in PCL microspheres using a double emulsion-like technique	(Kriegel and Amiji, 2011)
Gelatin	65 nm	+37 mV	Dry-eye syndrome	Plasmid	Complexes of spermine-modified, cationized gelatin with plasmid, prepared with ionic gelation	Plasmid delivery to the ocular surface for dry-eye treatment	(Contreras-Ruiz et al., 2013)
Zein	58 nm	-	Bactericidal agent	Silver nanoparticles	Silver-loaded acidified zein nanoparticles prepared by desolvation method and reduced pH	Formulation of silver-loaded zein particles with antimicrobial activity as well as good hemocompatibility for antiseptics	(Zhang et al., 2010)
Zein	100 nm	-23 mV (at pH 7.4)	Oral bioavailability enhancement	Daidzin	Tocopherol polyethylene glycol-Zein bioconjugate nanoparticles loaded with daidzin, prepared with phase-separation method	Oral administration and enhanced absorption of daidzin	(Zou and Gu, 2013)

Hydrophobin	56 nm	-	Drug delivery/contrast agent	Paclitaxel	Au nanoparticle-hydrophobin film hydration	Glutathione-sensitive carrier for theranostics stable *in vivo*	(Maiolo et al., 2017)

*at neutral pH unless otherwise indicated

Natural proteins represent a category of biological materials that can be efficiently employed as drug delivery vehicles. The methods employed lead to the formation of particles with a diameter ranging between 10-200 nm which were negatively charged in most cases (except for the case of gelatin and cationized albumin, see Table 1). These methods are generally straightforward which may facilitate the large-scale production of protein nanoparticles. Further information on the preparation methods of protein particles has been provided in previous reviews that the reader is welcome to consult (Herrera Estrada and Champion, 2015; Tarhini et al., 2017; Verma et al., 2018). Each natural protein was specifically employed for the treatment of a certain disease. For instance, albumin nanoparticles have been primarily focused on applications for cancer treatment, HDL for cardiovascular inflammation, gelatin for eye diseases, and zein for diseases of the GI tract. Nevertheless, the same protein particles are being investigated for other applications, *e.g*. in bacterial infections, expanding their potential in nanomedicine therapy. The nanoformulations revised have exhibited enhanced pharmacokinetics in comparison with the free drug *in vivo*. The animal models employed, however, were mainly mice. It is expected that these evaluations will also be conducted in more relevant animal models, as was done for example in the applications of HDL formulations in rabbits and pigs. The collection of such data will be critical in order to proceed with translation to the clinic. Last, carriers based on natural proteins often lack active targeting properties, which may be supplemented by means of chemical modifications and protein engineering.

3. Engineered protein-based particles

Since the construction of the first recombinant plasmid, scientists have been adapting natural proteins to change their properties. This has also been the case for the development of proteins with self-assembly properties to facilitate nanoparticle formation. A logical choice in this respect are proteins that have as their natural function the assembly into well-defined protein cages, such as heat-shock proteins, ferritin and virus capsid proteins. Regarding the latter class, viruses inherently self-assemble around their genetic material to form macromolecular particles. In some cases, the capsid proteins have the intrinsic property, or can be engineered to assemble without their native lipid bilayer and DNA/RNA, which results in protein mantles known as virus-like particles (VLPs). These capsid proteins may be modified to display or encapsulate antigens, toxic compounds or targeting moieties. For *in vivo* applications, they have been mainly used as vaccination agents (Noad and Roy, 2003). Another interesting group are native structural proteins that already show self-assembly properties, such as elastin, silk, resilin *etc*. Naturally, they may form connective tissues (elastin, resilin) or supramolecular materials (spider's silk). Using their basic sequences, responsive materials have been created that may control or participate in self-assembly. Here we focus on the creation of particles based on elastin- and silk-like polypeptides and their hybrids, since they have been most extensively studied *in vivo*.

3.1 Elastin-like polypeptides

Elastin-like polypeptides (ELPs) are repetitive biopolymers derived from natural elastin (Urry et al., 1991). The repeat unit may differ, though most commonly used is the GXGVP motif, in which X is the variable amino acid. ELPs are typically noted as [$A_XB_YC_Z$-n], where A, B and C denote the guest residues, X:Y:Z their ratio within the ELP block, and n the number of pentapeptide repeats. For example, [A_3G_2-60]-[I-60] denotes an ELP diblock that consists of one part with 60 pentapeptide repeats containing alanine and glycine in a ratio of 3 to 2 as guest residue, and one part with 60 pentapeptide repeats containing only isoleucine as guest residue; a protein with 600 amino acids total. Note that this notation does not define the exact position of each guest residue within a sequence if multiple guest residues are used. We will adhere to this notation but adapt for structures which cannot be fully described by it. These disordered proteins change structure upon heating towards type-II β-turns, type-I β-turns, and β-strands (Groß et al., 2003; Li et al., 2014), exposing hydrophobic residues and leading to their coacervation. Lowering the temperature results in the reversal of this structural change, dissolving the individual polymers. The transition temperature T_t is dependent on polymer concentration, salt concentration, number of repeats and the nature of the guest residue at position X (McDaniel et al., 2013). More hydrophilic residues shift the T_t higher, while more hydrophobic ones lowering the T_t. By combining ELP 'blocks' with different transition temperature, micellar and other shapes can be created (Fig. 6, Table 2). Here we focus on *in vivo* studies of ELPs that form micellar or similar structures in their aggregated state.

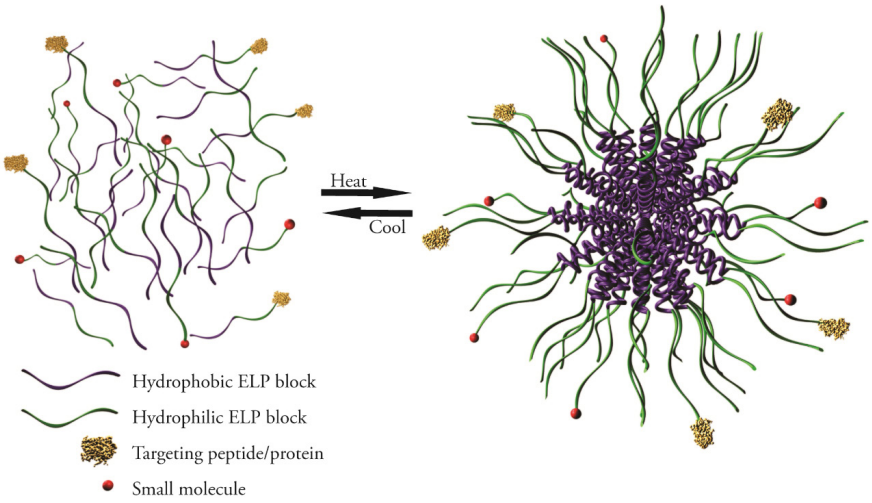

Figure 6. Scheme of elastin-like peptide diblocks reversibly forming micelles. Modifications are possible by recombinant fusion and/or chemical modification. Di-blocks with varying modifications can be mixed, creating diverse ELP micelles displaying and/or encapsulating drugs and targeting moieties (Pille et al., 2017). Adapted from Biomacromolecules, Vol 18 (4), 2017, J. Pille *et al.*, Self-Assembling VHH-Elastin-Like Peptides for Photodynamic Nanomedicine, 1302–1310.

3.1.1 ELPs in cancer research

ELPs have been used to target and treat different kinds of cancers. Simnick *et al.* fused the NGR tripeptide to $[V_1G_7A_8$-64]-[V-90] to target the aminopeptidase-N receptor overexpressed on endothelial cells in tumour tissue (Pasqualini et al., 2000; Simnick et al., 2011). In comparison with unmodified control particles, NGR-ELP particles showed accumulation in endothelial and perivascular regions of human squamous cell carcinoma derived tumors in female BALB/c nude mice. 45 minutes after injection, around 80 % of NGR-ELP was retained in the vascular region of tumors, significantly more than in normal tissue. There also was a significant increase in extravascular regions when compared to normal tissues. However, these results did not significantly differ from ELP particles alone.

Cancerous tissue often shows a decreased extracellular pH, ranging from 6.2 to 6.9. Callahan *et al* created a pH-sensitive ELP diblock, $[VG_7A_8$-80]-$[VH_4$-100], which forms a nanoparticle at physiological conditions with the addition of physiological concentrations of $ZnCl_2$ and disassembles into monomers upon reaching a pH of 6.4 (Callahan et al., 2012; Kasperek et al., 1977). This pH-sensitivity stems from using histidine, with its pKa of around 6, as a guest residue; it becomes protonated in slightly acidic conditions, increasing the transition temperature of the ELP. The resulting particle showed a CMC of 8.9 $\pm$ 3 µM (measured by pyrene fluorescence), a hydrodynamic radius of 29.5 nm and was on average composed of 73 ELP diblocks (measured by static light scattering). Injection of particles into nude mice bearing human colorectal adenocarcinoma-derived tumors showed a more homogenous distribution within tumor sections 4 h after injection than pH insensitive control ELP particles, but faster clearance from the tumor site 24 h and 48 h after injection. The system was not tested in combination with a therapeutic agent.

Sarangthem *et al.* used the construct $(AP1\text{-}[V\text{-}12])_6$-$(KLAK)_4$ to target tumor models in mice (Sarangthem et al., 2016). AP1 is a 7 amino acid peptide (RKRLDRN) that binds the interleukin-4 (IL-4) receptor, implicated in drug resistance of various cancers by amplifying the expression of anti-apoptotic proteins. The same group had previously shown that $(AP1\text{-}[V\text{-}12])_6$ accumulates in human breast cancer MDA-MB-231 xenografts in mice with increased affinity and uptake into IL-4 receptor expressing cells. KLAK-repeats destabilize eukaryotic membranes and induce apoptosis. The combined construct $(AP1\text{-}[V\text{-}12])_6$-$(KLAK)_4$ showed a micellar structure at physiological conditions with a hydrodynamic radius of 300 $\pm$ 61 nm (measured by DLS) and ~ 60 nm (measured by TEM). Particles induced an 80-85 % decrease in tumor growth in MDA-MB-231 xenografts in BALB/c female nude mice and in murine B16F10 tumors of C57BL/6 black female mice after intraperitoneal injection. All parameters tested to ensure liver, heart and kidney function as well as haematological markers indicated no systemic toxicity after two weeks of daily injection of 150 mg kg^{-1}. The material had a terminal half-life of 14.4 $\pm$ 1.2 h and plasma clearance of 4.5 $\pm$ 0.7 10^{-3} L hr^{-1} kg^{-1}.

Aluri *et al.* fused a single-chain antibody (scFV), derived from anti CD-20 rituximab, to the ELP [A-192] (Aluri et al., 2014). The resulting conjugate formed particles with hydrodynamic radii of 85.7 and 24.1 nm as determined by DLS and cryoTEM, respectively. According to size-exclusion chromatography (SEC) coupled to multi-angle light scattering (MALS), the particles possessed an average molecular weight of 25.5 MDa,

resulting in an aggregation number of about 250 monomers per particle. Assembly was observed below the expected transition temperature of the ELP (conjugate) and further processing of the particles was used. After denaturation with guanidine and renaturation, a major population was observed with rod-like morphologies (length 56.2 nm and width 17.9 nm). The molecular weight of these dropped significantly to an average of 8.4 MDa and an aggregation number of around 84. In a Raji xenograft mouse model, the scFV-ELP particles significantly reduced tumor growth when compared to Rituximab given alone.

Zhao *et al.* created a fusion of the ELP di-block $(GAGVPG)_{70}$-$(GVLPGVP)_{56}$-$(GC)_4$ and single-chain variable fragment (scFVv) of the antibody αPD-1, which suppresses the programmed cell death protein 1 (PD-1) (Zhao et al., 2017). This protein prevents both desirable immune reaction against various types of cancers as well as autoimmune reactions. The resulting scFv-ELP formed cross-linked micelles with a radius of 21.5 nm as determined by DLS. *In vitro*, the resulting particles showed an avidity effect towards binding PD-1 positive EL4 cells when compared to free scFv or scFv-ELP in a monomeric state. This effect was also seen in a competitive binding assay. *In vivo*, no significant difference in PD-1 inhibition could be seen in monobese diabetic female NOD/ShiLtJ mice between the scFv-ELP nanoparticle and its non-crosslinked counterpart.

The same group used the sequence $(GAGVPG)_{70}(GGGGGGGGC)_8$ to deliver salinomycin and paclitaxel to orthotopic breast cancers (P. Zhao et al., 2016, 2014). Salinomycin was modified with 4-(aminomethyl)benzaldehyde and 4-(4-N-maleimidophenyl)butyric acid hydrazide to obtain a maleimide-functionalized drug that could be conjugated to the polymer, but would be released after particle uptake due to acidification and hydrolysis of the hydrazone bond. Paclitaxel was non-covalently encapsulated together with α-tocopherol. The resulting particles had hydrodynamic radii of 25.6 nm and 42.6 nm at 25 µM in phosphate buffered saline (PBS) without and with paclitaxel, respectively. Tumor growth, metastasis and survival were monitored in BALB/c mice bearing 4T1 metastatic breast tumors. Salinomycin loaded particles decreased tumor growth and increased survival when compared to salinomycin alone. The combination of paclitaxel and salinomycin loaded particles further decreased tumor growth and increased metastasis-free survival and overall survival significantly than either particle alone.

Schaal *et al.* created stable depots for brachytherapy of prostate and pancreatic tumor models by inducing micelle-to-gel transition of [V-120]-$(GY)_7$, followed by ^{131}I induced β-irradiation mediated crosslinking (Schaal et al., 2016). The radiolabeled ELPs formed micellar structures around ambient temperature with a hydrodynamic radius of 41.2 nm and an average radius of gyration of 50.3 nm, measured by DLS and static light scattering (SLS), respectively. These micelles formed crosslinked gels at 37 °C that retained ^{131}I with very little off-target accumulation. In a mice model, prostate tumor regression was larger than 95 % with a median survival five-fold higher than the control, 60 versus 12 days, respectively.

Overall, the greatest effects in tumor treatment were achieved when self-assembly was either induced by covalent coupling to hydrophobic small molecules as in the case of doxorubicin(MacKay et al., 2009) and salinomycin, or when a formed micelle coacervated after injection to form a drug deposit as shown with brachytherapy (Schaal et al., 2016; P. Zhao et al., 2016, 2014). This might be due to increased circulation stability, since a coacervate core formed by ELPs might be susceptible to deformation and rapid clearance without cross-linking or stronger interactions such as pi-stacking. This has not been investigated yet systematically, but observations with polyplexes support this hypothesis (Takeda et al., 2017).

3.1.2 ELPs in wound healing

Koria *et al.* developed nanoparticles by fusing the keratinocyte growth factor (KGF) to the ELP [V-50] (Koria et al., 2011). The formed nanoparticles had radii of about 250 and 255 nm, as determined by TEM and DLS. *In vitro*, proliferation of keratinocytes was enhanced, albeit with a lower downstream phosphorylation of ERK1 and ERK2 when compared to free KGF. Proliferation of fibroblasts was increased for both free ELP and KGF-ELP particles, 4.9-fold and 1.6-fold compared to negative controls, respectively. *In vivo*, wounds of diabetic B6.BKS(D)-*Lepr^{db}*/J mice showed increased granulation and reepithelization when treated with KGF-ELP nanoparticles embedded in fibrin gels. Although granulation was even higher for either free ELP or KGF and ELP given simultaneously, the reepithelization was highest for KGF-ELP and the granulation to reepithelization ratio was most favorable for KGF-ELP, according to the authors.

In a follow-up study, Yeboah *et al.* fused stromal cell-derived growth factor 1 (SDF1) to the same ELP (Agnes Yeboah, Rick I. Cohen, Renea Faulknor, Rene Schloss, Martin L. Yarmush, 2016). They obtained nanoparticle sizes with radii of 300 and 280 nm as measured by TEM and DLS, respectively. Binding to the SDF1 receptor, CXCR4, was comparable with free SDF1 with dissociation constants of 1.14 nM and 0.3 nM, respectively, as measured by surface plasmon resonance (SPR). Intracellular calcium release of SDF1-ELP

nanoparticles in CXCR4-positive HL60 cells was lower at low concentrations when compared to free SDF1, but significantly higher at therapeutic relevant doses. *In vivo*, wound closure of diabetic BKS·Cg-Dock7^{m} +/+ Lepr^{db}/J mice was significantly accelerated when treated with SDF1-ELP particles embedded in fibrin gels, with wounds being completely closed after 28 days compared to 42 days when treated with free SDF. Additionally, a thicker epidermis and dermis were observed after 42 days in the SDF1-ELP treated mice.

These results show that nanoparticles formed by ELPs are good for the display of proteinaceous factors for wound healing, probably due to a more favorable release profile / retention. They can be easily combined with other materials for optimization. As gels made from ELPs can also be used for cell guidance for regenerative purposes (Coletta et al., 2017), tailoring release kinetics and degradation kinetics is feasible when using ELPs as a carrier materials.

3.1.3 ELPs in vaccination

García-Arévalo *et al.* fused a 20 amino acid antigen from *M. tuberculosis* to [E-50]-[I-60] (García-Arévalo et al., 2013). The resulting particles had a zeta potential -12.1 mV in PBS, and radii of 26.7, 27.7 and 33.2 nm, measured by SLS, cryo-TEM and atomic force microscopy (AFM), respectively. They had an average mass of 13.6 MDa, resulting in an aggregation number of 277. Curiously, the ρ ratio was 0.93, indicating a vesicular structure rather than a micellar one. After immunization of BALB/cByJ female mice with antigen-ELP, an initial immune response was observed, characterized by increased levels of IL-1β, IFN-γ and IL-5. Although isotype switching from IgM to IgG specific to antigen-ELP was observed, this strategy did not lead to IgGs specific to the antigen alone.

Cho *et al.* used elastin-like peptide micelles as a carrier material for stimulating the response of cytotoxic T lymphocytes (CTLs) to an eight amino peptide epitope (SIINFEKL) derived from ovalbumin (Cho et al., 2016). The polymeric di-block did not correspond to the canonical ELP sequence. Sequences where chosen directly by comparing mouse tropoelastin and human elastin and selecting regions resembling similarity to hydrophobic and hydrophilic ELP motifs, GVLPGVG and GAGVPG, respectively. These sequences were termed immune-tolerant elastin-like polypeptides (iTEPs) due to the hypothesis that they would be less immunogenic due to their natural occurrence. The resulting protein had the sequence $G(GAGVPG)_{70}G(GVLPGVG)_{28}G(ESIINFEKLT)_2GG$ and the assembled particles radii of 40.6 and 36.0 nm in PBS, depending on concentration. After immunization of C57BL/6 mice, these particles induced increased secretion of interferon gamma (IFN-γ) from splenocytes in response to the ovalbumin epitope, suggesting an increase in CTL activation. The stimulation was higher than with ovalbumin or the epitope alone.

Overall, there do not seem to be any undesired immunogenic response against ELP sequences, making them particularly interesting carriers for small antigens such as peptides, which would be quickly eliminated from circulation with an artificial increase in hydrodynamic radius. Whether a particle morphology by using ELP diblock copolymers is preferable to simply using ELP tags to increase circulation time of small epitopes remains however an active area of research. Multiple small epitopes from a known organism could be combined into a single particle, potentially leading to a more effective immunization against pathogens such as *M. tuberculosis.*

3.1.4 ELPs in eye-related diseases

Shah *et al.* developed rapamycin retaining nanoparticles by fusing the protein FKBP12, which binds rapamycin, to the ELP diblock [S-48]-[I-48] (Shah et al., 2013). The resulting particles had hydrodynamic radii of about 24 nm as determined by DLS. In male NOD mice, an animal model for Sjoegren's syndrome, the resulting particles positively influenced the pharmacokinetic parameters of rapamycin when compared to monomeric rapamycin-FKBP12-[S-48] or free drug alone. Plasma concentration declined according to a two-phase decay model with an initial half-life time of 0.36 $\pm$ 0.1 h^{-1} and terminal half-life of 8.8 $\pm$ 2.6 h^{-1} if administered in the nanoparticle formulation, compared to a single-phase decay with terminal half-lives of 5.1 $\pm$ 0.4 h^{-1} and 5.6 $\pm$ 0.8 h^{-1} for free drug and drug bound by the monomeric ELP fusion protein. Both free drug and rapamycin-containing micelles decreased lymphocytic infiltration of the lacrimal glands (LGs) significantly when compared to controls, albeit with no significant difference between the two. Both altered the RNA expression profiles of cytokine and chemokine genes as well as mTOR-related genes. Notably, the rapamycin-containing nanoparticles reduced both the gene expression and activity of a biomarker associated with dacryoadenitis in the LGs of NOD mice, CATS. The particles also showed reduced nephrotoxicity and inflammation/necrosis around the injection site. Of note, and showing synergies of studying one nanoparticle system for multiple diseases, Shi *et al.* used the same particles on MDA-MB-468 tumors grown in the fat pads of female nude mice

(Shi et al., 2013). Tumor volume stagnated over the course of 60 days, while treatment with rapamycin alone had to be abandoned due to severe toxicity of the free drug.

Hsueh *et al.* used ELP [S-48]-[I-48] fused to the terminal domain of the fiber capsid protein of adenovirus serotype 5 (Hsueh et al., 2015). This protein fragment with a molecular size of ~20 kDa is known to target the coxsackievirus and adenovirus receptor (Henry et al., 1994), present at high levels on the basolateral side of cells composing the lacrimal glands (Xie et al., 2006). The resulting particle had a zeta potential of -7.9 mV and radii of 16.0 and 21.6 nm, measured by TEM and DLS, respectively. After intra-lacrimal injection in male BALB/c mice, particles showed basolateral to apical transcytosis by acinar epithelial cells to the lumen of laminar glands *in vivo*. It was proposed to use these particles as a delivery system for therapeutics to the ocular surface from within the body.

Reducing (nephro-) toxicity of small molecules either by encapsulation within a nanoparticle or by having additional binding moieties, such as FKBP12 for rapamycin, is a powerful strategy to increase the maximum tolerable dose, potentially prolonging the therapeutic window, in which drug concentration is high enough to exert its desired effect. ELPs as proteinaceous carriers have the distinct advantage that displayed or encapsulated protein-based binding or targeting moieties are part of the fusion protein, making in additional coupling step unnecessary. Since ELPs itself show very good biocompatibility and low immunogenicity, continuous treatment of nanoparticles loaded with or displaying immuno-stimulatory antibodies, antigens and small molecules may allow powerful combinatorial therapies in one formulation. One potential issue is that there is currently no direct evidence of long-circulating ELP-based nanoparticles without stabilizing cargo, which may be a potential hindrance to their application. However, chemical and enzymatic cross-linking, as well as the introduction of hysteresis-inducing guest residues has not been studied *in vivo* to a significant extent. Studies that investigate the fate of ELP-based nanoparticles and possible modifications of the coacervate core would be highly interesting and useful to the field.

Table 2. Characteristics and applications of nanocarriers based on elastin-like polypeptides

Polypeptide	Radius of NPs	Morphology / Zeta potential	Application	Targeting / active compound	Method of application / Main findings	Synthesis / Preparation	Reference
Elastin-like polypeptides	20 nm	micellar	Cancer	No targeting peptide / doxorubicin via hydrazone linkage	Increased AUV vs free DOX (716 vs 4.7 µMh). Curative in 8 of 9 mice bearing C28 tumors for up to 66 days	Recombinant ELP with free cysteines, to which dox was coupled	(MacKay et al., 2009)
Elastin-like polypeptides	-	micellar	Cancer	NGR / none	Increased retention of particles in HSCCA tissue compared to normal, unclear effect of NGR	Recombinant ELP	(Simnick et al., 2011)
Elastin-like polypeptides	30 nm	micellar	Cancer	pH-sensitive ELP block / none	Increased homogenous distribution in HCAC tumors	Recombinant ELP	(Callahan et al., 2012)
Elastin-like polypeptides	60 nm by 20 nm	Rod-shape	Cancer	Anti-CD-20 single-chain antibody	Reduced tumor growth compared to full-length Anti-CD-20	Recombinant fusion protein, renaturation	(Aluri et al., 2014)
Elastin-like polypeptides	40 nm	micellar	Cancer	Salinomycin via hydrazone bond, paclitaxel by co-formulation with α-tocopherol	Decreased tumor growth and metastasis-free survival compared to free drugs	Recombinant protein, chemical attachment of salinomycin, co-formulation of paclitaxel and α-tocopherol	(P. Zhao et al., 2016, 2014)
Elastin-like polypeptides	60 – 300 nm	micellar	Cancer	AP1/KLAK	Decrease in tumor growth of 80% compared to control in MDA-MB-231 xenografts and murine B16F10 tumors	Recombinant fusion protein	(Sarangthem et al., 2016)
Elastin-like polypeptides	40 nm as micelles	Micellar, gel upon injection	Cancer	None/ ^{131}I	Direction injection for brachytherapy.	Recombinant ELP	(Schaal et al., 2016)
Elastin-like polypeptides	20 nm	Micellar, crosslinked by internal disulfide bridges	Cancer	αPD-1 single-chain antibody	*In vitro*, avidity effect was observed. *In vivo*, no difference could be seen between cross- and non-crosslinked particles	Recombinant fusion protein	(Zhao et al., 2017)

Elastin-like polypeptides	250 nm		Wound healing	Keratinocyte growth factor	*In vitro*, proliferation of fibroblasts was increased. Wounds of diabetic mice showed increased granulation and reepithelization when treated with KGF-ELP particles	Recombinant fusion protein, delivered via embedment in fibrin gels.	(Koria et al., 2011)
Elastin-like polypeptides	280 – 300 nm		Wound healing	Stromal cell-derived growth factor-1	Accelerated wound closure in diabetic mice with thicker epidermis and dermis	Recombinant fusion protein, delivered via embedment in fibrin gels.	(Agnes Yeboah, Rick I. Cohen, Renea Faulknor, Rene Schloss, Martin L. Yarmush, 2016)
Elastin-like polypeptides	30 nm	Micellar, –12 mV (in pH 7.4)	Vaccination	M. tuberculosis antigenic peptide	Increased levels of IL-1β, IFN-γ and IL-5. Isotype switching was observed, though no IgGs specific to antigen alone were observed.	Recombinant fusion protein	(García-Arévalo et al., 2013)
Elastin-like polypeptides	40 nm	micellar	Vaccination	CTL stimulating epitope from ovalbumin	Increased IFN-γ secretion after immunization compared to free ovalbumin or epitope alone	Recombinant fusion protein	(Cho et al., 2016)
Elastin-like polypeptides	20 nm	Micellar, – 8 mV (at pH 7.4)	Eye diseases	Rapamycin binding protein	Reduced toxicity compared to free drug, increased plasma half-life	Recombinant fusion protein, binding of rapamycin	(Shah et al., 2013)
Elastin-like polypeptides	40 nm	micellar	Eye diseases	Domain of adenovirus capsid protein	Transcytosis to the lumen of laminar grands after intra-lacrimal injection	Recombinant fusion protein	(Hsueh et al., 2015)

3.1.5 ELP-based hybrid systems

Integrating elastin-like polypeptides with other sequences or polymers can modify the performance of the nanoparticles. These hybrid nanoparticles include fusions of ELPs with poly(aspartic acid), small hydrophobic drugs, protein receptors, single-stranded DNA, virus coat proteins, silk-based polypeptides and synthetic polymers (Table 3) (Smits et al., 2015). Surface coating of the nanoparticles with synthetic polymers such as polyethylene glycol (PEG) can prevent agglomeration (Rahman et al., 2013). PEG is often used as the hydrophilic stealth component of amphiphilic block copolymers. In an aqueous solution, PEGylated polymers can form micelles by collapsing the insoluble hydrophobic block into a center core surrounded by a hydrophilic shell (Otsuka et al., 2012). Van Eldijk *et al.* fused PEG to ELP blocks with different lengths *via* strain-promoted alkyne−azide cycloaddition (SPAAC) (Fig. 7) (Van Eldijk et al., 2014). This conjugation resulted in stimulus-responsive amphiphilic block copolymers that self-assembled into micelles upon inducing the ELP phase transition. In addition, a fluorescent dye was easily encapsulated indicating the ability of these hybrid polymers to encapsulate hydrophobic drugs.

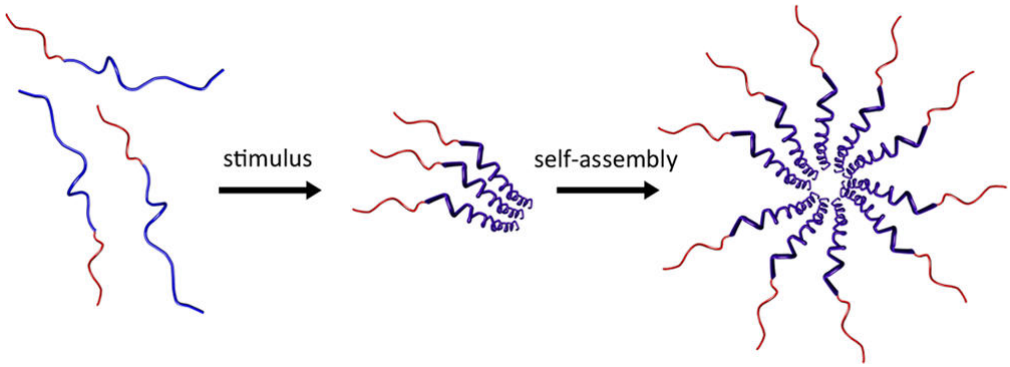

Figure 7. Schematic illustration of PEGylated-ELP hybrid system (Van Eldijk et al., 2014). Reprinted with permission from Biomacromolecules, Vol 15, M.B. van Eldijk *et al.*, Synthesis and self-assembly of well-defined elastin-like polypeptide-poly(ethylene glycol) conjugates, 2751-2759. © 2014 American Chemical Society.

Recently, Kim *et al.* fabricated α- elastin nanoparticles derived from human adipose tissue and functionalized it with methoxy-poly(ethylene glycol) (mPEG) (Kim et al., 2017). The formed conjugates (PhENPs) self-assembled into 330 nm spherical nanoparticles in water at 32 °C. DLS and SEM characterization data suggested that the increased mPEG molar ratio prevented particle aggregation over time and increased particle stability. PhENPs were tested for their ability to encapsulate proteins such as insulin and BSA. When insulin-loaded PhENPs were studied for their biological activity *in vitro*, they were capable to induce the translocation of the insulin-regulated glucose transporter (GLUT4) in mouse cells comparable to commercial insulin-treated cells, as shown by confocal microscopy. PhENPs showed a brust insulin and BSA over 12 hrs with slow and sustained release for 72hrs. This approach is considered as a good example for injectable protein delivery systems. Moreover, PEGylated-ELP nanoparticles were evaluated for their anti-cancer drug nuclear localization. pH-responsive, PEG-ELP/DOX micelles were generated in which doxorubicin was encapsulated in the ELP hydrophobic core (Huang et al., 2017b). The hybrid polymers, PEG-ELP[VH4-70] self-assembled into nanoparticles with size of 114 nm at pH 7.4 and disassembled when the pH dropped to 5.6. This behavior was controlled by addition of Zn^{2+} metal ions that stabilized the micelles structures, trapping the DOX in the hydrophobic core at pH 7.4, but also facilitated doxorubicin release in the lysosomal acidic environment. PEG-ELP/DOX nanoparticles showed *in vitro* biocompatibility with 85% cell viability. *In vivo* fluorescence images showed tumor reduction in a mouse model upon intravenous injection with PEG-ELP[VH_4-70]/DOX with no noticeable toxicity to murine liver cells.

Chilkoti's group rationally designed and produced the first chimeric polypeptides (CPs) that self-assemble into nanoparticles upon doxorubicin encapsulation, and showed *in vivo* efficacy in a murine tumor model (MacKay et al., 2009). The system was composed of two segments, a hydrophilic ELP with the guest residues being Val/Ala/Gly in [1:8:7] ratios, and a shorter $(Gly\text{-}Gly\text{-}Cys)_8$ at the C-terminal side for doxorubicin attachment through a pH-labile linker. TEM and DLS measurements confirmed near-monodisperse CP-DOX nanoparticles with hydrodynamic radius, Rh, of 21.1 ± 1.5 nm. Laser-scanning confocal microscopy images confirmed doxorubicin localization into the cell nucleus after 30 min of exposure to CP-DOX indicating cell uptake of CP-DOX, release of doxorubicin and subsequent trafficking of drug to the nucleus. Locally

administrated CP-DOX had about 3.5-fold higher drug accumulation in tumor tissue compared to free drug with decreased drug concentrations into healthy tissues such as lung and heart. CP-DOX outperformed free drug exhibiting significant anti-tumor efficacy when administrated to mice with eight-day-old C26 tumors as it increased animal survival up to 66 days compared to 27 days with free DOX. Interestingly, the authors studied genome array data to investigate the molecular mechanism CP-DOX nanoparticles. They found out that among DNA repair genes a specific gene, uracil-DNA glycosylase (Ung), was exclusively down-regulated by CP-DOX treatment compared to free DOX treatment. This gene is involved in chemotherapeutics resistance. This supports that CP nanoparticles can overcome drug resistance, as also suggested for other drug delivery systems (Seib et al., 2013).

Addition of poly(aspartic acid) can induce ELP self-assembly into nanoparticles. Kobatake's group previously produced genetically engineered ELPs with fused poly (aspartic acid) tails (ELP-D) displaying epidermal growth factor (EGF). However this system exhibited a problem of steric hindrance of the fused proteins (Matsumoto et al., 2014). They overcame this problem by using de novo-designed peptides with a coiled-coil structure to allow non-covalent tethering of growth factors to protein nanoparticles. The nanoparticles were formed with as building blocks a fusion of ELP with a poly (aspartic acid) sequence and helix B at its C-terminus. The surface of the nanoparticles was decorated with growth factor and paclitaxel was encapsulated in the core. EGF-decorated nanoparticles were recognized by the VEGF receptor and thus were taken up by HeLa cells. Paclitaxel-loaded growth factor-tethered ELP-Ds were effective against cancer cells by inducing cell apoptosis (Assal et al., 2015). Another approach to fabricating hybrid ELP-based delivery systems is to fuse protein receptor to ELPs. This was illustrated by a study in which an ELP of sequence [VH_4-40] was genetically fused to Tumor necrosis factor-Related Apoptosis-Inducing Ligand (TRAIL) and the RGD peptide. The RGD-TRAIL-ELP complex was able to self-assemble forming nanoparticles under physiological conditions (37 °C) (Huang et al., 2017a). DLS and freeze-fracture TEM images showed the formation of ~190 nm particles at body temperature. Compared to RGD-TRAIL alone, RGD-TRAIL-ELP nanoparticles exhibited longer half-life and systemic circulation in a mouse model and more accumulation at the tumor sites.

Table 3. Characteristics and applications of nanocarriers developed with ELP hybrid systems.

Components	Size of NPs	Morphology / Zeta potential	Application	Targeting / active compound	Method of application / Main findings	Synthesis / Preparation	Reference
α- elastin+ PEG	330 nm	Spherical	Protein delivery	-	*In vitro* insulin delivery- GLUT4 translocation in C2C12 cells treated with the nanoparticles	Mixing in water	(Kim et al., 2017)
ELP+PEG	114 nm in pH 7.4 and 20 nm in pH 5.6	Micelles, 0.189mV in pH 7.4 and 12.65 mV in pH 5.6	Cancer	Doxorubicin	pH-responsive and 4.8-fold suppressed effect relative to the free drug after intravenous injection *in vivo*	ELP coupled with 20 kDa Mal-PEG.	(Huang et al., 2017b)
DOX-ELP	21.1 ± 1.5 nm	Spherical	Cancer	Doxorubicin	Higher anti-tumor activity can overcome drug resistance	Dox was linked to chimeric polypeptides through pH-responsive linker	(MacKay et al., 2009)
ELP+poly (aspartic acid)	35nm (without EGF or Pax)	Spherical-shaped granulations	Cancer	Epidermal growth factor (EGF)/ Paclitaxel	PTX-loaded ELP-D-VEGF showed higher apoptotic activity compared to control	protein nanoparticle was formed *via* coiled-coil formation	(Assal et al., 2015)
RGD+TRAIL+ELP	~190 nm at 37 °C	--	Cancer	RGD/TRAIL	Intraperitoneal injection RGD-TRAIL-ELP 3-fold enhanced apoptosis-inducing capacity than RGD-TRAIL with no liver toxicity	ELP sequence fused to RGD-TRAIL *via* Gly linker	(Huang et al., 2017a)

3.2 Silk-like nanoparticles

Silk has been renowned for its unique mechanical properties. Both the *Bombyx mori* silkworm and the spider produce silks that outcompete the toughness of steel and Kevlar (Heim et al., 2009). Therefore, this protein-based material has been exploited in many applications through the years such as electronics and sensors; edible food packaging as well as medical applications such as wound dressing and tissue engineering (Kasoju and Bora, 2012; Marelli et al., 2016; Zhu et al., 2016). Silk can be produced through different ways; either by organisms such as silkworms and spiders, protein recombinant expression in micro-organisms or transgenic animals such as mice (Andersson et al., 2016; Tokareva et al., 2013; Xu et al., 2007). Due to its biocompatibility (Cattaneo et al., 2013; Maitz et al., 2017), biodegradability as well as its minimal adverse effects, the FDA has approved silk usage in humans for load bearing applications (Philipp Seib, 2017; Seib and Kaplan, 2013).

Bombyx mori produces two silk proteins; a central core of fibroin presenting 70% of the silk-fiber weight and an outer coating of sericin presenting the remaining 30% of the mass. Fibroins are mainly comprised of large hydrophobic domains, a core domain of β-sheets and β-spirals, spaced by terminal hydrophilic domains that facilitate self-assembly during the spinning process. Sericin is the gummy substance that holds the fibroin filaments together. Meanwhile, spider silk protein consists mainly of spidroins which are large proteins of 250-350 kDa. They are tandem repeats of 30 to 40 amino acids (Andersson et al., 2016). More insights into the molecular structure of different silk proteins can be found in the studies of Pallini and Lefèvre *et al* (Lefèvre et al., 2007; Pallini, 2009). Due to its versatility, silk proteins can be processed in diverse biopolymer architectures such as hydrogels, nanoparticles, silk films, and nanofibers (Fig. 8) (Chen et al., 2017; Jastrzebska et al., 2015; Kim et al., 2004; Min et al., 2018; Philipp Seib, 2017).

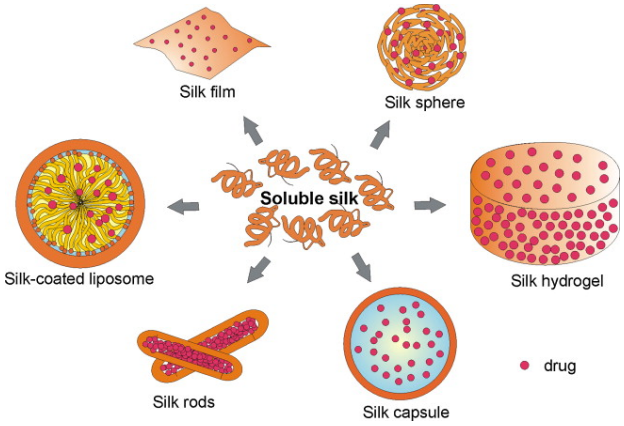

Figure 8. Variety of architectures formed by silk proteins at the nano level (Jastrzebska et al., 2015). Reprinted from Reports of Practical Oncology & Radiotherapy, Vol 20 (2), K. Jastrzebska *et al.*, Silk as an innovative biomaterial for cancer therapy, 87-98. © 2014, with permission from Elsevier.

Silk nanoparticles confer stability on small molecules and protein drugs as well as reduce payload mobility (Pritchard et al., 2012). Therefore, silk is considered as an excellent drug nanocarrier. Several methods have been employed to form silk nanoparticles with different particle size ; (1) polyvinyl alcohol blends (particle size range 300nm to 10, (2) emulsification (particle size range 170 nm), (3) spray-drying (5-µm particles), (4) salting out (particle size range 1 to 2 µm), (5) capillary microdot printing (particle size range 25 to 140 nm), or (6) organic solvents such as methanol (particle size range 35 to 170 nm) (Zhao et al., 2015). Silk-like nanoparticles can be designed either as (1) native nanoparticles where the protein molecules conjugate with each other triggering self-assembly into nanoparticles, or (2) other polymers can be introduced to the silk protein to confer new characteristics such as enhanced colloidal stability, avoiding the immune system, and increasing the circulation time in the blood (Table 4).

On account of the difficulty to produce recombinant spider silk, most studies were focused on silk nanoparticles from silk proteins of *Bombyx mori* (Mottaghitalab et al., 2015). The emphasis of these studies was to adjust the parameters to control nanoparticle generation; hence only few studies have been performed to test the *in vivo* behavior of the silk nanoparticles.

3.2.1 Silk fibroin-like nanoparticles

Since silk fibroin (SF) constitutes the biggest protein of *Bombyx mori,* it has been studied intensively for delivery of therapeutics for different diseases such as cancer and inflammatory diseases. Li *et al.* produced nanoparticles from natural silk fibroin as binary drug delivery system (H. Li et al., 2016). To form nanoparticles, the SF protein molecules conjugated together triggering self-assembly. The resulting nanoparticles, examined by DLS, had a hydrodynamic diameter of 217 ± 0.4 nm. The nanoparticles were loaded with curcumin and fluorouracil 5-FU to investigate their efficacy as binary-drug-loaded nanoparticles in cancer treatment. Cancer cells *in vitro* underwent more than 90% apoptosis two days after incubation with the drug-loaded nanoparticles. *In vivo*, tumor-loaded mice exhibited suppression in tumor size 5 days after injection with binary drug-loaded SF nanoparticles. In addition, the nanoparticles-treated mice showed longer survival rate compared to control groups. SF nanoparticles enhanced cellular uptake of curcumin and 5-FU *in vitro* and *in vivo.*

To enhance the performance of the silk nanoparticles, polyethylene glycol (PEG) was introduced to silk nanoparticles. It assisted the nanoparticles to evade the phagocytic system (MPS) (also known as the reticuloendothelial system, RES) (Wongpinyochit et al., 2015). Totten *et al.* developed PEGylated silk spherical nanoparticles using nanoprecipitation. The PEGylated nanoparticles were of a size 116 nm and polydispersity 0.12 with a net negative charge in water. Surface modification with PEG shielded the PEGylated surface charge to be −46.71 ± 2.59 mV. Both non-modified and PEGylated silk nanoparticles exhibited stability (shelf life) in water, but the former tended to aggregate in phosphate buffer compared to the PEGylated silk nanoparticles that retained their size. Moreover, PEGylated nanoparticles demonstrated enhanced biocompatibility when tested for macrophage response as they didn't induce an increase in tumor necrosis factor alpha (TNF-α) levels compared to the native silk nanoparticles that were associated with significant amounts of TNF-α release. Both types of silk particles were compared in a single and combined therapy with drugs doxorubicin and propranolol. The PEGylated NPs exhibited higher propranolol loading than the non-modified nanoparticles, they also showed excellent doxorubicin loading and release capacity as well as greater *in vitro* antitumor efficacy than freely diffusible controls at the equivalent doxorubicin concentration. Recently, the same group used a similar strategy to investigate the response of silk and PEGylated silk nanoparticles *in vitro* toward lysosomal conditions (Totten et al., 2017). In this study, homogenous spherical nanoparticles of size 105 nm were produced. When the human breast cancer cell line MCF-7 was treated with doxorubicin conjugated nanoparticles in presence of papain to mimic the enzymatic activity of the lysosomes, the PEGylated NPs demonstrated four-fold higher cumulative pH-dependent drug release than the native silk nanoparticles. Upon inhibiting the lysosomal proteolytic and pH induced activity using combination treatments with leupeptin and NH_4Cl, respectively, the doxorubicin nuclear localization was reduced by 42% and 33% for non-modified and PEGylated silk nanoparticles respectively. This confirmed that doxorubicin release from silk nanoparticles is both enzymatic and pH-dependent.

Surface decoration with polyvinyl alcohol (PVA) has also been studied. PVA is an FDA-approved non-toxic water-soluble polymer. Cao *et al.* blended the synthetic PVA with naturally generated SF and used coaxial electrospraying to form nanospheres where PVA formed an inner core surrounded by SF layers (Cao et al., 2017). The anti-cancer drug doxorubicin was incorporated in the PVA core to examine the efficiency of the PVA/SF particles as pH-dependent drug carriers *in vitro* and *in vivo*. Varying PVA ratios (0.1, 0.3, and 0.5 wt%) were used to investigate the effect of the polymer concentrations. Increasing the polymer concentration led to size diameter increase from 984 nm to 1270 nm. TEM and SEM confirmed the spherical structure of the nanoparticles where PVA was placed in the core. Although the higher PVA concentration encapsulated more doxorubicin, this high PVA concentration decreased the initial drug release compared to lower PVA concentrations (Fig. 9). This may be due to the molecular network interactions between doxorubicin and PVA molecules as well as to the fact that residual PVA polymer formed a hydrogel layer on the surface which slowed down the drug release. Therefore, ultrasound (US) was used to solve this problem as US promotes water permeation into the polymer, dissolving the hydrophilic PVA and enhancing the drug release. Doxorubicin encapsulated PVA/SF NPs showed increased drug release when the pH dropped to 5.0. Exposure of MDA-MB-231 cells to the PVA/SF NPs showed no cytotoxicity suggesting that the PVA/SF NPs are biocompatible. When the nanoparticles were tested for apoptosis, the particles composed of a lower PVA concentration had higher apoptotic activity. US significantly enhanced cell apoptosis, as it promoted cell permeability and cell uptake. The doxorubicin conjugated PVA/SF NPs were tested on BALB/c nude mice xenografted with MDA-MB-231 cells. US was found to improve drug accumulation in the tumor tissue. Moreover, US-stimulated NPs showed longer cumulative survival and were more effective in decreasing tumor size compared to the control groups.

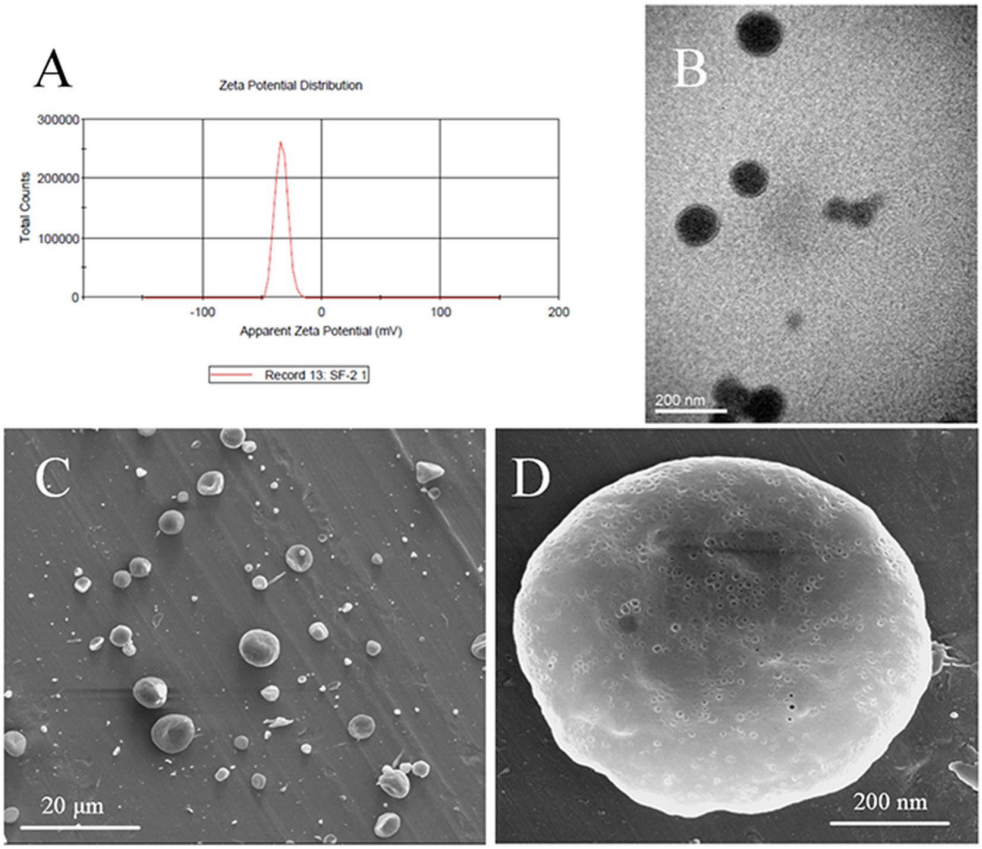

Figure 9. Physicochemical characteristics of PVA/SF nanoparticles: (A) Zeta potential distribution; (B) TEM image of nanoparticles; (C,D) SEM images of the nanoparticles. Reprinted with permission from Springer Nature, Drug release from core-shell PVA/silk fibroin nanoparticles fabricated by one-step electrospraying, Y. Cao et al. © 2017 (doi:10.1038/s41598-017-12351-1).

Similar results were obtained by Kaplan's group who successfully made pH-dependent doxorubicin (DOX) conjugated silk nanoparticles following an organic solvent precipitation strategy (Seib et al., 2013). Acetone precipitation of silk resulted in uniform 98 nm diameter nanoparticles with overall negative charge, -33.6 mV. The generated nanoparticles were able to overcome drug resistance when they were tested against doxorubicin-resistant human breast cancer cells, MCF-7/DOX, by changing the cellular uptake mechanism. Live cell confocal microscopy confirmed accumulation of the nanoparticles in the lysosomes. These observations indicated that silk nanoparticles serve as a lysosomotropic drug delivery platform. Paclitaxel silk fibroin nanoparticles (PTX-SF-NPs) were produced and tested *in vitro* and *in vivo* (P. Wu et al., 2013). With Fourier transform infrared (FTIR) spectroscopy and X-ray diffraction (XRD), it was found that the drug paclitaxel served as the hydrophobic core of the NPs and coassembled with the hydrophobic domain of the SF during self-assembly in aqueous solution. The drug release *in vitro* reached 47% after 100 h. Gastric cancer cells, SGC-7901 and BCG-823 showed cell viability of respectively 76 % and 80% after exposure to PTX-SF-NPs for 48 h. The nanoparticles induced 65.6% apoptosis in the BCG-823 cells as evidenced by their change in morphology compared to the control when examined by inverted microscopy. *In vivo*, human gastric cancer nude mice xenografts were injected by intraperitoneal injection (IP) with drug-loaded NPs. PTX-SF-NPs showed significantly slower tumor growth compared to the PTX control after 14 days treatment. PTX-SF-NPs served effectively as drug carrier for locoregional chemotherapy offering *in vivo* biocompatibility.

In vivo applications of silk nanoparticles are not confined to cancer, Rodriguez-Nogales *et al.* reported the efficacy of SNPs in gastrointestinal tract inflammatory bowel disease (IBD) (Rodriguez-Nogales et al., 2016). Nanoprecipitation in methanol was used to fabricate globular granular silk fibroin nanoparticles ranging in size from 60 to 100 nm as characterized by DLS and orange II spectrophotometric assay. The nanoparticles' surface was functionalized by the RGD peptide (Gly-Arg-Gly-Asp-Ser), which has great affinity to integrins, cell surface proteins that are involved in the pathogenesis of IBD (Smith and Mohammad, 2014). When the nanoparticles were tested on a model of rat colitis, both bare and RGD-functionalized silk fibroin nanoparticles exhibited an anti-inflammatory effect as they significantly decreased the extension of the colon damage compared to

control groups. These results were confirmed by a histological evaluation of the colon section. The same results were obtained by Lozano-Pérez *et al.* who investigated the intestinal anti-inflammatory properties of resveratrol-loaded silk fibroin nanoparticles (Lozano-Pérez et al., 2014). Reveratrol-loaded NPs showed controlled and prolonged drug release up to 80 days. Such results open the door for more investigations to study the biological applications of silk nanoparticles other than being inert carriers.

3.2.2 Silk sericin-like nanoparticles

Recently, Hu *et al.* fabricated silk-sericin-based nanoparticles (SSC@NPS) via a two-step cross-linking approach, in which negatively charged silk sericin was complexed with positively charged chitosan, followed by EDC cross-linking for stabilization (Hu et al., 2017). This procedure resulted in monodisperse spherical nanoparticles that had the ability to undergo surface charge conversion from −11.2 mV to +15.7 mV upon reducing the pH, a characteristic that enhanced the cellular uptake of the nanoparticles in the tumor intercellular acidic microenvironment. The SSC@NPs loaded and successfully delivered the anticancer drug doxorubicin to the nucleus of HeLa cells in low pH culture medium. The SSC@NPs were loaded with doxorubicin and successfully delivered to HeLa cells. The DOX-SSC@NPs followed a ph-dependent drug release to the nucleus.

In a follow up study (Hu et al., 2018), it was found that these water-soluble SSC@NPs exhibited two outstanding properties; (1) they could act as a dispersion stabilizer maintaining their colloidal stability in blood serum, and (2) they preserve their integrity during cryopreservation. Upon intravenous injection of doxorubicin loaded nanoparticles (DOX-SSC@NPs) in HepG2 tumor-bearing mice, the drug retention in the heart decreased compared to free-drug treatment. Moreover, the SSC@NPs showed blood compatibility while decreasing the hemolysis associated with free drug.

This is in accordance with the results obtained by Guo *et al.* where a ring-opening polymerization strategy was used to produce micellar nanoparticles with a silk sericin backbone and sidechains of poly(γ-benzyl-L-glutamate), PBLG (W. Guo et al., 2018). The Sericin-PBLG micelles had a size of about 100 nm which increased to 110 nm after of loading of doxorubicin (DOX). The hydrophobic DOX was used to facilitate a pH-triggered release mechanism. In vitro, 50% of the DOX was released into the media throughout 72 hrs at pH 4.5. The DOX-Sericin-PBLG micelles harbored a negative charge of −25 mV that allowed a prolonged circulation time of the nanoparticles. *In vivo*, DOX-Sericin-PBLG nanoparticles suppressed tumor growth by 70% compared to 30% for free DOX.

3.2.3 Silk-elastin-like nanoparticles

Integrating the high strength mechanical properties of silk blocks with other protein polymers has been used to construct smart materials with a wide range of physical and biological properties, such as in thermosensitive, pH-dependent hydrogels (Nagarsekar et al., 2003; Qiu et al., 2009). In particular, the recombinant production of silk-elastin-like polypeptides (SELPs) has been intensively explored (Collins et al., 2013). The beta sheets of the silk blocks provide thermal and chemical stability as well as cross-linking sites for the SELP system, whereas elastin-like polypeptides display stimuli-sensitivity (Anderson et al., 1994). SELP nanoparticles can be fabricated *via* different approaches including directed self-assembly of block copolymers and triggered self-assembly using gold nanoparticles or hydrophobic drugs. The formation of SELP nanoparticles depends on the hydrophobicity difference between the silk and elastin blocks, the ratio between these two blocks as well as the hydrogen bonding between silk domains (W. Huang et al., 2015).

Kaplan's group genetically engineered three SELPs with varying silk to elastin ratios named SE8Y, S2E8Y, and S4E8Y. They found out that the higher the silk to elastin ratio the more uniform particles were formed as detected by SEM and DLS. The formed SELPs behaved differently upon heating, various nanostructures including nanoparticles, hydrogels, or nanofibers were triggered either reversibly or irreversibly. The hydrophobic drug doxorubicin was also used to trigger-self-assembly. Using the same SELP constructs as mentioned above, doxorubicin was used as hydrophobic core to form micellar-like nanoparticles upon thermal triggering. When these nanoparticles were tested on HeLa cells, no toxicity was observed. The DOX-SE8Y particles (R_h 50 ± 10 nm) showed higher drug loading and better cell uptake. Long exposure of these nanoparticles with HeLa cells led to doxorubicin diffusion into the nuclei (Xia et al., 2014). Lin *et al.* fabricated and characterized gold/SELP core/shell nanoparticles. Below the transition temperature the size of the nanoparticles was about 30 nm with the Au core surrounded by a uniform silk-elastin shell. Heating above the transition temperature led to aggregation in larger particles. Particle characterization using DLS and TEM

confirmed that the elastin blocks triggered the thermal response of the Au-SELPs NPs while the silk β-sheet structure served to stabilize the packed aggregates (Lin et al., 2014).

Despite the interesting and promising properties of SELPs as drug carriers, there is no *in vivo* data published yet. More studies are to be done to show the full potential of these protein-based nanoparticle structures.

Table 4. Characteristics and applications of nanocarriers based on silk proteins.

Components	Size of NPs	Morphology / Zeta potential	Application	Targeting / active compound	Method of application / Main findings	Synthesis / Preparation	Reference
PEGylated Silk	116.40 ± 3.23 nm	Spherical / -47± 3 mV in pH7	Cancer	Doxorubicin and propranolol (single and combined)	PEG enhanced the biocompatibility and reduced macrophage response compared to native NPS	Organic precipitation	(Wongpinyochit et al., 2015)
PEGylated Silk	105.30nm	Spherical / -37 mV[#]	Cancer	Doxorubicin	PEGylation increased the drug release >4 fold than native NP. Drug release relevant to lysosomal pH and enzymatic activity	Organic precipitation	(Totten et al., 2017)
PVA-Silk	984 - 1270 nm	Nanospheres / -34 mV[#]	Cancer	Doxorubicin	Ultrasound was used to enhance and control the drug release *in vitro*	Electrospraying	(Cao et al., 2017)
DOX-silk	98 nm	Nanospheres/ -34 ± 6 mV[#]	Cancer	Doxorubicin	Low toxicity *in vitro* suitable for lysomotropic delivery system	Organic solvent precipitation	(Seib et al., 2013)
Paclitaxel-silk fibroin	158-206 nm according to the solvent	Spherical/ -7 to -21 mV acc. to solvent	Cancer	Paclitaxel	Significant anti-tumor efficacy and *in vivo* biocompatibility	Organic solvent precipitation	(P. Wu et al., 2013)
RGD-SF	60-100 nm	Globular granules -7.5 to -33 mV in pH4.3 to 7.4	Inflammatory bowel disease	Silk fibroin	Silk fibroin showed anti-inflammatory effect	Organic precipitation	(Rodriguez-Nogales et al., 2016)
Resveratrol-loaded SF nanoparticles (RL-FNPs)	68 nm	Aggregates	Inflammatory bowel disease	Resveratrol	Efficient immunomodulatory properties	Organic precipitation	(Lozano-Pérez et al., 2014)
DOX-Silk sericin-Chiston	231 ± 7.3 nm	Spherical / -6.25±1.2 in pH7.4	Cancer	Doxorubicin	The nanoparticles can act as drug carrier, dispersion stabilizer and cryoprotectant	Cross-linking	(Hu et al., 2018, 2017)
Sericin-PBLG-DOX	110 nm	Micelles/ −15 to −25 mV[#]	Cancer	Doxorubicin	Restore the response of DOX-resistant cells	Ring-opening polymerization (ROP)	(W. Guo et al., 2018)

pH of the zeta potential measurements unknown

3.3 Capsules designed from native self-assembly structures: Virus-like particles

Viruses, in the arms race with the (human) immune system, have developed intricate ways to both avoid recognition as foreign species as well as pathways to infiltrate target cells and proliferate within. Virus-like particles (VLPs) lack the genetic information and hence the ability to proliferate but still have many of their other features intact to enter cells effectively. Especially in vaccination studies, VLPs are used extensively to ensure antigen uptake and – processing, sometimes working as an adjuvant themselves or in combination with additional ones (Cimica and Galarza, 2017; Lua et al., 2014). Here we give some examples of different types of modified virus-like particles that were studied *in vivo* (Table 5).

Spohn *et al.* coupled an inactivated form of the interleukin-1β (IL-1β) to Qβ, an icosahedral VLP with a diameter of 25 nm, *via* maleimide-thiol chemistry (Spohn et al., 2014). IL-1β is an inflammatory cytokine that is produced by β-cells at high glucose concentration, leading to β-cell death and impaired insulin production. Immunization of mice with this VLP resulted in the stimulation of T-helper cells and transient production of IgGs against IL-1β. This led to increased insulin production in the murine diet-induced model of diabetes.

An antigen against *Malaria tertiana* induced by *Plasmodium vivax,* the thrombospondin-related adhesive protein (TRAP), was coupled *via* maleimide-thiol chemistry to the cucumber mosaic virus fused to a universal T-cell epitope of the tetanus toxin (Cabral-Miranda et al., 2017). The resulting VLP was mixed with microcrystalline tyrosine (MCT), acting as an adjuvant, before administration. In mice, the VLP combined with MCT yielded the highest titre of IgGs and $CD8^+$ cytotoxic T cell activation, indicated by IFN-γ and TNF-α levels. While delaying the development of malaria when challenging immunized mice with *P. vivax* significantly, no vaccination was achieved.

Zochowska *et al.* used the adenovirus dodecahedron (Dd) to target hepatocellular carcinoma (HCC) (Zochowska et al., 2015). They coupled cap analogues, nucleoside polyphosphate derivatives, and/or doxorubicin to the amino groups of lysine side chains of the virus-like particle (Dd-cap and Dd-dox, respectively). The average loading was 100 molecules of cap analogues and 60 molecules of Dox per virus particle, respectively. In an orthotopic rat model of HCC, the combined treatment of Dd-cap and Dd-dox resulted in a significant tumor growth inhibition of 40% compared to the control.

Hutzler *et al.* displayed claudin-6, a transmembrane protein acting as an antigen to induce immunological responses towards various kinds of cancers, on VLPs composed of the structural proteins of measles virus (MV) by recombinant DNA technology (Hutzler et al., 2017). The resulting VLPs had radii of about 40 nm when analyzed with electron microscopy. In syngeneic $IFNAR^{-/-}$-CD46Ge mice challenged with tumor cells forming lung metastasis, immunization with antigen presenting VLPs significantly reduced or prevented tumor metastasis and reduced tumor growth.

So far, VLPs have been mostly used for immunotherapy and vaccination as reviewed elsewhere (Anzaghe et al., 2018; Ma et al., 2012; Shirbaghaee and Bolhassani, 2016).

Table 5. Characteristics and applications of nanocarriers based on virus-like particles.

Virus	Radius of NPs	Morphology	Application	Targeting / active compound	Method of application / Main findings	Synthesis / Preparation	Reference
Qβ virus-like particles	-	Proteinaceous vesicle	Vaccination	Inactivated form of IL-1β	Stimulation of T-helper cell, IgG production against IL-1β in mouse model	Chemical conjugation	(Spohn et al., 2014)
CMV virus-like particles	-	Proteinaceous vesicle	Vaccination	TRAP protein, epitope of tetanus toxin	Significant delay of malaria development in mice when co-formulated with MCT in mouse models.	Chemical conjugation, recombinant fusion protein, co-formulation with MCT	(Cabral-Miranda et al., 2017)
Adenovirus dodecahedron virus-like particles	-	Proteinaceous vesicle	Cancer	Nucleoside polyphosphate derivatives, doxorubicin	Significant growth inhibition in a HCC rat model	Chemical conjugation	(Zochowska et al., 2015)
Measles Virus gag virus-like particle	40 nm	Proteinaceous vesicle	Vaccination/Cancer	Claudin-6	Immunization significantly reduced tumour growth and metastasis	Recombinant fusion protein	(Hutzler et al., 2017)

4. Polypeptide-based nanoparticles

In the previous chapters, the building blocks were either proteins derived from natural sources or polypeptides produced *via* protein engineering techniques. Other methods to produce polypeptides include microbial synthesis (van Hest and Tirrell, 2001), solid phase peptide synthesis (SPPS) (Merrifield, 1963), or ring opening polymerization (ROP) of activated amino acid monomers such as *N*-carboxyanhydrides (NCAs) (Hadjichristidis et al., 2009). The two first methods enable producing sequence-controlled and unimolecular polypeptides, while ROP of NCAs is an attractive alternative to produce polypeptides in larger scale with a chemical diversity beyond canonical amino acid residues. This technique has been widely explored for the design of amphiphilic block copolymers using primary amines as initiator, the polymerization being well controlled and leading to polymers and copolymers with good control over molecular weight and distribution (Carlsen and Lecommandoux, 2009; Deng et al., 2014; Huang and Heise, 2013; Song et al., 2017). Polypeptide blocks exhibit versatile properties, with well-defined block sizes and functionalities, unique ability to stabilize specific secondary structures (such as α-helix, β-sheet, β-turn, etc.) and most of them have biomimicry, biocompatibility and also biodegradability features (He et al., 2012; Rodríguez-Hernández and Lecommandoux, 2005). Polypeptide-based nanomedicines have been engineered from different building blocks, mainly using poly(L-glutamic acid) (PGlu), poly(α,β aspartic acid) PAsp or poly(L-lysine) PLys as hydrophilic segments and poly(γ-benzyl,*L*-glutamate) PBLG as the hydrophobic one, with different shape and structure, ranging from spherical micelles, vesicles or gels. Polypeptide segments have been often conjugated to other synthetic or biological blocks, mainly PEG, for its stealth behavior. These particles have been used as nanocarriers for therapeutic agents, including hydrophobic anticancer drugs and hydrophilic biomolecules (DNA, siRNA, peptide, proteins). As the literature is very abundant and the research very active in this area, we will highlight here only what we believe are the most promising examples of such polypeptide-based nanostructures, focusing on the ones that include *in vivo* studies.

4.1 Poly(*L*-glutamate) and poly(aspartate)-based polypeptide nanocarriers

Poly(*L*-glutamic acid)-based micelles have been used as promising carriers for delivery of cisplatin and platinum for treatment of various cancer types. As a typical example, an active complex of oxaliplatin (1,2-diaminocyclohexane) platinum(II) (DACHP) with a strong therapeutic activity as evaluated in phase I clinical studies, was successfully loaded by metal complexation through the carboxyl side chains of PGlu. Loading of DACHP in polymeric micelles led to enhanced delivery of the oxaliplatin complex to cancer cells with a reduced systemic toxicity (Cabral and Kataoka, 2014). All the platinum-based drug loaded nanocarriers that have been developed are summarized in Table 6.

In the very comprehensive and elegant work of Kataoka *et al*., the efficiency of PEG-*b*-PGlu based micelles as drug delivery vehicles was effectively evaluated in various cancer models such as pancreatic cancer, glioblastoma, orthotopic and lung metastasis models of melanoma, an orthotopic scirrhous gastric cancer model and peritoneal metastasis. In a recent example, the same group prepared antibody fragment-connected polymeric micelles by one-to-one tailored conjugation of anti-tissue factor (TF) antibody (anti-TF Fab') and DACHPt/m (micelle loaded with DACHP) *via* maleimide-thiol chemistry (Fig. 10) (Ahn et al., 2015). Anti-TF Fab' was used to target TF overexpressed on the surface of cancer cells, such as human pancreatic, colorectal, breast and lung cancers. The so-called immunomicelles, with sizes around 31 nm, suppressed the growth of tumors for approximately 40 days ($p < 0.01$). Co-injection of non-conjugated anti- TF Fab' and Mal-DACHPt/m was also investigated and lower antitumor activity was observed compared to anti-TF Fab'-DACHPt/m ($p < 0.01$) which confirmed that conjugation to polymeric micelles can be an effective strategy for enhancing drug delivery (Ahn et al., 2015).

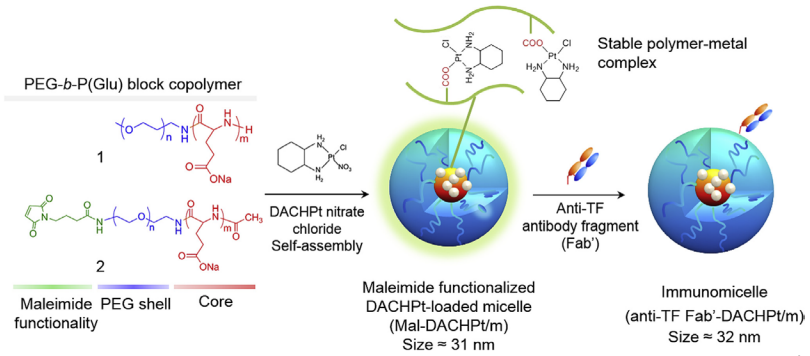

Figure 10. Schematic illustration of the preparation of anti-TF Fab' fragment-installed DACHPt/m (Ahn et al., 2015). Reprinted from Biomaterials, Vol 39, J. Ahn, Antibody fragment-conjugated polymeric micelles incorporating platinum drugs for targeted therapy of pancreatic cancer, 23-30. © 2014 with permission from Elsevier.

PEG-*b*-PGlu nanoparticles with two different sizes (20 and 70 nm) and loaded with 1,2-diaminocyclohexane-platinum(II) (DACHPt) were further evaluated by using intravital confocal laser scanning microscopy (IVCLSM) to demonstrate permeability of tumor blood vessels caused by dynamic vents (vigorously outward flowing fluids called eruptions). Human pancreatic cancer-derived BxPC3 mice and human glioblastoma-derived U87MG bearing mice were used for eruption identification up to 10 hr. General outcome of this study is that whereas smaller nanoparticles can enter tumor tissue *via* both eruption and static permeability, larger nanoparticles mostly depend on eruption. This study highlights how the EPR effect gives drug carriers access to the tumor extravascular space, which is then followed by release of the small molecule therapeutics to diffuse throughout the tumor tissue (Matsumoto et al., 2016). The size effect of such nanoparticles was also investigated in other contributions from the same group (with diameters of 30, 50, 70 and 100 nm) for a comparison study regarding accumulation and effectiveness of long-circulating nanoparticles. This study revealed that in highly permeable hypervascular tumors, sub-100 nm micellar nanoparticles could penetrate with no size-dependent restrictions. In previous studies of Kano *et al.*, a transforming growth factor (TGF)-β inhibitor with low doses was used to decrease the pericyte coverage of the endothelium in the neovasculature of pancreatic tumors by accumulation (Kano et al., 2007). By employing a TGF-β signaling inhibitor, permeability of hypovascular tumors was increased and this improved the accumulation of nanoparticles which are bigger than 70 nm (Cabral et al., 2011).

Another interesting work conducted by the group of Kataoka studied the effect of stereoisomerism of polypeptides on micellar formulations. Polypeptides have the tendency to adopt secondary structures upon self-assembly which directly affects their biological behavior. For this reason, polypeptide-based micelles composed of PEG-*b*-poly(Glu) with different glutamic acid stereoisomers, namely either *L* or *D*, or the *D,L* racemic mixture were developed. These micelles were used for the delivery of cisplatin (CDDP/m) to pancreatic cancer cells. The *in-vitro* release profiles of L- and D-CDDP/m showed similar release kinetics in a sustained manner but the D,L-CDDP/m showed relatively accelerated and faster release than the other micelles after 10 h. Biodistribution and antitumor efficacy of these micelles with a size ≈24 nm (confirmed by TEM) on mice bearing subcutaneous BxPC3 tumors were evaluated. This study demonstrated that accelerated release of *D,L*-CDDP/m was observed causing less antitumor efficacy compared to D or L configuration CDDP loaded micelles. The α-helix core bundled assembly seem therefore to be an important parameter since it leads to extended bioavailability while avoiding nonspecific biodistribution, and increased accumulation and efficacy against tumors (Mochida et al., 2014).

Head and neck tumors, which are treated by cis-platinum based drugs, could recur due to presence of drug-resistant, cancer stem cell (CSC) niches. PEG-*b*-PGlu micelles incorporating cisplatin (CDDP/m) were used to inhibit the growth of a CD44v-rich head and neck cancer. CD44v is a variant form of CD44 that induces metastasis and resists therapies. Tumor growth was reduced and the population of cancer stem cells was efficiently suppressed by the cisplatin containing micelles in HSC2 tumor tissue, as was shown by immunohistochemistry. This result was explained by the micelle-mediated delivery of cisplatin to the cell nucleus and high cellular expression of glutathione leading to successful delivery of Pt to nuclear DNA (Wang et al., 2016).

PEG-*b*-PGlu copolymers were also reported as MRI contrast agents for imaging tumors in response to pH (Fig. 11). Mn^{2+} was confined within pH-sensitive calcium phosphate (CaP) aggregates, which were stabilized by PEG-*b*-PGlu copolymers (PEGMnCaP) to yield particles of around 60 nm. In solid tumors Mn^{2+} was released due to disintegration of CaP because of the low pH, and subsequent binding to proteins led to its increased

relaxivity, allowing the identification of hypoxic regions within tumor mass and also enabling to detect invisible millimetre-sized metastatic tumors in the liver. PEGMnCaP nanoparticles were compared with the clinically approved contrast agent gadopentetate dimeglumine (Gd-DTPA) and PEGylated Mn_2O_3 nanoparticles ($PEGMn_2O_3$). Results indicated that only PEGMnCaP showed enhanced tumor contrast when measured with T^1-weighted MRI at 1 T magnetic field. This comparison study revealed the importance of pH triggered release of Mn^{2+} ions for enhancing tumor probing. The PEGMnCaP nanoparticles served as promising contrast agents without any limitation in tissue penetration, enhancing MRI contrast. The MRI results had a higher spatial resolution, implying that the ionizing radiation of positron emission tomography (PET) may therefore be avoided (Mi et al., 2016).

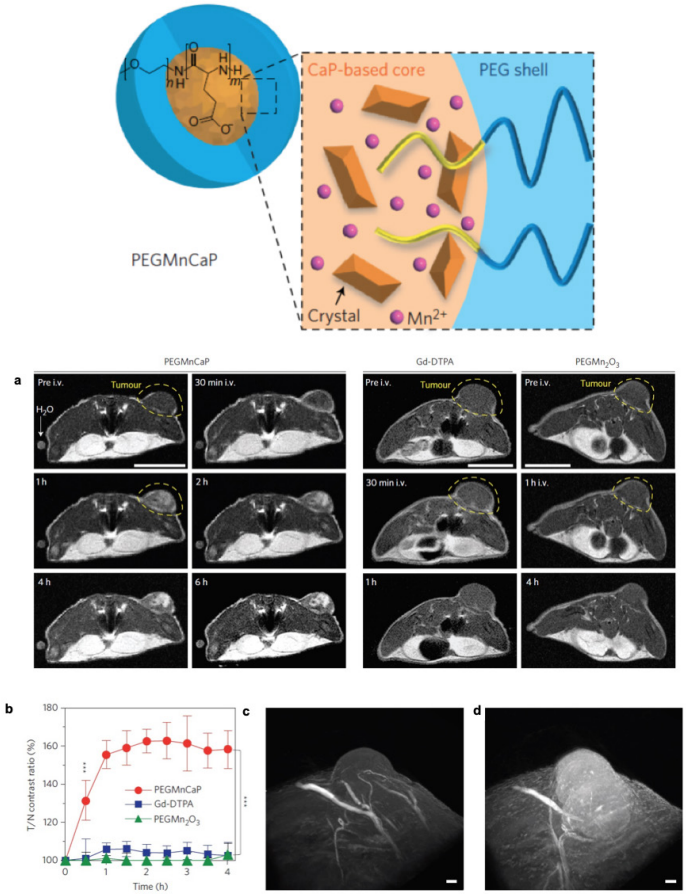

Figure 11. Top: PEGMnCaP (CaP based core and PEG shell, in the core poly(glutamic acid) blocks control the growth of the core by inhibiting the mineralization of large CaP blocks), could specifically enhance the contrast of solid tumors for cancer diagnosis. Bottom: **a**, In vivo MR images of subcutaneous C26 tumor-bearing mice pre- and post-intravenous injection of PEGMnCaP (left), Gd-DTPA (center) and $PEGMn_2O_3$ (right) measured with 1 T MRI. Only PEGMnCaP showed a selective and high enhancement of tumor contrast. Scale bar, 1 cm. **b**, A comparison of the T/N contrast ratio after administration of PEGMnCaP (number of mice, n = 7), Gd-DTPA (n = 5) and $PEGMn_2O_3$ (n = 3). Data are shown as mean ± s.d., ***P < 0.001, unpaired Student's t-test. **c,d**, 3D MRI of C26 tumors before **(c)** and 1 h after **(d)** the intravenous injection of PEGMnCaP measured with 7 T MRI. After the administration of PEGMnCaP, the contrast of the entire tumor tissue was enhanced with no contrast enhancement in the surrounding normal tissues, demonstrating that there is a broad distribution of Mn^{2+} ions in the tumors, as the relaxivity enhancement from protein binding is reduced in the 7 T magnetic field (Mi et al., 2016). Scale bars, 50 µm. Adapted with permission from Springer Nature: Nature, Nature Nanotechnology, Vol 11, A pH-activatable nanoparticle with signal- amplification capabilities for non-invasive imaging of tumour malignancy, P. Mi et al. © 2016.

In recent work by the group of Kataoka, PEG-*b*-PGlu was conjugated to boron clusters for effective boron neutron capture therapy of solid tumors. High amounts of ^{10}B compounds (sodium boracaptate) were conjugated to thiolated poly(ethylene glycol)-*b*-poly(L-glutamic acid) PEG-*b*-PGlu to deliver this isotope in to deep tumor regions. Boron cluster conjugated particles were intravenously injected and irradiated by a

thermal neutron beam after 24 h injection; after 20 days of irradiation, a 20-fold decrease in tumor volume was observed compared to control groups (Mi et al., 2017).

In another example, micelles based on poly(*L*-glutamic acid) *grafted* with PEG (PGlu-*g*-PEG) copolymers were also reported for delivery of Pt(II) to different *in vivo* cancer models, such as MCF-7 bearing mice, melanoma (B16F1) and non-small cell lung cancer (Shi et al., 2015; Yu et al., 2016, 2015). These polymeric micelles are more flexible drug carriers in terms of controlling PEG density of micelles compared to PEG-*b*-PGlu. Different aspects in terms of molecular weight of PGlu, weight ratio of PEG to PGlu, chain length of PEG and loading content of CDDP were found to have a significant influence on the plasma pharmacokinetics. Polymeric micelles prepared from $PGlu_{160}$-*g*-PEG_{5K} purified by ultrafiltration showed a sustained release profile up to 336 h, therefore this system was chosen for further *in-vivo* studies. These nanoparticles allowed for 46-fold higher platinum plasma levels in LLC tumor-bearing mice than those of mice receiving equivalent doses of free CDDP. These types of nanoparticles, prepared by ultrafiltration, showed highly promising results for inhibiting C26 tumors with safety and high tolerance *in vivo* (Yu et al., 2015).

In another study, grafted polymers were prepared for the design of nanoparticles for targeted delivery applications. An amphiphilic PGlu-*g*-α-tocopherol /PEG graft copolymer was designed for co-loading of docetaxel (DTX) and cisplatin (CDDP) by hydrophobic interactions and chelation. α-Tocopherol and PEG were grafted to the poly(*L*-glutamic acid) main-chain. The resulting polymeric micelles were decorated with the $\alpha_v\beta_3$ integrin targeting peptide *cyclo*(RGDfK) for efficient receptor mediated endocytosis and multi drug delivery. DTX and CDDP were loaded by the nanoprecipitation method and micelles were obtained with a size around 28 nm and a surface potential of -8 mV. *In vivo* anti-tumor and anti-metastasis efficacy of both targeted and undecorated dual loaded polymeric micelles were studied. After 10 days of injection to B16F10 bearing cells, anti-metastasis efficiency of dual drug loaded and targeted polymeric micelles was demonstrated by the strong inhibition on melanoma metastasis to the lungs (Song et al., 2014).

In another example, poly(amido amine) dendrimers (PAMAM) have been used as multifunctional initiator for ROP of NCAs to yield linear-dendritic block copolymers with one, two, four, and eight PGA arms for doxorubicin hydrochloride (DOX) delivery. Detailed *in vivo* studies revealed that linear and Y-shaped PEG-*b*-PAMAM-*b*-PGA block copolymers have higher anti-tumor efficacy and are less toxic than the other linear dendritic copolymers based DOX formulations (Yu Zhang et al., 2016). The same group prepared nanoparticles using an amphiphilic poly(ethylene glycol)-*b*-poly(*L*-glutamic acid)-*b*-poly(*L*-lysine) triblock copolymer decorated with deoxycholate (PEG-*b*-PLG-*b*-PLys-DOCA). The particles were additionally loaded with DOX and paclitaxel (PTX) and used for treatment of A549 human lung adenocarcinoma cells. This co-delivery system with different functional antitumor drugs provided clinical potential in cancer therapy (Lv et al., 2014b).

PEG-*b*-PBLG block copolymers were also used for targeted delivery of disrupted aortic aneurysm micro-structure. PBLG is used as the hydrophobic core of micellar structures. As an example, Alexa647-labeled rapamycin loaded nanoparticles of around 106 nm were prepared by nanoprecipitation and injected into an elastase induced rat model of abdominal aortic aneurysm (AAA). Their distribution and therapeutic effect against AAA were evaluated. Rapamycin-loaded nanoparticles specifically accumulated in AAA areas. MMP-2, which is the responsible protease for formation of aortic aneurysm, was suppressed by the injected nanoparticles. The rapamycin nanoparticles suppressed the infiltration of macrophages, activity of MMP-2, and expression of inflammatory cytokines in the AAA wall (Shirasu et al., 2016).

Poly(α,β-aspartic acid) based copolymers are another class for efficient and targeted drug delivery systems which could also be used as potential contrast agents. In early studies of Kataoka *et al*., micellar formulations of PEG-*b*-poly(α,β-aspartic acid) PEG-*b*-PAsp for loading of Adriamycin in the core of the polymeric micelles showed high anti-cancer activity compared to free Adriamycin which is a hydrophobic drug with low aqueous solubility (Yokoyama et al., 1990, 1989). In a further study, the same polymeric system was used as novel magnetic resonance contrast agent for *in vivo* cancer imaging. Electrostatic complexation of iron oxide nanoparticles (β-FeOOH) with PEG-*b*-poly(α,β-aspartic acid) showed better colloidal stability under physiological saline conditions. After intravenous injection into mice, the PEG-*b*-PAsp coated nanoparticles showed higher accumulation up to 3 hr, compared to a commercial magnetic resonance contrast agent (called Feridex®) (Kumagai et al., 2007). PEG-*b*-poly(α,β-aspartic acid) copolymers were also complexed with calcium phosphate and the clinical MRI contrast agent Gd-diethylenetriaminepentaacetic acid (GdDTPA/CaP) to produce nanoparticles. Gadolinium (Gd) chelates have high potential for efficient MRI guided Gd neutron capture therapy of tumors. This study highlighted that the required dose of Gd-DTPA/CaP was much lower than that of Gd-DTPA-based MRI contrast enhancement in clinical uses (Mi et al., 2015). In further work, SPIO nanoparticles, which were coated by PEG-*b*-poly(α,β-aspartic acid), were developed to enhance magnetic resonance imaging in pancreatic cancer cells, with the aid of a conjugated TGF-β (transforming growth factor)

inhibitor. The TGF-β inhibitor was introduced to prevent tumor growth and metastasis. This system was also proven to be successful in an *in vivo* study (Kumagai et al., 2009). Notably, the metal-ion complexations based on PEG-*b*-PAsp had degraded more rapidly than those based on PEG-*b*-PGlu in the bloodstream (Cabral et al., 2018).

The PAsp block may also be used in the development of micellar systems for delivery in cancer. For example, DOX loaded micelles composed of poly(aspartic acid-*g*-imidazole)-*b*-PEG were designed because the conjugation of imidazole rings (pKa = ~7.0) to the carboxyl groups in the PAsp block would lead to enhanced targeting of the acidic pH. The micelles effectively accumulated at the tumor tissue, compared to the healthy one, in an *in vivo* model of breast cancer (Lee et al., 2014). After injection of the DOX-loaded micellar system, passive targeting was achieved and release was facilitated due to the pH responsiveness of the system, which was shown by *in vivo* non-invasive fluorescent images of nude mice with MCF-7.

An overview of PGlu and PAsp-based micellar systems is provided in Table 6. One can note that hydrophobic polypeptide segments such as poly*(L*-phenyl alanine) and p(*D,L* lactide-*co*-glycolic acid) may also be used to increase drug loading, micellar stability and affect particle size (Desale et al., 2013; Li et al., 2013; Lv et al., 2014a, 2013; Xu et al., 2015).

Table 6. Characteristics and applications of micellar structures bearing anionic polypeptides.

Polymer	Radius of NPs	Zeta potential*	Application	Targeting / active compound	Method of application / Main findings	Synthesis / Preparation	Reference
PEG-*b*-P(Glu)	15 - 50 nm	-2 to 0 mV	Cancer	DACHPt, CDDP, (Gd-DTPA), sodium boracaptate (BSH), Doxorubicin	Intravenous injection to various cancer types for treatment	Polymer-metal complexation and self-assembly	(Ahn et al., 2015; Cabral et al., 2011; Cabral and Kataoka, 2014; Kano et al., 2007; Li et al., 2013; Matsumoto et al., 2016; Mi et al., 2017, 2016; Mochida et al., 2014; Wang et al., 2016)
PGlu-*g*-mPEG	18 nm	-8 mV	Cancer	CDDP	Non-small cell lung cancer	Nanoprecipitation	(Shi et al., 2015; Yu et al., 2016, 2015)
PGlu-*g*-Ve-PEG decorated with peptide (*cyclo*(RGDfK)	28 nm	-8 mV	Cancer	CDDP, Docetaxel	Melanoma B26F1 cells	Nanoprecipitation	(Song et al., 2014)
PEG-*b*-PLG-*b*-PLL/DOCA	36 nm	-18 mV	Cancer	Doxorubicin, Paclitaxel	Lung cancer (A549)	Nanoprecipitation	(Lv et al., 2014b)
PEG-*b*-P(Glu-*co*-Phe) and PEG–*b*–PGlu–*b*–PPhe	70 nm	-23 mV	Cancer	Doxorubicin	Lung Cancer (A549)	Nanoprecipitation	(Desale et al., 2013; Li et al., 2013; Lv et al., 2014a, 2013)
(PEG-*b*-PAMAM-*b*-PGA) dendrimers	7 to 50 nm	-35 to -40 mV	Cancer	Doxorubicin	MCF-7 tumor (breast cancer)	Dialysis (solvent displacement)	(Yu Zhang et al., 2016)
PEG-*b*-PLGA-*b*-PGlu	50 nm	-14 mV	Cancer	Doxorubicin	MCF-7 tumor (breast cancer)	Nanoprecipitation	(Xu et al., 2015)
PEG-*b*-poly(α,β-aspartic acid)	20 - 50 nm	-40 to 0 mV depending on pH (6.5 to 8.5)	Cancer	Adriamycin, (GdDTPA/CaP), SPIO, Doxorubicin	Intravenous injection to various cancer types for treatment	Polymer metal complexation and self-assembly	(Kumagai et al., 2009, 2007; Lee et al., 2014; Mi et al., 2015; Yokoyama et al., 1990, 1989)

mPEG-*b*-PBLG	45 nm	-30 to -40 mV	Cancer	Doxorubicin	A549 (lung cancer)	Nanoprecipitation	(Shirasu et al., 2016)

*at pH 7.4 unless otherwise indicated

Besides the micellar systems described above, also nanogels and vesicles composed of synthetically prepared and modified amphiphilic polypeptides have been used for drug delivery and tissue engineering applications. Studies involving their *in vivo* applications are summarized in Table 7.

As a typical example of a polypeptide-based nanogel system, a thermosensitive hydrogel composed of methoxy-poly(ethylene glycol*)-b*-(poly(γ-ethyl-*L*-glutamate-*co*-*L*-glutamic acid) (mPEG-*b*-poly(ELG-*co*-LG)) was designed for local delivery of CDDP for tumor treatment. Suppressed tumor growth was achieved with a therapeutic efficacy which was revealed by *in vivo* studies (Yu et al., 2017). Another polypeptide-based nanogel system was reported by Bronich *et al*. The nanogel was based on PEG-*b*-poly(glutamic acid) which was functionalized with phenyl alanine moieties by polymer-analogous modification of the PGA segment with PME (*L*-phenylalanine methyl ester (PME)) using carbodiimide chemistry. This strategy was followed to increase the hydrophobicity of the system and thus reach better drug loading capacities. This gel was used to co-encapsulate doxorubicin with 17-allyl amino demethoxygeldanamycin (17-AAG) to inhibit tumor activity in an ErbB2-driven breast cancer model. ErB2, which is overexpressed in breast cancer, is sensitive to HSP90 inhibition (a heat shock protein associated with ErB2) by 17-AAG. DOX was encapsulated *via* electrostatic interactions and 17-AAG was incorporated *via* hydrophobic interactions. Antitumor efficacy *in vivo* was clearly demonstrated and the therapeutic index of the co-loaded polypeptide based nanogel showed promising results with only l ~5% body weight loss during the 2-week study period in mice (Desale et al., 2015).

As an example for nanogels which possess dual response, polypeptide triblock copolymers based on poly[(2-(dibutylamino)ethyl-*L*-glutamate)-*co*-(γ-benzyl-*L*-glutamate)]-poly(ethylene glycol)-*b*-(γ-benzyl-*L*-glutamate)]-*co*-poly[(2-(dibutylamino)ethyl-*L*-glutamate) (PNLG-*co*-PBLG-*b*-PEG-*b*-PBLG-*co*-PNLG) were developed as temperature and pH responsive injectable hydrogel. The polypeptide copolymers were molecularly dissolved at low temperature and pH and assembled into a soft hydrogel under physiological conditions (37 °C and pH 7.4) showed form. A water-soluble therapeutic protein, human growth hormone (hGH), was loaded through polypeptide complexation due to ionic interactions. The prepared gels were injected into the dorsal region of Sprague–Dawley (SD) rats. Human growth hormone-loaded gels were found biodegradable and bioresorbable after 6 weeks of injection without any toxicity (Turabee et al., 2017).

Polymer vesicles, or polymersomes, which are obtained by self-assembly of amphiphilic copolymers are versatile drug carriers to load both hydrophobic and hydrophilic cargos with their tunable membrane and aqueous core (L. Zhao et al., 2014). Lecommandoux *et al*., designed antibody-functionalized polymersomes loaded with USPIONS (ultra-small iron oxide magnetic nanoparticles) to target bone metastases using high resolution MRI. This study was one of the first examples where polypeptide-based polymersomes were used as contrast agents. Maleimide bearing polymersomes composed of poly(trimethylene carbonate)-*b*-poly(glutamic acid) PTMC-*b*-PGlu were reacted with thiol-derivatized trastuzumab to obtain the targeted multifunctional polymer vesicles. A bone cancer model was developed by injecting BT-474 cells (a HER2-positive cell line) directly in the femoral bone of NOD/SCID mice. This study revealed that only targeted polymersomes showed a more persistent T_2* dynamic contrast enhancement at the tumor site, associated with increased residence time of the contrast agent (Pourtau et al., 2013). In a comparative study, 99mTc-radiolabeled poly(ethylene glycol)-*b*-poly(γ-benzyl-*L*-glutamate) (PEG-*b*-PBLG) micelles and poly(trimethylene carbonate)-*b*-poly(glutamic acid) (PTMC-*b*-PGlu) vesicles were evaluated regarding their biodistribution and circulation behavior. This study revealed that these hybrid vesicles would show higher *in vitro* stability in comparison with the hybrid micelles; *in vivo* experiments demonstrated a higher uptake in the liver, spleen and lungs for hybrid vesicles when compared with hybrid micelles, showing potential theranostic properties (Psimadas et al., 2014). The same polymeric system was used for the delivery of the hydrophobic anticancer agent plitidepsin for the treatment of multiple myeloma (ADMYRE). The pharmacokinetics study showed lower plasma clearance for PEG-*b*-PBLG micelles in terms of higher AUC and C_{max} compared to commercial Cremophor® and PTMC-*b*-PGlu vesicles. In this study, empty nanoparticles showed a maximum tolerated dose higher than 200 mg/kg with non-toxic profile and they could therefore be potential alternative vehicles for drug delivery applications (Oliveira et al., 2014).

Polymersomes based on a hybrid polymeric system composed of a polypeptide block and a water-soluble hyaluronan block, Poly(γ-benzyl *L*-glutamate)-*b*-hyaluronan (PBLG-*b*-Hya), were developed by Lecommandoux *et al*. for intracellular delivery of DOX. DOX was loaded through the nanoprecipitation method and pH dependent release was achieved up to 10 days in an *in vitro* assay. DOX-loaded polymersomes were used to inhibit breast tumors in a female Sprague–Dawley (SD) rat model. Hyaluronic acid, which fully covered the surface of the nanoparticles, was used both to provide good colloidal stability *in vitro* and *in vivo*, but also to target CD44 receptors over-expressed in some cancer cell models. The results showed a significant tumor suppression effect in CD44 overexpressed breast cancer models *in vivo,* together with a significant

improvement in survival (Upadhyay et al., 2010). The same vesicular structure ($PBLG_{23}$-*b*-Hya_{10}) was further studied in Ehrlich ascites tumor (EAT) bearing mice to evaluate the *in vivo* efficacy of DOX loaded vesicles. Intracellular uptake of DOX loaded vesicles was achieved via CD44 receptor mediated endocytosis in the EAT tumor, with as a result a prolonged tumor doubling time and an increase in life span of the mice (Upadhyay et al., 2012). These nanoparticles are highly efficient in different tumor models due to their targeting ability of the CD44 receptor. Furthermore, hyaluronan-based NP were effectively loaded with both vorinostat, a histone deacetylase inhibitor, and gefitinib, an EGFR-TKI. These systems combined anti-tumor efficacy with less toxic drug delivery (Jeannot et al., 2018, 2016).

A versatile class of PEG-*b*-polypeptide conjugates was developed by Hammond *et al*. The group synthesized poly(γ-propargyl *L*-glutamate) (PPLG) by *N*-carboxyanhydride (NCA) polymerization. The pendant alkyne groups along the polypeptide chain were modified effectively *via* Cu catalyzed azide-alkyne cycloaddition (CuAAC) with tertiary amine moieties. Vesicular structures were observed from these polymers and DOX loading was achieved during the self-assembly process. The DOX loaded vesicles were shown to reduce tumor growth (Quadir et al., 2014). In a further study of the same group, folate conjugated nanoparticles were further assessed for targeted drug delivery. Folic acid-conjugated nanoparticles could enhance more accumulation in tumor cells especially in folate-receptor-overexpressing cancer cells (KB), compared to untargeted carriers. PEG-*b*-PPLG, substituted with diethyl amine side chains, was functionalized with folate using NHS/EDC chemistry and DOX loading was achieved subsequently during self-assembly process. Delivery of nanoparticles was achieved with minimal toxicity and good reduction in tumor growth in hind flank xenograft mouse model (Quadir et al., 2017). In this section, we summarized only *in vivo* studies of carriers possessing negatively charged, biodegradable polypeptide blocks. Due to their pH-responsive nature, nanoparticles based on these polymers can disassemble in acidic environment (of organelles in cells or tumor tissue) due to the change of their secondary structure, releasing their therapeutic cargo in a controlled manner. These characteristics were exploited in the above studies to develop drug delivery and contrast agents for future biomedical applications.

Table 7. Characteristics and applications of nanogels and vesicular structures bearing acidic units.

Polymer	Radius of NPs	Zeta potential / Surface charge	Application	Targeting / active compound	Method of application/ Main findings	Synthesis / Preparation	Reference
mPEG-*b*-P(ELG-*co*-LG)	-	-	Cancer	CDDP	Improving Localized Antitumor Efficacy	Complexation with CDDP	(Yu et al., 2017)
PEG-*b*-Poly(glutamic acid)(*L*-phenylalanine methylester (PME)	~30 nm	-21 mv at pH 7.0	Cancer	17 AAG and Doxorubicin	Combination of drugs to target breast cancer	Complexation with DOX through ionic interactions	(Desale et al., 2015)
PTMC-*b*-PGlu	100 nm	Negatively charged at pH 7.4	Cancer	Doxorubicin, antibody, SPIONS	Magnetic resonance imaging and targeting cancer cells	Functionalization and nanoprecipitation	(Oliveira et al., 2014; Pourtau et al., 2013; Psimadas et al., 2014)
PBLG-*b*-Hya	~100 nm	Negatively charged at pH 7.4	Cancer	Doxorubicin	CD44 targeting for cancer targeting	Nanoprecipitation	(Jeannot et al., 2018, 2016, Upadhyay et al., 2012, 2010)
PEG-*b*-PPLG	~25-50 nm	-	Cancer	Doxorubicin	Targeted drug delivery depending on pH	Self-assembly by nanoprecipitation	(Quadir et al., 2017, 2014)
PNLG-*co*-PBLG-*b*-PEG-*b*-PBLG-*co*-PNLG	-	-	Therapeutic protein delivery	Human Growth Hormone	Biodegradable and bioresorbable hydrogels	Copolymer protein complexes	(Turabee et al., 2017)

4.2 Cationic polypeptide-based nanoparticle systems

Cationic polypeptide-based systems including poly(*L*-lysine) (PLL) and *N*-substituted poly(aspartamide)s are the most studied systems for the complexation of genetic materials such as DNA, siRNA, mRNA and their application in gene transfection, while they also have great potential for the delivery of anticancer agents (Fig. 12, Table 8). In this section, we will summarize all *in vivo* applications of nanocarriers based on cationic polypeptides.

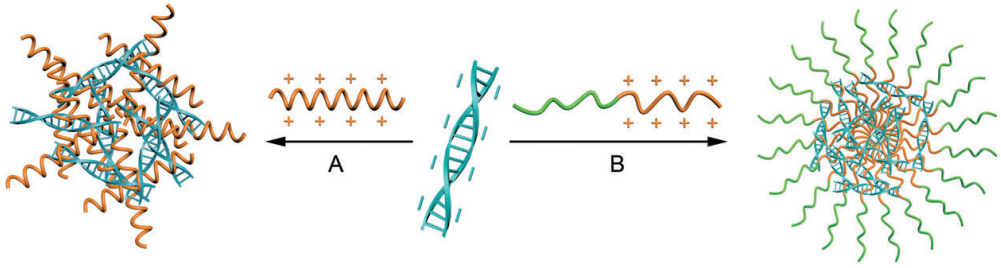

Figure 12. Schematic illustration showing the complex formation of nucleic acids with α-helical, cationic polypeptides (A) and PEG-*b*-poly(*N*-aspartamide) copolymers (B) (Song et al., 2017). Republished with permission of The Royal Society of Chemistry, from Chemical Society Reviews, Synthetic polypeptides: from polymer design to supramolecular assembly and biomedical application, Z. Song et al., Vol 46. © 2017, permission conveyed through Copyright Clearance Center, Inc.

Self-assembled cationic micelles based on amphiphilic poly(ethylene glycol)-*b*-poly(*L*-Lysine)-*b*-poly(*L*-Leucine) PEG-*b*-PLL-*b*-PLeu have been studied by Cai *et al.* for different purposes such as gene therapy, vaccine delivery systems and for intracellular imaging. A co-delivery system was obtained by complexation of PLL with siRNA and entrapment of docetaxel (DTX) into the PLeu core. Even at low dosages of DTX the particles proved to be very promising for down-regulation of the anti-apoptotic Bcl-2 gene, associated with inhibition of tumor growth on MCF-7 murine xenograft by passive targeting (Zheng et al., 2013). The same polymer system was also used for encapsulation of poorly aqueous soluble Indocyanine green (ICG), which is approved by the FDA for photothermal therapy. Polymeric micelles composed of PEG-*b*-PLL_{30}-*b*-$PLLeu_{40}$ and loaded with ICG (in a 5: 1 ratio) showed enhanced tumor localization with a prolonged circulation time by *in vivo* studies on H460 cells (L. Wu et al., 2013). As an example for nanoparticle-based antigen delivery, encapsulated ovalbumin antigens with this polymeric micelle system enhanced vaccine-induced antibody production by 70–90 fold and cytotoxic T-lymphocyte (CTL) responses were suppressed (Luo et al., 2013).

Redox-sensitive disulfide links were incorporated in polymeric micelles to exploit the significant concentration difference of glutathione (GSH) between the extracellular (~2.0 to 20.0 μM) and intracellular (~10 mM) environment for redox sensitive drug delivery applications (K. Huang et al., 2015). PEG-*b*-poly(*L*-lysine) was modified first with 3,3'-dithiodipropionic acid, after which PTX was conjugated to the carboxylic acid moieties. The resulting polymeric micelles showed both pH and redox sensitivity, and this dual effect enhanced the antitumor activity against B16F1 melanoma bearing C57BL/6 mice compared to the free drug. In another study, poly(*L*-lysine-*r*-histidine) was conjugated via a disulfide bond with PEG (PEG-SS-Lys-*r*-His) to form particles suitable for siRNA delivery and tumor therapy. The His moieties introduced the necessary hydrophobicity for polymer assembly. The cleavable SS bond allowed a more efficient release of the siRNA payload to silence the expression of the endogenous vascular endothelial growth factor (VEGF), which led to tumor suppression. Both the biodistribution profile and anti-tumor activity of the complexes verified the efficient delivery of nucleic acid for targeted tumor gene therapy. (Lv et al., 2014c; Zhu et al., 2014).

Poly(*L*-lysine) modified with branched PEI(25k) poly(ethyleneimine) was developed by Chen *et al*. (Tian et al., 2013), because PEI is a well-known polymer due to its effective endosomal escape property even though it is non-biodegradable and toxic (Cabral et al., 2018). The low endosomal escape ability of PLL was improved by PEI and the copolymers were used to encapsulate pKH3-rev-casp-3 plasmid DNA, which encodes the apoptosis-inducing caspase 3 enzyme. The polymer-DNA complex inhibited tumor growth by poly (ADP-ribose) polymerase-1 cleavage, leading to tumor apoptosis. In another study, poly(ethylene imine)-*b*-poly(*L*-lysine)-*b*-poly(*L*-glutamic acid) (PELG) was designed as a zwitterionic polymer to shield the ternary complex of PEI25k/DNA to obtain high cell uptake efficiency and high transfection efficiency. The complex containing the pKH3-rev-casp-3 plasmid inhibited HeLa tumor growth (Tian et al., 2014).

Poly(*L*-Lysine) cannot only be used for interaction with single biomolecules or inorganic particles, but has also found use for the decoration of virus particles such as adenoviruses. These viruses normally trigger an

immune response and a polymer coating could reduce the toxic effect by altering the net charge of the viral particles. Physical complexation of the adenoviral particles was performed with these polymeric micelles composed of poly(*L*-lysine) and poly(*L*-lysine)-*b*-poly(Nε-2-[2-(2-methoxyethoxy)ethoxy]acetyl-*L*-lysine) diblock copolymers (Jiang et al., 2013). Studies with the coated particles on immunocompetent mice showed a reduced antigenicity and an enhanced lung transduction as a result of the altered interactions with cells and organs. Enhanced gene transfer in both *in vitro* and *in vivo* studies was observed, demonstrating the potential of these coated Ad vectors to target cancer metastasis.

Recently, another drug loaded polycationic based polypeptide micelle was developed with multiple functionalities. The micelle was based on the self-assembly of poly(*L*-methionine-*block*-*L*-lysine)-PLGLAG-PEG (MLMP), and DOX was loaded into the core. PLGLAG is a short amino acid sequence cleavable by MMP-2 proteases, which is overexpressed in cancer cells. This would lead to removal of the PEG chains. Methionine is responsive to reactive oxygen species (ROS), which turns this amino acid into a more hydrophilic oxidized form. ROS is highly abundant in cancer cells, which would allow efficient oxidation and the transition from an amphiphilic block copolymer to a fully water soluble one. The combination of both mechanisms would lead to effective release of DOX. Indeed, DOX loaded MLMP micelles demonstrated higher tumor inhibition with the smaller tumor volume compared to free DOX, which was examined on NCI-H460 tumor bearing nude mice (Yoo et al., 2017). Poly(*L*-Lysine) was one of the first biodegradable polymers developed as an alternative to PEI. However, poly(*L*-Lysine) lacks amino groups with pKa between 5 and 7 which limits endosomal escape, resulting in lower transfection efficacy compared to PEI. In this context, the biodegradable poly(*N*-aspartamide) can be alternatively used for polymeric micelles based on cationic polypeptides, because they have a better buffering capacity that leads to better transfection efficacy (Doane and Burda, 2012).

Poly(*N*-aspartamide) based polymeric micelles are also often employed in nanomedicine, primarily by Kataoka's group. In particular, poly{*N*-[*N*-(2-aminoethyl)-2-aminoethyl] aspartamide} (poly(Asp(DET)) which has two amino ethylene units in the side chains has interesting properties, because of the lower pKa of the amino groups which facilitates endosomal escape, and its effective complexation with siRNA. Different functionalized poly(Asp(DET)) derived polymeric micelles have been studied *in vivo*. Disulfide containing stearoyl conjugates were complexed with vascular endothelial growth factor siRNA and systematic administration of complexes was examined in a mouse model bearing a subcutaneous pancreatic tumor. The stearoyl modification improved the bioavailability of the complexes and resulted in a 40% tumor regression (Kim et al., 2012).

In a further study, poly(Asp(DET) was used to design a smart multilayered assembly (SMA). As inner core a polyion complex was formed composed of siRNA and poly(Asp(DET). This core was stabilized with an inorganic silica layer. On top of this structure, a layer of PEG-SS-PAsp(DET) was complexed. The resulting system had a spherical morphology with a size of 160 nm. The silica interlayer improved the siRNA tolerability against anionic lipid dissociation. The therapeutic effect of the system was investigated with an OS-RC-2 tumor model by intravenous tail injection. Vascular endothelial growth factor (VEGF) was used as the target gene. A significant reduction (50 %) in VEGF mRNA level was found in tumor tissues (Suma et al., 2012a).

The cyclic pentapeptide (*cyclo*(-Arg-Gly-Asp-d-Phe-Lys) (*cyclo*(RGDfK)) is a potent binder and inhibitor of $\alpha_v\beta_3$ and $\alpha_v\beta_5$ integrins, which are overexpressed in tumor tissue. The peptide was conjugated to PEG-*b*-poly(Asp(DET))/pDNA polyplexes to improve its targeting efficiency. Nano-assembly with pDNA was successfully achieved with different N/P ratios. Polyplex complexes with an N/P ratio of 5 were administered into the arteries of rats. Sustained gene expression was detected after delivery in rats with neointimal hyperplasia (Kagaya et al., 2012). In another study, cholesterol modified *cyclo*(RGDfK) conjugated PEG-*b*-PAsp(DET) based particles were used for delivery of pDNA for systemic treatment of pancreatic tumors. Cholesterol modification was performed to enhance particle stability due to hydrophobic interactions. Antiangiogenic gene expression at the targeted tumor site with an effect for inhibition on neo-vasculature growth was observed, which would eventually lead to suppression of tumor growth (Kim et al., 2014). Similarly, a cholesterol- and cRGD-modified polyaspartamide derivative with a tetraethylenepentamine (TEP) moiety was used for complexation with siRNA. PolyAsp (TEP) has proven to be better in forming stable siRNA complexes with less toxic endosomal escape (Kim et al., 2014). siRNA loaded polymeric micelles were subcutaneously administrated to mice bearing A549 lung cancer with a N/P ratio 3. Significant tumor suppression leading to cancer cell apoptosis was observed via this gene silencing approach (Suma et al., 2012b).

PEGylated calcium phosphate hybrid micelles derived from (PolyAsp(DET) were also reported (Pittella et al., 2014). The calcium phosphate nanoparticles were efficient in encapsulating negatively charged molecules. To make the system stimulus-responsive, cis-aconitic acid (Aco) groups were incorporated through

the amine side chains. Upon exposure to lysosomal pH conditions, the Aco groups were removed from the polymer side chain, thereby restoring the amine functionalities. This facilitated endosomal escape. These nanoparticles were used for the delivery of VEGF siRNA. Enhanced accumulation of siRNA and significant VEGF gene silencing (~68%) was detected in subcutaneous BxPC3 tumors in mice (Pittella et al., 2012). The same polymeric micelle hybrid system was also used to treat spontaneous bioluminescent pancreatic tumors in transgenic mice. Gene silencing was achieved on pancreatic cancer cells with 60% tumor regression with ~40 ng siRNA.

A block/homo-mixed polyplex micelle composed of poly[Asp(DET)] and PEG-*b*-poly[Asp(DET)] was applied in immunotherapy. Granulocyte macrophage colony stimulating factor (GM-CSF) gene was encapsulated into the polymeric micelles and the particles were administered intraperitoneally (i.p) to treat pancreatic cancer in mice. The safety profile of the polymeric micelles was also tested in cynomolgus monkeys. Polymeric micelles did not show any immune response in related organs such as liver, spleen and lymph nodes after i.p administration both in mice and monkey (Ohgidani et al., 2013). This key study demonstrating gene transfection using a block/homo-mixed polyplex micelle in a primate may have great potential for further gene therapy applications in the clinic.

As a variant to the poly(aspartimides), PEG-*b*-poly(aspartate hydrazide) was used for micelle formation and drug conjugation. The hydrazide moieties were used for the coupling of the anthracycline epiburicin (Epi) via a pH sensitive hydrazone linker. Besides that, staurosporine (STS) a pan-kinase inhibitor which is very potent in cancer stem cell (CSC) inhibition, was loaded into the Epi-stabilized polymeric micelle *via* hydrophobic interactions. Polymeric micelles with a size around 50 nm were used to treat orthotopic mesothelioma xenografts bearing a recalcitrant CSC subpopulation. Because of the synergistic effect of this pH sensitive dual delivery system STS proved to be effective already at low doses. STS/Epi/m could therefore eradicate orthotopic mesothelioma without any body weight loss (Kinoh et al., 2016). Derivatives of poly(aspartate) were also used by Hammond *et al*. to facilitate tumor-specific RNA interference therapy for advanced ovarian tumor therapy. They engineered end functional NCA polymers using different chemical strategies. These polymers were used to form nanoplexes with siRNA to target silencing of protein kinase, MK2, which is overexpressed in ovarian cancer cells. Compared to platinum/taxane chemotherapy alone, these nanoplexes led to an overall survival of 37% with lower toxic side effects (Dreaden et al., 2018).

Micelles of polypeptides composed of arginine and cysteine have been also reported for gene and drug delivery applications. As a relevant example, poly(*L*-arginine)-based nanoparticles were prepared by complexation with chondroitin sulfate and used for nitric oxide (NO) based anticancer therapy. M1 macrophages overexpress inducible nitric oxide synthase (iNOS) intracellularly, which produces NO using L-arginine as a substrate. This is applied as a cytotoxic agent at an early stage of cancer. After particle administration *in vivo* protease degradation of poly(L-arginine) liberated the substrate for iNOS, which led to tumor suppression in C26 tumor bearing mice 4h after injection (Kudo and Nagasaki, 2015).

Table 8. Characteristics and applications of micelles bearing cationic groups.

Polymer	Radius of NPs	Zeta potential*/ Surface charge	Application	Targeting / active compound	Method of application / Main findings	Synthesis / Preparation	Reference
PEG-*b*-PLL-*b*-PLLeu	60 nm	Positively charged	Cancer, cell imaging, vaccine	Docetaxel and siRNA ICG (Indocyanine green) OVA	Cancer treatment	Nanoprecipitation and complexation	(Luo et al., 2013; L. Wu et al., 2013; Zheng et al., 2013)
(PEG-*b*-P(LL-DTPA) and PEG-SS-LL-*r*-His	100 nm	Positively charged	Gene delivery -cancer	siRNA	HepG2	Nucleic acid complexes	(K. Huang et al., 2015; Lv et al., 2014c; Zhu et al., 2014)
PEI-*b*-PLL and PEG-*b*-PLL-*b*-PGlu	75 nm	+52 and +36 mV	Gene therapy-cancer	pKH3-rev-casp-3 plasmid DNA	HeLa Cells	complexation	(Tian et al., 2014, 2013)
poly(*L*-lysine)-*b*-poly(Nε-2-[2-(2 methoxyethoxy)ethoxy]acetyl-*L*-lysine)	~100 nm	-20 to +30 mV (pH 7.5 to 8.0)	Vaccine	Adenovirus complex for vaccine theraphy	Immunodeficiency	Complexation and nanoprecipitation	(Jiang et al., 2013)
poly(L-methionine-*b*-L-lysine)-PLGLAG-PEG	100 nm to 2500 nm	+20 mV	Cancer	Doxorubicin	NCI-H460(lung cancer)	Covalent conjugation and self-assembly	(Yoo et al., 2017)
P(Asp(DET), PEG-SS-P(Asp(DET)), and cRGD-PEG-*b*-PAsp(DET)	50 nm	Positively charged	Cancer	pDNA,siRNA,	Chemical modifications Nucleic acid complexation for gene silencing	Nucleic acid complexation	(Kagaya et al., 2012; Kim et al., 2012; Ohgidani et al., 2013; Suma et al., 2012a)
cRGD-PEG-b-P(Asp(TEP)	50 nm	Slightly positive	Gene therapy	siRNA	A549 (Lung cancer) and	complexation	(Kim et al., 2014;

							Suma et al., 2012b)
PEG-*b*-PAsp(DET) with CaP	30 nm	-2 mV	Gene therapy	siRNA	Pancreatic cells	Chemical modifications then Nucleic acid complexation	(Pittella et al., 2014, 2012)
PEG-*b*-poly(aspartate hydrazide-epirubicin)	50 nm	-	Cancer	Epirubicin	tumors harboring recalcitrant cancer stem cells (CSCs)	Chemical modifications and self-assembly for micelles	(Kinoh et al., 2016)
PEG-*b*-poly(*L*-Arg)	~25 nm	-	Cancer	none	Targeting nitric oxide expression in cancer cells	Chemical modifications and complexation with ionic counterpart	(Kudo and Nagasaki, 2015)
PEG-*b*-poly(HEA)	~20 nm	~3 mV	Cancer	Doxorubicin, DMXAA	Solid tumor targeting (breast cancer)	Chemical modifications and complexation with ionic counterpart	(Lv et al., 2017)
PEG-b-poly(hydrazinyl-aspartamide)	10 nm	-	Cancer	MG132	Lung Cancer	Chemical modifications and self-assembly in aqueous solution	(Quader et al., 2014)

*at pH 7.4 unless otherwise indicated

Nanogels based on cationic amphiphilic copolypeptides are also attractive for different biomedical applications. A positively charged disulfide-core-crosslinked block copolypeptide nanogel of poly(*L*-lysine)-*b*-poly(*L*-phenylalanine-*co*-*L*-cystine) (PLL-*b*-P(LP-*co*-LC)) was reported to deliver 10-hydroxycamptothecin (HCPT) into orthotopic bladder cancer cells. HCPT is a derivative of camptothecin which can inhibit topoisomerase I thereby blocking DNA replication and RNA transcription of a broad spectrum of tumor cells. *In-vitro* experiments revealed that HCTP was released from the nanogel in a sustained manner for up to 72 h. The disulfide crosslinked polypeptide gel enabled glutathione (GSH) dependent release due to the increased GSH concentration in the intracellular environment of cancer cells. Tumor cell growth was successfully inhibited and the apoptosis level was increased, demonstrating efficient delivery of HCPT to bladder cancer cells (Guo et al., 2017). Diblock amphiphilic copolypeptide hydrogels were also designed to treat injured central nervous system (CNS). As hydrophobic block poly-L-leucine (*L*), poly(*L*-alanine) (A), poly(*L*-leucine-*stat*-*L*-alanine) (L/A) or poly(*L*-phenylalanine) (F) were employed and poly(*L*-lysine) (K) was used as hydrophilic domain. The amphiphilic character of the designed hydrogel enabled the loading of hydrophobic components more effectively than other types of hydrogels. One of the gels, $K_{180}L_{20}$, was loaded with the hydrophobic gene regulatory compound tamoxifen and was injected locally into the CNS of genetically modified mice. Tamoxifen was released from the hydrogel and efficiently activated reporter gene expression locally (Song et al., 2012; Zhang et al., 2014). Among DCHs, the properties and *in vivo* applications of polycationic nanogels and vesicles are provided in Table 6.

Given the results on both polyacidic and polycationic polypeptides, their use in amphiphilic block copolymers may lead to the development of carriers for a wide range of biomedical applications. The primary challenges regarding the fabrication of such carriers are the hydrolytic sensitivity of NCA monomers as well as the use of organic solvents for the self-assembly process.

4.3 Polyion complex micellar systems

PICsomes, standing for “Poly Ion Complex vesicles”, were first prepared by Kataoka’s group and are mostly based on PEG-*b*-polypeptide blocks. These nanocarriers are very efficient for encapsulation of water-soluble drugs. Interestingly, their preparation does not require any organic solvent, which makes them also highly applicable for biomedical studies. The usage of oppositely charged polypeptide blocks enables PIC membrane formation and the PEG units serve as an inner or outer shell layer, improving prolonged lifetime in the blood stream. Examples of PICsomes that were used for *in vivo* applications are summarized in this part.

PICsomes have a semi permeable vesicle wall which allow the exchange of small molecules with the environment. Larger molecules such as enzymes remain entrapped inside. As a result, PICsomes can be used as therapeutic nanoreactors, in which enzymatic activity is retained under *in vivo* conditions. PICsomes from PEG-based anionic polypeptide block (PEG-*b*-PAsp) and cationic homopolypeptide (poly(Asp-AP)) were prepared by vortex mixing, and EDC chemistry to maintain the structure. During the formation process enzymes were encapsulated in the aqueous lumen. Two different studies were described by Kataoka’s lab with enzyme loaded PICsomes. In one study, β-galactosidase-loaded PICsomes were evaluated as *in vivo* reactor by administration to murine C26 tumor bearing mice (Fig. 13). Enzymatic activity in PICsomes was followed by a model prodrug called hydroxymethyl-*N,N*-diethylrhodol-β-galactopyranoside (HMDER-βGal) which could be converted to the highly fluorescent product of HMDER. Even after 4 days of injection of enzyme loaded PICsomes, HMDER was found in tumor tissues which means enzymatic activity was maintained for this time period (Anraku et al., 2016). In a more recent study, *L*-asparaginase loaded PICsomes (ASNase@PICsomes) were evaluated after systemic injection into mice, corroborating their functionality as *in vivo* nanoreactors. ASNase is an enzyme, which has anti-proliferative effects on asparagine synthetase-deficient cancer cells, such as leukemic cells, by hydrolyzing L-asparagine in the circulation. Intravenous injection of enzyme loaded PICsomes into BALB/c mice was performed and prolonged enzymatic was found compared to free ASNase (Sueyoshi et al., 2017).

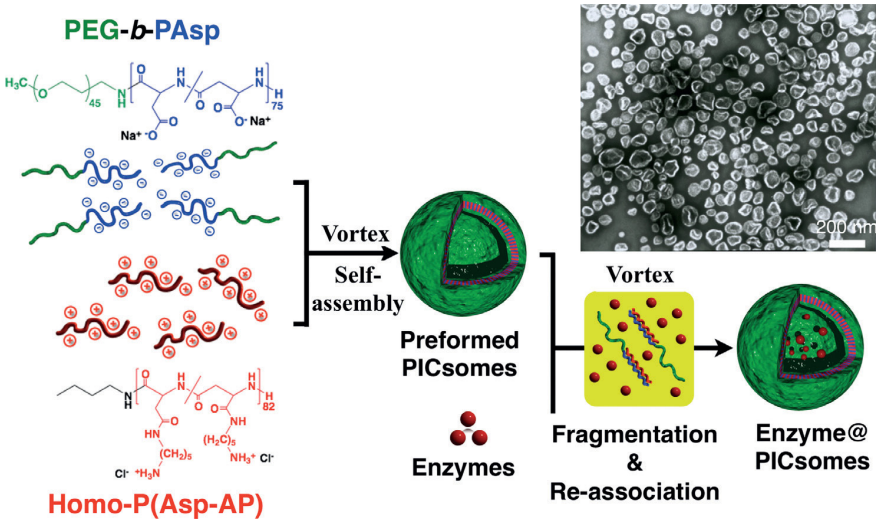

Figure 13. Chemical structures of the constituent polymers of PICsomes, and preparation of enzyme@PICsomes via preformed PICsomes. Top right: TEM image of β-gal@PICsomes (scale bar: 200 nm). PEG=poly(ethylene glycol). Reprinted with permission from Angewandte Chemie Int. Ed., Systemically Injectable Enzyme-Loaded Polyion Complex Vesicles as in Vivo Nanoreactors Functioning in Tumors, Y. Anraku et al., © 2016, with permission from John Wiley and Sons.

The high membrane permeability of PICsomes makes it difficult to load water soluble low molecular weight compounds such as Gemcitabine (GEM). Drug retaining capacity of PICsomes was improved by the application of mesoporous silica nanoparticles (MSN). Both sulfonate and amine functional MSNs were loaded through ionic interactions with the polyelectrolytes into PICsomes. Absorption and release studies of GEM from modified MSN@PICsome revealed that the sulfonate modified particles were more efficient for loading of GEM. Biodistribution and *in vivo* therapeutic efficacy of GEM-MSN@PICsome were evaluated for cancer treatment in a mouse model bearing subcutaneous A549 lung tumor. After 7 days of injection, GEM-MSN@PICsome showed significant tumor suppression compared to free GEM (Goto et al., 2017).

PICsomes have also been applied as diagnostic agents. For this purpose, superparamagnetic iron oxide nanoparticle-loaded Cy5-cross-linked PICsomes (SPIO-Cy5-PICsomes) were synthesized to detect tumor sites more precisely with MRI. SPIO-Cy5-PICsomes were prepared by vortex mixing and cross-linking of Cy5-PEG-*b*-PAsp, poly([5-aminopentyl]-α,β-aspartamide) (P(Asp-AP), and SPIO, resulting in particles of around 100 nm in size. Due to the larger size of SPIO compared to USPIO it is more effective in inducing a signal change in T2-weighted MRI due to T2 and T2* shortening. Furthermore, it was shown that the transverse relaxivity (r2) of the SPIO-Cy5-PICsomes was 2.5 times higher than that of bare SPIO. When applied in a subcutaneously grafted colon carcinoma tumor bearing mouse, 3 hrs after administration, MRI signals were detected and maintained for 24 hrs. This system also demonstrated that early stage tumors could be detected *in vivo* (after 3 days approximately 4 mm^3) with MRI (Kokuryo et al., 2013).

There are still many ongoing studies related to PICsomes for the targeted delivery of enzymes, water-soluble hydrophilic drugs, and oligonucleotides, since these carriers may ensure the long circulation of the therapeutics in the bloodstream. The simplicity of the self-assembly process of PICsomes is beneficial to develop next-generation, pioneering polymeric micellar systems that have more chances to be translated to the clinic.

5. Conclusions

Proteins and polypeptides are advantageous building blocks for the design of therapeutic nanocarriers. Indeed, composed of amino acid residues linked by natural amide bonds as monomer units, they are fully biodegradable, but also amenable to chain-end or side-chain modifications. These modifications can serve in multiple ways, for instance *i*) to tune physico-chemical properties (*e.g.*, hydrophilic-lipophilic balance) to control the folding and self-assembly behavior, *ii*) to anchor ligands to endow nanocarriers with specific receptor targeting properties, *iii*) to directly and covalently couple cytotoxic drugs or introduce pendant groups to increase non-covalent drug payloads, or *iv*) to append

contrast-enhancing agents for *in vitro* and *in vivo* imaging during preclinical developments in particular.

Proteins extracted from natural resources can present suitable properties for nanocarrier formulations. Naturally folded into 3D structures, some proteins such as albumin exhibit hydrophobic pockets where poorly-water soluble low molecular weight drugs can be confined. Self-assembled protein particles such as zein particles can additionally sustain hostile media found for instance in the gastrointestinal tract. Food resources can in particular provide abundant, safe (GRAS) and cost-effective proteins for drug nanocarrier formulation.

Synthetic polypeptides on the other hand constitute highly simplified analogs of proteins. They are however accessible at large scale and reduced costs as compared to natural human-derived or recombinant proteins. A major difference also relies on their inherent polydispersity resulting from the synthetic polymerization process, even if well controlled. Polydispersity can actually be advantageous for self-assembly behavior and/or nanoparticles' stability, but may present some additional difficulties and drawbacks from analytical point of view and validation from drug safety agencies. Ring opening polymerization is typically achieved in anhydrous organic solvents, however new approaches are arising to access synthetic polypeptides in aqueous media. The variety of accessible monomers provides the possibility for numerous chemical structures and compositions.

Engineered polypeptides are interesting compromises between proteins and synthetic polypeptides. Their chemical composition can indeed reach the complexity of natural proteins, while they can also be engineered with great liberty at the gene level to provide fully artificial proteins. Recombinant proteins and polypeptides are mostly produced in *Escherichia coli* bacteria as the cheapest host to achieve recombinant expression (over yeast or mammalian production). *E. coli* however provides few post-translational modification possibilities and cloning steps necessary for artificial gene construction can be long and tedious. Dual recombinant and synthetic approaches could be an advantageous way to circumvent these limitations. Protein engineering and recombinant expression can be used to provide monodisperse polypeptide backbones, while chemoselective bioconjugation methods can be applied to append various additional functions. Such a strategy is currently explored in many research groups, including ours, for the design of bioactive and thermo-sensitive elastin-like polypeptides.

Over the years, a broad range of peptide-based materials have been developed to fulfill all the complex requirements for biomaterials design, ranging from small synthetic peptides that can self-assemble into hierarchical assemblies (especially peptide amphiphiles), synthetic polypeptides, bioengineered polypeptides and proteins or bio-extracted and possibly modified proteins. Each system presents specific properties, advantages and limitations, from their synthetic viewpoint, cost, accessibility, *etc*. Altogether, we believe that the combination of these different approaches into controlled and functional biomacromolecules with predictable conformation and properties may open new avenue towards future biomaterials design. However, as recently highlighted by Faria *et al*., this multidisciplinary area undoubtedly requires standardization of evaluation methods in terms of materials and biological characterizations for improved reproducibility, as well as for the construction of a database enabling quantitative comparisons and meta-analyses (Faria et al., 2018).

Acknowledgements

This research was done within the NANOMED project which has received funding from the European Union's Horizon 2020 research and innovation program Marie Skłodowska-Curie Innovative Training Networks (ITN) under grant No. 676137. This work was also supported by the French National Research Agency (ANR-14-CE08-0013, ANR-15-CE07-0002) and by the Dutch Ministry of Education, Culture and Science (Gravitation Program 024.001.035).
Authors wish to address special thanks to Anne-Laure Wirotius (Univ. Bordeaux, CNRS, Bordeaux INP, LCPO) for her help in the design of Figure 1.

References

Agnes Yeboah, Rick I. Cohen, Renea Faulknor, Rene Schloss, Martin L. Yarmush, F.B., 2016. The development and characterization of SDF1α -elastin-like-peptide nanoparticles for wound healing. J. Control. Release 232, 238–247. https://doi.org/10.1016/j.jconrel.2016.04.020

Ahn, J., Miura, Y., Yamada, N., Chida, T., Liu, X., Kim, A., Sato, R., Tsumura, R., Koga, Y., Yasunaga, M., Nishiyama, N., Matsumura, Y., Cabral, H., Kataoka, K., 2015. Antibody fragment-conjugated polymeric

micelles incorporating platinum drugs for targeted therapy of pancreatic cancer. Biomaterials 39, 23–30. https://doi.org/10.1016/j.biomaterials.2014.10.069

Aluri, S.R., Shi, P., Gustafson, J.A., Wang, W., Lin, Y.A., Cui, H., Liu, S., Conti, P.S., Li, Z., Hu, P., Epstein, A.L., Mackay, J.A., 2014. A hybrid protein-polymer nanoworm potentiates apoptosis better than a monoclonal antibody. ACS Nano 8, 2064–2076. https://doi.org/10.1021/nn403973g

Anderson, J.P., Cappello, J., Martin, D.C., 1994. Morphology and primary crystal structure of a silk-like protein polymer synthesized by genetically engineered Escherichia coli bacteria. Biopolymers 34, 1049–1058. https://doi.org/10.1002/bip.360340808

Andersson, M., Johansson, J., Rising, A., 2016. Silk Spinning in Silkworms and Spiders. Int. J. Mol. Sci. 17, 1290. https://doi.org/10.3390/ijms17081290

Anraku, Y., Kishimura, A., Kamiya, M., Tanaka, S., Nomoto, T., Toh, K., Matsumoto, Y., Fukushima, S., Sueyoshi, D., Kano, M.R., Urano, Y., Nishiyama, N., Kataoka, K., 2016. Systemically Injectable Enzyme-Loaded Polyion Complex Vesicles as in Vivo Nanoreactors Functioning in Tumors. Angew. Chemie - Int. Ed. 55, 560–565. https://doi.org/10.1002/anie.201508339

Anzaghe, M., Schülke, S., Scheurer, S., 2018. Virus-Like Particles as Carrier Systems to Enhance Immunomodulation in Allergen Immunotherapy. Curr. Allergy Asthma Rep. 18, 71. https://doi.org/10.1007/s11882-018-0827-1

Assal, Y., Mizuguchi, Y., Mie, M., Kobatake, E., 2015. Growth Factor Tethering to Protein Nanoparticles via Coiled-Coil Formation for Targeted Drug Delivery. Bioconjug. Chem. 26, 1672–1677. https://doi.org/10.1021/acs.bioconjchem.5b00266

Beck, A., Goetsch, L., Dumontet, C., Corvaïa, N., 2017. Strategies and challenges for the next generation of antibody–drug conjugates. Nat. Rev. Drug Discov. 16, 315–337. https://doi.org/10.1038/nrd.2016.268

Bhavsar, M.D., Amiji, M.M., 2008. Development of Novel Biodegradable Polymeric Nanoparticles-in-Microsphere Formulation for Local Plasmid DNA Delivery in the Gastrointestinal Tract. AAPS PharmSciTech 9, 288–294. https://doi.org/10.1208/s12249-007-9021-9

Bhavsar, M.D., Amiji, M.M., 2007. Gastrointestinal distribution and in vivo gene transfection studies with nanoparticles-in-microsphere oral system (NiMOS). J. Control. Release 119, 339–348. https://doi.org/10.1016/j.jconrel.2007.03.006

Boutros, C., Tarhini, A., Routier, E., Lambotte, O., Ladurie, F.L., Carbonnel, F., Izzeddine, H., Marabelle, A., Champiat, S., Berdelou, A., Lanoy, E., Texier, M., Libenciuc, C., Eggermont, A.M.M., Soria, J.-C., Mateus, C., Robert, C., 2016. Safety profiles of anti-CTLA-4 and anti-PD-1 antibodies alone and in combination. Nat. Rev. Clin. Oncol. 13, 473–486. https://doi.org/10.1038/nrclinonc.2016.58

Cabral-Miranda, G., Heath, M., Mohsen, M., Gomes, A., Engeroff, P., Flaxman, A., Leoratti, F., El-Turabi, A., Reyes-Sandoval, A., Skinner, M., Kramer, M., Bachmann, M., 2017. Virus-Like Particle (VLP) Plus Microcrystalline Tyrosine (MCT) Adjuvants Enhance Vaccine Efficacy Improving T and B Cell Immunogenicity and Protection against Plasmodium berghei/vivax. Vaccines 5, 10. https://doi.org/10.3390/vaccines5020010

Cabral, H., Kataoka, K., 2014. Progress of drug-loaded polymeric micelles into clinical studies. J. Control. Release 190, 465–476. https://doi.org/10.1016/j.jconrel.2014.06.042

Cabral, H., Matsumoto, Y., Mizuno, K., Chen, Q., Murakami, M., Kimura, M., Terada, Y., Kano, M.R., Miyazono, K., Uesaka, M., Nishiyama, N., Kataoka, K., 2011. Accumulation of sub-100 nm polymeric micelles in poorly permeable tumours depends on size. Nat. Nanotechnol. 6, 815–823. https://doi.org/10.1038/nnano.2011.166

Cabral, H., Miyata, K., Osada, K., Kataoka, K., 2018. Block Copolymer Micelles in Nanomedicine Applications. Chem. Rev. 118, 6844–6892. https://doi.org/10.1021/acs.chemrev.8b00199

Callahan, D.J., Liu, W., Li, X., Dreher, M.R., Hassouneh, W., Kim, M., Marszalek, P., Chilkoti, A., 2012. Triple stimulus-responsive polypeptide nanoparticles that enhance intratumoral spatial distribution. Nano Lett. 12, 2165–2170. https://doi.org/10.1021/nl300630c

Cao, Y., Liu, F., Chen, Y., Yu, T., Lou, D., Guo, Y., Li, P., Wang, Z., Ran, H., 2017. Drug release from core-shell PVA/silk fibroin nanoparticles fabricated by one-step electrospraying. Sci. Rep. 7, 1–9. https://doi.org/10.1038/s41598-017-12351-1

Carlsen, A., Lecommandoux, S., 2009. Self-assembly of polypeptide-based block copolymer amphiphiles. Curr. Opin. Colloid Interface Sci. 14, 329–339. https://doi.org/10.1016/j.cocis.2009.04.007

Casa, D.M., Scariot, D.B., Khalil, N.M., Nakamura, C.V., Mainardes, R.M., 2018. Bovine serum albumin nanoparticles containing amphotericin B were effective in treating murine cutaneous leishmaniasis and reduced the drug toxicity. Exp. Parasitol. 192, 12–18. https://doi.org/10.1016/j.exppara.2018.07.003

Caster, J.M., Patel, A.N., Zhang, T., Wang, A., 2017. Investigational nanomedicines in 2016: a review of

nanotherapeutics currently undergoing clinical trials. Wiley Interdiscip. Rev. Nanomedicine Nanobiotechnology 9, e1416. https://doi.org/10.1002/wnan.1416

Catanzaro, G., Curcio, M., Cirillo, G., Spizzirri, U.G., Besharat, Z.M., Abballe, L., Vacca, A., Iemma, F., Picci, N., Ferretti, E., 2017. Albumin nanoparticles for glutathione-responsive release of cisplatin: New opportunities for medulloblastoma. Int. J. Pharm. 517, 168–174. https://doi.org/10.1016/j.ijpharm.2016.12.017

Cattaneo, I., Figliuzzi, M., Azzollini, N., Catto, V., Farè, S., Tanzi, M.C., Alessandrino, A., Freddi, G., Remuzzi, A., 2013. In vivo regeneration of elastic lamina on fibroin biodegradable vascular scaffold. Int. J. Artif. Organs 36, 166–174. https://doi.org/10.5301/IJAO.5000185

Che, H., van Hest, J.C.M., 2016. Stimuli-responsive polymersomes and nanoreactors. J. Mater. Chem. B 4, 4632–4647. https://doi.org/10.1039/C6TB01163B

Chen, L., Hébrard, G., Beyssac, E., Denis, S., Subirade, M., 2010. In vitro study of the release properties of soy-zein protein microspheres with a dynamic artificial digestive system. J. Agric. Food Chem. 58, 9861–9867. https://doi.org/10.1021/jf101918w

Chen, L., Zhou, M.-L., Qian, Z.-G., Kaplan, D.L., Xia, X.-X., 2017. Fabrication of Protein Films from Genetically Engineered Silk-Elastin-Like Proteins by Controlled Cross-Linking. ACS Biomater. Sci. Eng. 3, 335–341. https://doi.org/10.1021/acsbiomaterials.6b00794

Cho, S., Dong, S., Parent, K.N., Chen, M., 2016. Immune-tolerant elastin-like polypeptides (iTEPs) and their application as CTL vaccine carriers. J. Drug Target. 24, 328–339. https://doi.org/10.3109/1061186X.2015.1077847

Cimica, V., Galarza, J.M., 2017. Adjuvant formulations for virus-like particle (VLP) based vaccines. Clin. Immunol. 183, 99–108. https://doi.org/10.1016/j.clim.2017.08.004

Coletta, D.J., Ibáñez-Fonseca, A., Missana, L.R., Jammal, M. V., Vitelli, E.J., Aimone, M., Zabalza, F., Issa, J.P.M., Alonso, M., Rodríguez-Cabello, J.C., Feldman, S., 2017. Bone Regeneration Mediated by a Bioactive and Biodegradable Extracellular Matrix-Like Hydrogel Based on Elastin-Like Recombinamers. Tissue Eng. Part A 23, 1361–1371. https://doi.org/10.1089/ten.tea.2017.0047

Collins, T., Azevedo-Silva, J., da Costa, A., Branca, F., Machado, R., Casal, M., 2013. Batch production of a silk-elastin-like protein in E. coli BL21(DE3): Key parameters for optimisation. Microb. Cell Fact. 12, 1–16. https://doi.org/10.1186/1475-2859-12-21

Contreras-Ruiz, L., Zorzi, G.K., Hileeto, D., López-García, A., Calonge, M., Seijo, B., Sánchez, A., Diebold, Y., 2013. A nanomedicine to treat ocular surface inflammation: Performance on an experimental dry eye murine model. Gene Ther. 20, 467–477. https://doi.org/10.1038/gt.2012.56

Cormode, D.P., Skajaa, T., van Schooneveld, M.M., Koole, R., Jarzyna, P., Lobatto, M.E., Calcagno, C., Barazza, A., Gordon, R.E., Zanzonico, P., Fisher, E.A., Fayad, Z.A., Mulder, W.J.M., 2008. Nanocrystal core high-density lipoproteins: A multimodal molecular imaging contrast agent platform. Nano Lett. 8, 3715–3723.

Damiano, M.G., Mutharasan, R.K., Tripathy, S., McMahon, K.M., Thaxton, C.S., 2013. Templated high density lipoprotein nanoparticles as potential therapies and for molecular delivery. Adv. Drug Deliv. Rev. 65, 649–662. https://doi.org/10.1016/j.addr.2012.07.013

Deng, C., Wu, J., Cheng, R., Meng, F., Klok, H.A., Zhong, Z., 2014. Functional polypeptide and hybrid materials: Precision synthesis via α-amino acid N-carboxyanhydride polymerization and emerging biomedical applications. Prog. Polym. Sci. 39, 330–364. https://doi.org/10.1016/j.progpolymsci.2013.10.008

Desale, S.S., Cohen, S.M., Zhao, Y., Kabanov, A. V., Bronich, T.K., 2013. Biodegradable hybrid polymer micelles for combination drug therapy in ovarian cancer. J. Control. Release 171, 339–348. https://doi.org/10.1016/j.jconrel.2013.04.026

Desale, S.S., Raja, S.M., Kim, J.O., Mohapatra, B., Soni, K.S., Luan, H., Williams, S.H., Bielecki, T.A., Feng, D., Storck, M., Band, V., Cohen, S.M., Band, H., Bronich, T.K., 2015. Polypeptide-based nanogels co-encapsulating a synergistic combination of doxorubicin with 17-AAG show potent anti-tumor activity in ErbB2-driven breast cancer models. J. Control. Release 208, 59–66. https://doi.org/10.1016/j.jconrel.2015.02.001

Doane, T.L., Burda, C., 2012. The unique role of nanoparticles in nanomedicine: imaging, drug delivery and therapy. Chem. Soc. Rev. 41, 2885. https://doi.org/10.1039/c2cs15260f

Dong, C., Li, B., Li, Z., Shetty, S., Fu, J., 2016. Dasatinib-loaded albumin nanoparticles possess diminished endothelial cell barrier disruption and retain potent anti-leukemia cell activity. Oncotarget 7, 49699–49709. https://doi.org/10.18632/oncotarget.10435

Dreaden, E.C., Kong, Y.W., Quadir, M.A., Correa, S., Suárez-López, L., Barberio, A.E., Hwang, M.K., Shi, A.C., Oberlton, B., Gallagher, P.N., Shopsowitz, K.E., Elias, K.M., Yaffe, M.B., Hammond, P.T., 2018. RNA-Peptide nanoplexes drug DNA damage pathways in high-grade serous ovarian tumors. Bioeng. Transl.

Med. 3, 26–36. https://doi.org/10.1002/btm2.10086
Du, J., Li, B., Zhang, P., Wang, Y., 2016. Cationized bovine serum albumin as gene carrier: Influence of specific secondary structure on DNA complexibility and gene transfection. Colloids Surfaces B Biointerfaces 143, 37–46. https://doi.org/10.1016/j.colsurfb.2016.03.023
Duivenvoorden, R., Tang, J., Cormode, D.P., Mieszawska, A.J., Izquierdo-garcia, D., Ozcan, C., Otten, M.J., Zaidi, N., Mark, E., Rijs, S.M. Van, Priem, B., Kuan, E.L., Martel, C., Sager, H., Nahrendorf, M., Randolph, G.J., Erik, S.G., Fuster, V., Fisher, E.A., Fayad, Z.A., Mulder, W.J.M., 2014. A Statin-Loaded Reconstituted High-Density Lipoprotein Nanoparticle Inhibits Atherosclerotic Plaque Inflammation. Nat. Commun. 1–23. https://doi.org/10.1038/ncomms4065.A
Elzoghby, A.O., Abo El-Fotoh, W.S., Elgindy, N.A., 2011. Casein-based formulations as promising controlled release drug delivery systems. J. Control. Release 153, 206–216. https://doi.org/10.1016/j.jconrel.2011.02.010
Elzoghby, A.O., Helmy, M.W., Samy, W.M., Elgindy, N.A., 2013. Novel ionically crosslinked casein nanoparticles for flutamide delivery: Formulation, characterization, and in vivo pharmacokinetics. Int. J. Nanomedicine 8, 1721–1732. https://doi.org/10.2147/IJN.S40674
Elzoghby, A.O., Samy, W.M., Elgindy, N.A., 2012. Albumin-based nanoparticles as potential controlled release drug delivery systems. J. Control. Release 157, 168–182. https://doi.org/10.1016/j.jconrel.2011.07.031
Erokhina, S., Konovalov, O., Bianchini, P., Diaspro, A., Ruggiero, C., Erokhin, V., Pastorino, L., 2013. Release kinetics of gold nanoparticles from collagen microcapsules by total reflection X-ray fluorescence. Colloids Surfaces A Physicochem. Eng. Asp. 417, 83–88. https://doi.org/10.1016/j.colsurfa.2012.11.012
Esfandyari-Manesh, M., Mohammadi, A., Atyabi, F., Nabavi, S.M., Ebrahimi, S.M., Shahmoradi, E., Varnamkhasti, B.S., Ghahremani, M.H., Dinarvand, R., 2016. Specific targeting delivery to MUC1 overexpressing tumors by albumin-chitosan nanoparticles conjugated to DNA aptamer. Int. J. Pharm. 515, 607–615. https://doi.org/10.1016/j.ijpharm.2016.10.066
Fang, G., Tang, B., Liu, Z., Gou, J., Zhang, Y., Xu, H., Tang, X., 2014. Novel hydrophobin-coated docetaxel nanoparticles for intravenous delivery: In vitro characteristics and in vivo performance. Eur. J. Pharm. Sci. 60, 1–9. https://doi.org/10.1016/j.ejps.2014.04.016
Faria, M., Björnmalm, M., Thurecht, K.J., Kent, S.J., Parton, R.G., Kavallaris, M., Johnston, A.P.R., Gooding, J.J., Corrie, S.R., Boyd, B.J., Thordarson, P., Whittaker, A.K., Stevens, M.M., Prestidge, C.A., Porter, C.J.H., Parak, W.J., Davis, T.P., Crampin, E.J., Caruso, F., 2018. Minimum information reporting in bio–nano experimental literature. Nat. Nanotechnol. 13, 777–785. https://doi.org/10.1038/s41565-018-0246-4
Foox, M., Zilberman, M., 2015. Drug delivery from gelatin-based systems. Expert Opin. Drug Deliv. 12, 1547–1563. https://doi.org/10.1517/17425247.2015.1037272
Fu, Q., Sun, J., Zhang, W., Sui, X., Yan, Z., He, Z., 2009. Nanoparticle albumin-bound (NAB) technology is a promising method for anti-cancer drug delivery. Recent Pat. Anticancer. Drug Discov. 4, 262–272. https://doi.org/10.2174/157489209789206869
Gai, X., Jiang, Z., Liu, M., Li, Q., Wang, S., Li, T., Pan, W., Yang, X., 2018. Therapeutic Effect of a Novel Nano-Drug Delivery System on Membranous Glomerulonephritis Rat Model Induced by Cationic Bovine Serum. AAPS PharmSciTech 19, 2195–2202. https://doi.org/10.1208/s12249-018-1034-z
García-Arévalo, C., Bermejo-Martín, J.F., Rico, L., Iglesias, V., Martín, L., Rodríguez-Cabello, J.C., Arias, F.J., 2013. Immunomodulatory nanoparticles from elastin-like recombinamers: Single-molecules for tuberculosis vaccine development. Mol. Pharm. 10, 586–597. https://doi.org/10.1021/mp300325v
Girija Aswathy, R., Sivakumar, B., Brahatheeswaran, D., Fukuda, T., Yoshida, Y., Maekawa, T., Sakthi Kumar, D., 2012. Biocompatible fluorescent zein nanoparticles for simultaneous bioimaging and drug delivery application. Adv. Nat. Sci. Nanosci. Nanotechnol. 3, 025006. https://doi.org/10.1088/2043-6262/3/2/025006
Gorgieva, S., Kokol, V., 2011. Collagen- vs. Gelatine-Based Biomaterials and Their Biocompatibility: Review and Perspectives, in: Biomaterials Applications for Nanomedicine. InTech, pp. 17–51. https://doi.org/10.5772/24118
Goto, A., Yen, H.C., Anraku, Y., Fukushima, S., Lai, P.S., Kato, M., Kishimura, A., Kataoka, K., 2017. Facile Preparation of Delivery Platform of Water-Soluble Low-Molecular-Weight Drugs Based on Polyion Complex Vesicle (PICsome) Encapsulating Mesoporous Silica Nanoparticle. ACS Biomater. Sci. Eng. 3, 807–815. https://doi.org/10.1021/acsbiomaterials.6b00562
Gradishar, W.J., Tjulandin, S., Davidson, N., Shaw, H., Desai, N., Bhar, P., Hawkins, M., O'Shaughnessy, J., 2005. Phase III trial of nanoparticle albumin-bound paclitaxel compared with polyethylated castor oil-based paclitaxel in women with breast cancer. J. Clin. Oncol. 23, 7794–7803. https://doi.org/10.1200/JCO.2005.04.937

Groß, P.C., Possart, W., Zeppezauer, M., 2003. An Alternative Structure Model for the Polypentapeptide in Elastin. Zeitschrift fur Naturforsch. - Sect. C J. Biosci. 58, 873–878.

Guo, H., Xu, W., Chen, J., Yan, L., Ding, J., Hou, Y., Chen, X., 2017. Positively charged polypeptide nanogel enhances mucoadhesion and penetrability of 10-hydroxycamptothecin in orthotopic bladder carcinoma. J. Control. Release 259, 136–148. https://doi.org/10.1016/j.jconrel.2016.12.041

Guo, W., Deng, L., Yu, J., Chen, Z., Woo, Y., Liu, H., Li, T., Lin, T., Chen, H., Zhao, M., Zhang, L., Li, G., Hu, Y., 2018. Sericin nanomicelles with enhanced cellular uptake and pH-triggered release of doxorubicin reverse cancer drug resistance. Drug Deliv. 25, 1103–1116. https://doi.org/10.1080/10717544.2018.1469686

Guo, Y., Yuan, W., Yu, B., Kuai, R., Hu, W., Morin, E.E., Garcia-Barrio, M.T., Zhang, J., Moon, J.J., Schwendeman, A., Eugene Chen, Y., 2018. Synthetic High-Density Lipoprotein-Mediated Targeted Delivery of Liver X Receptors Agonist Promotes Atherosclerosis Regression. EBioMedicine 28, 225–233. https://doi.org/10.1016/j.ebiom.2017.12.021

Guo, Z., Wang, F., Di, Y., 2018. Antitumor effect of gemcitabine-loaded albumin nanoparticle on gemcitabine-resistant pancreatic cancer induced by low hENT1 expression 4869–4880.

Hadjichristidis, N., Iatrou, H., Pitsikalis, M., Sakellariou, G., 2009. Synthesis of Well-Defined Polypeptide-Based Materials via the Ring-Opening Polymerization of r -Amino Acid N -Carboxyanhydrides. Chem. Rev. 109, 5528–5578. https://doi.org/10.1021/cr900049t

He, C., Zhuang, X., Tang, Z., Tian, H., Chen, X., 2012. Stimuli-sensitive synthetic polypeptide-based materials for drug and gene delivery. Adv. Healthc. Mater. 1, 48–78. https://doi.org/10.1002/adhm.201100008

He, Y.J., Xing, L., Cui, P.F., Zhang, J.L., Zhu, Y., Qiao, J. Bin, Lyu, J.Y., Zhang, M., Luo, C.Q., Zhou, Y.X., Lu, N., Jiang, H.L., 2017. Transferrin-inspired vehicles based on pH-responsive coordination bond to combat multidrug-resistant breast cancer. Biomaterials 113, 266–278. https://doi.org/10.1016/j.biomaterials.2016.11.001

Heim, M., Keerl, D., Scheibel, T., 2009. Spider Silk: From Soluble Protein to Extraordinary Fiber. Angew. Chemie Int. Ed. 48, 3584–3596. https://doi.org/10.1002/anie.200803341

Henry, L.J., Xia, D., Wilke, M.E., Deisenhofer, J., Gerard, R.D., 1994. Characterization of the knob domain of the adenovirus type 5 fiber protein expressed in Escherichia coli. J. Virol. 68, 5239–5246.

Herrera Estrada, L.P., Champion, J.A., 2015. Protein nanoparticles for therapeutic protein delivery. Biomater. Sci. 3, 787–799. https://doi.org/10.1039/C5BM00052A

Hsueh, P.Y., Edman, M.C., Sun, G., Shi, P., Xu, S., Lin, Y.A., Cui, H., Hamm-Alvarez, S.F., Mackay, J.A., 2015. Tear-mediated delivery of nanoparticles through transcytosis of the lacrimal gland. J. Control. Release 208, 2–13. https://doi.org/10.1016/j.jconrel.2014.12.017

Hu, D., Li, T., Xu, Z., Liu, D., Yang, M., Zhu, L., 2018. Self-stabilized silk sericin-based nanoparticles: In vivo biocompatibility and reduced doxorubicin-induced toxicity. Acta Biomater. 74, 385–396. https://doi.org/10.1016/j.actbio.2018.05.024

Hu, D., Xu, Z., Hu, Z., Hu, B., Yang, M., Zhu, L., 2017. PH-triggered charge-reversal silk sericin-based nanoparticles for enhanced cellular uptake and doxorubicin delivery. ACS Sustain. Chem. Eng. 5, 1638–1647. https://doi.org/10.1021/acssuschemeng.6b02392

Huang, J., Heise, A., 2013. Stimuli responsive synthetic polypeptides derived from N-carboxyanhydride (NCA) polymerisation. Chem. Soc. Rev. 42, 7373–7390. https://doi.org/10.1039/c3cs60063g

Huang, K., Duan, N., Zhang, C., Mo, R., Hua, Z., 2017a. Improved antitumor activity of TRAIL fusion protein via formation of self-assembling nanoparticle. Sci. Rep. 7, 1–13. https://doi.org/10.1038/srep41904

Huang, K., Shi, B., Xu, W., Ding, J., Yang, Y., Liu, H., Zhuang, X., Chen, X., 2015. Reduction-responsive polypeptide nanogel delivers antitumor drug for improved efficacy and safety. Acta Biomater. 27, 179–193. https://doi.org/10.1016/j.actbio.2015.08.049

Huang, K., Zhu, L., Wang, Y., Mo, R., Hua, Z.-C., 2017b. Targeted delivery and release of Doxorubicin using pH-responsive and self-assembling copolymer. J. Mater. Chem. B 5, 6356–6365. https://doi.org/10.1039/C7TB00190H

Huang, W., Rollett, A., Kaplan, D.L., 2015. Silk-elastin-like protein biomaterials for the controlled delivery of therapeutics. Expert Opin. Drug Deliv. 12, 779–91. https://doi.org/10.1517/17425247.2015.989830

Hutzler, S., Erbar, S., Jabulowsky, R.A., Hanauer, J.R.H., Schnotz, J.H., Beissert, T., Bodmer, B.S., Eberle, R., Boller, K., Klamp, T., Sahin, U., Mühlebach, M.D., 2017. Antigen-specific oncolytic MV-based tumor vaccines through presentation of selected tumor-associated antigens on infected cells or virus-like particles. Sci. Rep. 7, 16892. https://doi.org/10.1038/s41598-017-16928-8

Iwao, Y., Tomiguchi, I., Domura, A., Mantaira, Y., Minami, A., Suzuki, T., Ikawa, T., Kimura, S. ichiro, Itai, S., 2018. Inflamed site-specific drug delivery system based on the interaction of human serum albumin

nanoparticles with myeloperoxidase in a murine model of experimental colitis. Eur. J. Pharm. Biopharm. 125, 141–147. https://doi.org/10.1016/j.ejpb.2018.01.016

Jao, D., Xue, Y., Medina, J., Hu, X., 2017. Protein-based drug-delivery materials. Materials (Basel). 10, 1–24. https://doi.org/10.3390/ma10050517

Jastrzebska, K., Kucharczyk, K., Florczak, A., Dondajewska, E., Mackiewicz, A., Dams-Kozlowska, H., 2015. Silk as an innovative biomaterial for cancer therapy. Reports Pract. Oncol. Radiother. 20, 87–98. https://doi.org/10.1016/j.rpor.2014.11.010

Jeannot, V., Gauche, C., Mazzaferro, S., Couvet, M., Vanwonterghem, L., Henry, M., Didier, C., Vollaire, J., Josserand, V., Coll, J.L., Schatz, C., Lecommandoux, S., Hurbin, A., 2018. Anti-tumor efficacy of hyaluronan-based nanoparticles for the co-delivery of drugs in lung cancer. J. Control. Release 275, 117–128. https://doi.org/10.1016/j.jconrel.2018.02.024

Jeannot, V., Mazzaferro, S., Lavaud, J., Vanwonterghem, L., Henry, M., Arboléas, M., Vollaire, J., Josserand, V., Coll, J.L., Lecommandoux, S., Schatz, C., Hurbin, A., 2016. Targeting CD44 receptor-positive lung tumors using polysaccharide-based nanocarriers: Influence of nanoparticle size and administration route. Nanomedicine Nanotechnology, Biol. Med. 12, 921–932. https://doi.org/10.1016/j.nano.2015.11.018

Jiang, Z.K., Koh, S.B.S., Sato, M., Atanasov, I.C., Johnson, M., Zhou, Z.H., Deming, T.J., Wu, L., 2013. Engineering polypeptide coatings to augment gene transduction and in vivo stability of adenoviruses. J. Control. Release 166, 75–85. https://doi.org/10.1016/j.jconrel.2012.10.023

Kagaya, H., Oba, M., Miura, Y., Koyama, H., Ishii, T., Shimada, T., Takato, T., Kataoka, K., Miyata, T., 2012. Impact of polyplex micelles installed with cyclic RGD peptide as ligand on gene delivery to vascular lesions. Gene Ther. 19, 61–69. https://doi.org/10.1038/gt.2011.74

Kano, M.R., Bae, Y., Iwata, C., Morishita, Y., Yashiro, M., Oka, M., Fujii, T., Komuro, A., Kiyono, K., Kaminishi, M., Hirakawa, K., Ouchi, Y., Nishiyama, N., Kataoka, K., Miyazono, K., 2007. Improvement of cancer-targeting therapy, using nanocarriers for intractable solid tumors by inhibition of TGF-beta signaling. Proc. Natl. Acad. Sci. 104, 3460–3465. https://doi.org/10.1073/pnas.0611660104

Kasoju, N., Bora, U., 2012. Silk Fibroin in Tissue Engineering. Adv. Healthc. Mater. 1, 393–412. https://doi.org/10.1002/adhm.201200097

Kasperek, K., Feinendegen, L.E., Lombeck, I., Bremer, H.J., 1977. Serum zinc concentration during childhood. Eur. J. Pediatr. 126, 199–202. https://doi.org/10.1007/BF00477045

Kaur, A., Jain, S., Tiwary, A.K., 2008. Mannan-coated gelatin nanoparticles for sustained and targeted delivery of didanosine: In vitro and in vivo evaluation. Acta Pharm. 58, 61–74. https://doi.org/10.2478/v10007-007-0045-1

Kim, H.J., Ishii, T., Zheng, M., Watanabe, S., Toh, K., Matsumoto, Y., Nishiyama, N., Miyata, K., Kataoka, K., 2014. Multifunctional polyion complex micelle featuring enhanced stability, targetability, and endosome escapability for systemic siRNA delivery to subcutaneous model of lung cancer. Drug Deliv. Transl. Res. 4, 50–60. https://doi.org/10.1007/s13346-013-0175-6

Kim, H.J., Oba, M., Pittella, F., Nomoto, T., Cabral, H., Matsumoto, Y., Miyata, K., Nishiyama, N., Kataoka, K., 2012. PEG-detachable cationic polyaspartamide derivatives bearing stearoyl moieties for systemic siRNA delivery toward subcutaneous Bxpc3 pancreatic tumor. J. Drug Target. 20, 33–42. https://doi.org/10.3109/1061186X.2011.632010

Kim, J.D., Jung, Y.J., Woo, C.H., Choi, Y.C., Choi, J.S., Cho, Y.W., 2017. Thermo-responsive human α-elastin self-assembled nanoparticles for protein delivery. Colloids Surfaces B Biointerfaces 149, 122–129. https://doi.org/10.1016/j.colsurfb.2016.10.012

Kim, U.J., Park, J., Li, C., Jin, H.J., Valluzzi, R., Kaplan, D.L., 2004. Structure and properties of silk hydrogels. Biomacromolecules 5, 786–792. https://doi.org/10.1021/bm0345460

Kinoh, H., Miura, Y., Chida, T., Liu, X., Mizuno, K., Fukushima, S., Morodomi, Y., Nishiyama, N., Cabral, H., Kataoka, K., 2016. Nanomedicines Eradicating Cancer Stem-like Cells in Vivo by pH-Triggered Intracellular Cooperative Action of Loaded Drugs. ACS Nano 10, 5643–5655. https://doi.org/10.1021/acsnano.6b00900

Kokuryo, D., Anraku, Y., Kishimura, A., Tanaka, S., Kano, M.R., Kershaw, J., Nishiyama, N., Saga, T., Aoki, I., Kataoka, K., 2013. SPIO-PICsome: Development of a highly sensitive and stealth-capable MRI nano-agent for tumor detection using SPIO-loaded unilamellar polyion complex vesicles (PICsomes). J. Control. Release 169, 220–227. https://doi.org/10.1016/j.jconrel.2013.03.016

Konat Zorzi, G., Contreras-Ruiz, L., Párraga, J.E., López-García, A., Romero Bello, R., Diebold, Y., Seijo, B., Sánchez, A., 2011. Expression of MUC5AC in ocular surface epithelial cells using cationized gelatin nanoparticles. Mol. Pharm. 8, 1783–1788. https://doi.org/10.1021/mp200155t

Koria, P., Yagi, H., Kitagawa, Y., Megeed, Z., Nahmias, Y., Sheridan, R., Yarmush, M.L., 2011. Self-assembling

elastin-like peptides growth factor chimeric nanoparticles for the treatment of chronic wounds. Proc. Natl. Acad. Sci. U. S. A. 108, 1034–9.

Kriegel, C., Amiji, M., 2011. Oral TNF-α gene silencing using a polymeric microsphere-based delivery system for the treatment of inflammatory bowel disease. J. Control. Release 150, 77–86. https://doi.org/10.1016/j.jconrel.2010.10.002

Kudo, S., Nagasaki, Y., 2015. A novel nitric oxide-based anticancer therapeutics by macrophage-targeted poly(l-arginine)-based nanoparticles. J. Control. Release 217, 256–262. https://doi.org/10.1016/j.jconrel.2015.09.019

Kumagai, M., Imai, Y., Nakamura, T., Yamasaki, Y., Sekino, M., Ueno, S., Hanaoka, K., Kikuchi, K., Nagano, T., Kaneko, E., Shimokado, K., Kataoka, K., 2007. Iron hydroxide nanoparticles coated with poly(ethylene glycol)-poly(aspartic acid) block copolymer as novel magnetic resonance contrast agents for in vivo cancer imaging. Colloids Surfaces B Biointerfaces 56, 174–181. https://doi.org/10.1016/j.colsurfb.2006.12.019

Kumagai, M., Kano, M.R., Morishita, Y., Ota, M., Imai, Y., Nishiyama, N., Sekino, M., Ueno, S., Miyazono, K., Kataoka, K., 2009. Enhanced magnetic resonance imaging of experimental pancreatic tumor in vivo by block copolymer-coated magnetite nanoparticles with TGF-β inhibitor. J. Control. Release 140, 306–311. https://doi.org/10.1016/j.jconrel.2009.06.002

Kumar, R., Nagarwal, R.C., Dhanawat, M., Pandit, J.K., 2011. In-Vitro and In-Vivo study of indomethacin loaded gelatin nanoparticles. J. Biomed. Nanotechnol. 7, 325–333. https://doi.org/10.1166/jbn.2011.1290

Kuntworbe, N., Ofori, M., Addo, P., Tingle, M., Al-Kassas, R., 2013. Pharmacokinetics and in vivo chemosuppressive activity studies on cryptolepine hydrochloride and cryptolepine hydrochloride-loaded gelatine nanoformulation designed for parenteral administration for the treatment of malaria. Acta Trop. 127, 165–173. https://doi.org/10.1016/j.actatropica.2013.04.010

Kuwahara, H., Nishina, K., Yoshida, K., Nishina, T., Yamamoto, M., Saito, Y., Piao, W., Yoshida, M., Mizusawa, H., Yokota, T., 2011. Efficient in vivo delivery of siRNA into brain capillary endothelial cells along with endogenous lipoprotein. Mol. Ther. 19, 2213–2221. https://doi.org/10.1038/mt.2011.186

Lai, L.F., Guo, H.X., 2011. Preparation of new 5-fluorouracil-loaded zein nanoparticles for liver targeting. Int. J. Pharm. 404, 317–323. https://doi.org/10.1016/j.ijpharm.2010.11.025

Larsen, M.T., Kuhlmann, M., Hvam, M.L., Howard, K.A., 2016. Albumin-based drug delivery: harnessing nature to cure disease. Mol. Cell. Ther. 4, 3. https://doi.org/10.1186/s40591-016-0048-8

Lee, E.S., Kim, J.H., Sim, T., Youn, Y.S., Lee, B.J., Oh, Y.T., Oh, K.T., 2014. A feasibility study of a pH sensitive nanomedicine using doxorubicin loaded poly(aspartic acid-graft-imidazole)-block-poly(ethylene glycol) micelles. J. Mater. Chem. B 2, 1152–1159. https://doi.org/10.1039/c3tb21379j

Lee, S., Alwahab, N.S.A., Moazzam, Z.M., 2013. Zein-based oral drug delivery system targeting activated macrophages. Int. J. Pharm. 454, 388–393. https://doi.org/10.1016/j.ijpharm.2013.07.026

Lefèvre, T., Rousseau, M.E., Pézolet, M., 2007. Protein secondary structure and orientation in silk as revealed by Raman spectromicroscopy. Biophys. J. 92, 2885–2895. https://doi.org/10.1529/biophysj.106.100339

Li, F., Zheng, C., Xin, J., Chen, F., Ling, H., Sun, L., Webster, T.J., Ming, X., Liu, J., 2016. Enhanced tumor delivery and antitumor response of doxorubicin-loaded albumin nanoparticles formulated based on a schiff base. Int. J. Nanomedicine 11, 3875–3890. https://doi.org/10.2147/IJN.S108689

Li, H., Tian, J., Wu, A., Wang, J., Ge, C., Sun, Z., 2016. Self-assembled silk fibroin nanoparticles loaded with binary drugs in the treatment of breast carcinoma. Int. J. Nanomedicine 11, 4373–4380. https://doi.org/10.2147/IJN.S108633

Li, M., Song, W., Tang, Z., Lv, S., Lin, L., Sun, H., Li, Q., Yang, Y., Hong, H., Chen, X., 2013. Nanoscaled poly(l-glutamic acid)/doxorubicin-amphiphile complex as pH-responsive drug delivery system for effective treatment of nonsmall cell lung cancer. ACS Appl. Mater. Interfaces 5, 1781–1792. https://doi.org/10.1021/am303073u

Li, N.K., Quiroz, F.G., Hall, C.K., Chilkoti, A., Yingling, Y.G., 2014. Molecular description of the lcst behavior of an elastin-like polypeptide. Biomacromolecules 15, 3522–3530. https://doi.org/10.1021/bm500658w

Lin, Y., Xia, X., Wang, M., Wang, Q., An, B., Tao, H., Xu, Q., Omenetto, F., Kaplan, D.L., 2014. Genetically Programmable Thermoresponsive Plasmonic Gold/Silk-Elastin Protein Core/Shell Nanoparticles. Langmuir 30, 4406–4414. https://doi.org/10.1021/la403559t

Liu, X., Zheng, C., Luo, X., Wang, X., Jiang, H., 2019. Recent advances of collagen-based biomaterials: Multi-hierarchical structure, modification and biomedical applications. Mater. Sci. Eng. C 99, 1509–1522. https://doi.org/10.1016/j.msec.2019.02.070

Lohcharoenkal, W., Wang, L., Chen, Y.C., Rojanasakul, Y., 2014. Protein Nanoparticles as Drug Delivery Carriers for Cancer Therapy. Biomed Res. Int. 2014, 1–12. https://doi.org/10.1155/2014/180549

Lozano-Pérez, A.A., Rodriguez-Nogales, A., Ortiz-Cullera, V., Algieri, F., Garrido-Mesa, J., Zorrilla, P., Rodriguez-Cabezas, M.E., Garrido-Mesa, N., Pilar Utrilla, M., de Matteis, L., de la Fuente, J.M., Cenis, J.L., Gálvez, J., 2014. Silk fibroin nanoparticles constitute a vector for controlled release of resveratrol in an experimental model of inflammatory bowel disease in rats. Int. J. Nanomedicine 9, 4507–4520. https://doi.org/10.2147/IJN.S68526

Lua, L.H.L., Connors, N.K., Sainsbury, F., Chuan, Y.P., Wibowo, N., Middelberg, A.P.J., 2014. Bioengineering virus-like particles as vaccines. Biotechnol. Bioeng. 111, 425–440. https://doi.org/10.1002/bit.25159

Luo, Y., Wang, Q., 2014. Zein-based micro- and nano-particles for drug and nutrient delivery: A review. J. Appl. Polym. Sci. 131. https://doi.org/10.1002/app.40696

Luo, Z., Li, P., Deng, J., Gao, N., Zhang, Y., Pan, H., Liu, L., Wang, C., Cai, L., Ma, Y., 2013. Cationic polypeptide micelle-based antigen delivery system: A simple and robust adjuvant to improve vaccine efficacy. J. Control. Release 170, 259–267. https://doi.org/10.1016/j.jconrel.2013.05.027

Lv, S., Li, M., Tang, Z., Song, W., Sun, H., Liu, H., Chen, X., 2013. Doxorubicin-loaded amphiphilic polypeptide-based nanoparticles as an efficient drug delivery system for cancer therapy. Acta Biomater. 9, 9330–9342. https://doi.org/10.1016/j.actbio.2013.08.015

Lv, S., Song, W., Tang, Z., Li, M., Yu, H., Hong, H., Chen, X., 2014a. Charge-conversional peg-polypeptide polyionic complex nanoparticles from simple blending of a pair of oppositely charged block copolymers as an intelligent vehicle for efficient antitumor drug delivery. Mol. Pharm. 11, 1562–1574. https://doi.org/10.1021/mp4007387

Lv, S., Tang, Z., Li, M., Lin, J., Song, W., Liu, H., Huang, Y., Zhang, Y., Chen, X., 2014b. Co-delivery of doxorubicin and paclitaxel by PEG-polypeptide nanovehicle for the treatment of non-small cell lung cancer. Biomaterials 35, 6118–6129. https://doi.org/10.1016/j.biomaterials.2014.04.034

Lv, S., Tang, Z., Song, W., Zhang, D., Li, M., Liu, H., Cheng, J., Zhong, W., Chen, X., 2017. Inhibiting Solid Tumor Growth In Vivo by Non-Tumor-Penetrating Nanomedicine. Small 13, 1–10. https://doi.org/10.1002/smll.201600954

Lv, S., Tang, Z., Zhang, D., Song, W., Li, M., Lin, J., Liu, H., Chen, X., 2014c. Well-defined polymer-drug conjugate engineered with redox and pH-sensitive release mechanism for efficient delivery of paclitaxel. J. Control. Release 194, 220–227. https://doi.org/10.1016/j.jconrel.2014.09.009

Ma, Y., Nolte, R.J.M., Cornelissen, J.J.L.M., 2012. Virus-based nanocarriers for drug delivery. Adv. Drug Deliv. Rev. 64, 811–825. https://doi.org/10.1016/j.addr.2012.01.005

MacKay, J.A., Chen, M., McDaniel, J.R., Liu, W., Simnick, A.J., Chilkoti, A., 2009. Self-assembling chimeric polypeptide-doxorubicin conjugate nanoparticles that abolish tumours after a single injection. Nat. Mater. 8, 993–9. https://doi.org/10.1038/nmat2569

Madan, J., Dhiman, N., Sardana, S., Aneja, R., Chandra, R., Katyal, A., 2011. Long-circulating poly(ethylene glycol)-grafted gelatin nanoparticles customized for intracellular delivery of noscapine: Preparation, in-vitro characterization, structure elucidation, pharmacokinetics, and cytotoxicity analyses. Anticancer. Drugs 22, 543–555. https://doi.org/10.1097/CAD.0b013e32834159b8

MaHam, A., Tang, Z., Wu, H., Wang, J., Lin, Y., 2009. Protein-based nanomedicine platforms for drug delivery. Small 5, 1706–1721. https://doi.org/10.1002/smll.200801602

Maiolo, D., Pigliacelli, C., Sánchez Moreno, P., Violatto, M.B., Talamini, L., Tirotta, I., Piccirillo, R., Zucchetti, M., Morosi, L., Frapolli, R., Candiani, G., Bigini, P., Metrangolo, P., Baldelli Bombelli, F., 2017. Bioreducible Hydrophobin-Stabilized Supraparticles for Selective Intracellular Release. ACS Nano 11, 9413–9423. https://doi.org/10.1021/acsnano.7b04979

Maitz, M.F., Sperling, C., Wongpinyochit, T., Herklotz, M., Werner, C., Seib, F.P., 2017. Biocompatibility assessment of silk nanoparticles: hemocompatibility and internalization by human blood cells. Nanomedicine Nanotechnology, Biol. Med. 13, 2633–2642. https://doi.org/10.1016/J.NANO.2017.07.012

Manca, M.L., Cassano, R., Valenti, D., Trombino, S., Ferrarelli, T., Picci, N., Fadda, A.M., Manconi, M., 2013. Isoniazid-gelatin conjugate microparticles containing rifampicin for the treatment of tuberculosis. J. Pharm. Pharmacol. 65, 1302–1311. https://doi.org/10.1111/jphp.12094

Marelli, B., Brenckle, M.A., Kaplan, D.L., Omenetto, F.G., 2016. Silk Fibroin as Edible Coating for Perishable Food Preservation. Sci. Rep. 6, 25263. https://doi.org/10.1038/srep25263

Matsumoto, R., Hara, R., Andou, T., Mie, M., Kobatake, E., 2014. Targeting of EGF-displayed protein nanoparticles with anticancer drugs. J. Biomed. Mater. Res. - Part B Appl. Biomater. 102, 1792–1798. https://doi.org/10.1002/jbm.b.33162

Matsumoto, Y., Nichols, J.W., Toh, K., Nomoto, T., Cabral, H., Miura, Y., Christie, R.J., Yamada, N., Ogura, T., Kano, M.R., Matsumura, Y., Nishiyama, N., Yamasoba, T., Bae, Y.H., Kataoka, K., 2016. Vascular bursts

enhance permeability of tumour blood vessels and improve nanoparticle delivery. Nat. Nanotechnol. 11, 533–538. https://doi.org/10.1038/nnano.2015.342

McDaniel, J.R., Radford, D.C., Chilkoti, A., 2013. A unified model for de novo design of elastin-like polypeptides with tunable inverse transition temperatures. Biomacromolecules 14, 2866–2872. https://doi.org/10.1021/bm4007166

Merrifield, R.B., 1963. Solid Phase Peptide Synthesis. I. The Synthesis of a Tetrapeptide. J. Am. Chem. Soc. 85, 2149–2154. https://doi.org/10.1021/ja00897a025

Mi, P., Dewi, N., Yanagie, H., Kokuryo, D., Suzuki, M., Sakurai, Y., Li, Y., Aoki, I., Ono, K., Takahashi, H., Cabral, H., Nishiyama, N., Kataoka, K., 2015. Hybrid Calcium Phosphate-Polymeric Micelles Incorporating Gadolinium Chelates for Imaging-Guided Gadolinium Neutron Capture Tumor Therapy. ACS Nano 9, 5913–5921. https://doi.org/10.1021/acsnano.5b00532

Mi, P., Kokuryo, D., Cabral, H., Wu, H., Terada, Y., Saga, T., Aoki, I., Nishiyama, N., Kataoka, K., 2016. A pH-activatable nanoparticle with signal-amplification capabilities for non-invasive imaging of tumour malignancy. Nat. Nanotechnol. 11, 724–730. https://doi.org/10.1038/nnano.2016.72

Mi, P., Yanagie, H., Dewi, N., Yen, H.C., Liu, X., Suzuki, M., Sakurai, Y., Ono, K., Takahashi, H., Cabral, H., Kataoka, K., Nishiyama, N., 2017. Block copolymer-boron cluster conjugate for effective boron neutron capture therapy of solid tumors. J. Control. Release 254, 1–9. https://doi.org/10.1016/j.jconrel.2017.03.036

Michell, D.L., Vickers, K.C., 2016. HDL and microRNA therapeutics in cardiovascular disease. Pharmacol. Ther. 168, 43–52. https://doi.org/10.1016/j.pharmthera.2016.09.001

Min, K., Kim, S., Kim, S., 2018. Silk protein nanofibers for highly efficient, eco-friendly, optically translucent, and multifunctional air filters. Sci. Rep. 8, 9598. https://doi.org/10.1038/s41598-018-27917-w

Mitraki, A., 2010. Protein aggregation: from inclusion bodies to amyloid and biomaterials. Adv. Protein Chem. Struct. Biol. 79, 89–125. https://doi.org/10.1016/S1876-1623(10)79003-9

Mo, Z.C., Ren, K., Liu, X., Tang, Z.L., Yi, G.H., 2016. A high-density lipoprotein-mediated drug delivery system. Adv. Drug Deliv. Rev. 106, 132–147. https://doi.org/10.1016/j.addr.2016.04.030

Mochida, Y., Cabral, H., Miura, Y., Albertini, F., Fukushima, S., Osada, K., Nishiyama, N., Kataoka, K., 2014. Bundled assembly of helical nanostructures in polymeric micelles loaded with platinum drugs enhancing therapeutic efficiency against pancreatic tumor. ACS Nano 8, 6724–6738. https://doi.org/10.1021/nn500498t

Mottaghitalab, F., Farokhi, M., Shokrgozar, M.A., Atyabi, F., Hosseinkhani, H., 2015. Silk fibroin nanoparticle as a novel drug delivery system. J. Control. Release 206, 161–176. https://doi.org/10.1016/j.jconrel.2015.03.020

Nagarsekar, A., Crissman, J., Crissman, M., Ferrari, F., Cappello, J., Ghandehari, H., 2003. Genetic Engineering of Stimuli-Sensitive Silkelastin-like Protein Block Copolymers. Biomacromolecules 4, 602–607. https://doi.org/10.1021/bm0201082

Nicolas, J., Mura, S., Brambilla, D., Mackiewicz, N., Couvreur, P., 2013. Design, functionalization strategies and biomedical applications of targeted biodegradable/biocompatible polymer-based nanocarriers for drug delivery. Chem. Soc. Rev. 42, 1147–1235. https://doi.org/10.1039/C2CS35265F

Niu, Z., Conejos-Sánchez, I., Griffin, B.T., O'Driscoll, C.M., Alonso, M.J., 2016. Lipid-based nanocarriers for oral peptide delivery. Adv. Drug Deliv. Rev. 106, 337–354. https://doi.org/10.1016/j.addr.2016.04.001

Noad, R., Roy, P., 2003. Virus-like particles as immunogens. Trends Microbiol. 11, 438–444. https://doi.org/10.1016/S0966-842X(03)00208-7

Ohgidani, M., Furugaki, K., Shinkai, K., Kunisawa, Y., Itaka, K., Kataoka, K., Nakano, K., 2013. Block/homo polyplex micelle-based GM-CSF gene therapy via intraperitoneal administration elicits antitumor immunity against peritoneal dissemination and exhibits safety potentials in mice and cynomolgus monkeys. J. Control. Release 167, 238–247. https://doi.org/10.1016/j.jconrel.2013.02.006

Oliveira, H., Thevenot, J., Garanger, E., Ibarboure, E., Calvo, P., Aviles, P., Guillen, M.J., Lecommandoux, S., 2014. Nano-encapsulation of plitidepsin: In vivo pharmacokinetics, biodistribution, and efficacy in a renal xenograft tumor model. Pharm. Res. 31, 983–991. https://doi.org/10.1007/s11095-013-1220-3

Otsuka, H., Nagasaki, Y., Kataoka, K., 2012. PEGylated nanoparticles for biological and pharmaceutical applications. Adv. Drug Deliv. Rev. 64, 246–255. https://doi.org/10.1016/j.addr.2012.09.022

Pallini, V., 2009. The Structure of Silk Proteins. Ital. J. Zool. 39, 263–282. https://doi.org/10.1080/11250007209430061

Pasqualini, R., Koivunen, E., Kain, R., Lahdenranta, J., Sakamoto, M., Stryhn, A., Ashmun, R.A., Shapiro, L.H., Arap, W., Ruoslahti, E., 2000. Aminopeptidase N is a receptor for tumor-homing peptides and a target for inhibiting angiogenesis. Cancer Res. 60, 722–727.

Pastorino, L., Erokhina, S., Soumetz, F.C., Bianchini, P., Konovalov, O., Diaspro, A., Ruggiero, C., Erokhin, V., 2011. Collagen containing microcapsules: Smart containers for disease controlled therapy. J. Colloid Interface Sci. 357, 56–62. https://doi.org/10.1016/j.jcis.2011.02.010

Patel, A., Hu, Y., Tiwari, J.K., Velikov, K.P., 2010. Synthesis and characterisation of zein–curcumin colloidal particles. Soft Matter 6, 6192. https://doi.org/10.1039/c0sm00800a

Pérez-Medina, C., Binderup, T., Lobatto, M.E., Tang, J., Calcagno, C., Giesen, L., Wessel, C.H., Witjes, J., Ishino, S., Baxter, S., Zhao, Y., Ramachandran, S., Eldib, M., Sánchez-Gaytán, B.L., Robson, P.M., Bini, J., Granada, J.F., Fish, K.M., Stroes, E.S.G., Duivenvoorden, R., Tsimikas, S., Lewis, J.S., Reiner, T., Fuster, V., Kjær, A., Fishe, E.A., Fayad, Z.A., Mulder, W.J.M., 2016. In vivo PET imaging of high-density lipoprotein in multiple atherosclerosis models. JACC Cardiovasc Imaging 9, 950–961. https://doi.org/10.1016/j.jcmg.2016.01.020.In

Philipp Seib, F., 2017. Silk nanoparticles—an emerging anticancer nanomedicine. AIMS Bioeng. 4, 239–258. https://doi.org/10.3934/bioeng.2017.2.239

Pille, J., van Lith, S.A.M., van Hest, J.C.M., Leenders, W.P.J., 2017. Self-Assembling VHH-Elastin-Like Peptides for Photodynamic Nanomedicine. Biomacromolecules 18, 1302–1310. https://doi.org/10.1021/acs.biomac.7b00064

Pittella, F., Cabral, H., Maeda, Y., Mi, P., Watanabe, S., Takemoto, H., Kim, H.J., Nishiyama, N., Miyata, K., Kataoka, K., 2014. Systemic siRNA delivery to a spontaneous pancreatic tumor model in transgenic mice by PEGylated calcium phosphate hybrid micelles. J. Control. Release 178, 18–24. https://doi.org/10.1016/j.jconrel.2014.01.008

Pittella, F., Miyata, K., Maeda, Y., Suma, T., Watanabe, S., Chen, Q., Christie, R.J., Osada, K., Nishiyama, N., Kataoka, K., 2012. Pancreatic cancer therapy by systemic administration of VEGF siRNA contained in calcium phosphate/charge-conversional polymer hybrid nanoparticles. J. Control. Release 161, 868–874. https://doi.org/10.1016/j.jconrel.2012.05.005

Posadas, I., Monteagudo, S., Ceña, V., 2016. Nanoparticles for brain-specific drug and genetic material delivery, imaging and diagnosis. Nanomedicine 11, 833–849. https://doi.org/10.2217/nnm.16.15

Pourtau, L., Oliveira, H., Thevenot, J., Wan, Y., Brisson, A.R., Sandre, O., Miraux, S., Thiaudiere, E., Lecommandoux, S., 2013. Antibody-functionalized magnetic polymersomes: In vivo targeting and imaging of bone metastases using high resolution MRI. Adv. Healthc. Mater. 2, 1420–1424. https://doi.org/10.1002/adhm.201300061

Pritchard, E.M., Dennis, P.B., Omenetto, F., Naik, R.R., Kaplan, D.L., 2012. Physical and chemical aspects of stabilization of compounds in silk. Biopolymers 97, 479–498. https://doi.org/10.1002/bip.22026

Psimadas, D., Oliveira, H., Thevenot, J., Lecommandoux, S., Bouziotis, P., Varvarigou, A.D., Georgoulias, P., Loudos, G., 2014. Polymeric micelles and vesicles: Biological behavior evaluation using radiolabeling techniques. Pharm. Dev. Technol. 19, 189–193. https://doi.org/10.3109/10837450.2013.763264

Puthli, S., Vavia, P., 2008. Gamma irradiated micro system for long-term parenteral contraception: An alternative to synthetic polymers. Eur. J. Pharm. Sci. 35, 307–317. https://doi.org/10.1016/j.ejps.2008.07.009

Qiu, W., Teng, W., Cappello, J., Wu, X., 2009. Wet-Spinning of Recombinant Silk-Elastin-Like Protein Polymer Fibers with High Tensile Strength and High Deformability. Biomacromolecules 10, 602–608. https://doi.org/10.1021/bm801296r

Quader, S., Cabral, H., Mochida, Y., Ishii, T., Liu, X., Toh, K., Kinoh, H., Miura, Y., Nishiyama, N., Kataoka, K., 2014. Selective intracellular delivery of proteasome inhibitors through pH-sensitive polymeric micelles directed to efficient antitumor therapy. J. Control. Release 188, 67–77. https://doi.org/10.1016/j.jconrel.2014.05.048

Quadir, M.A., Morton, S.W., Deng, Z.J., Shopsowitz, K.E., Murphy, R.P., Epps, T.H., Hammond, P.T., 2014. PEG − Polypeptide Block Copolymers as pH-Responsive Endosome- Solubilizing Drug Nanocarriers. Mol. Pharm. 11, 2420–2430. https://doi.org/10.1021/mp500162w

Quadir, M.A., Morton, S.W., Mensah, L.B., Shopsowitz, K., Dobbelaar, J., Effenberger, N., Hammond, P.T., 2017. Ligand-decorated click polypeptide derived nanoparticles for targeted drug delivery applications. Nanomedicine Nanotechnology, Biol. Med. 13, 1797–1808. https://doi.org/10.1016/j.nano.2017.02.010

Rahman, M., Laurent, S., Tawil, N., Yahia, L., Mahmoudi, M., 2013. Protein-Nanoparticle Interactions, Protein-Nanoparticle Interactions, Springer Series in Biophysics. Springer Berlin Heidelberg, Berlin, Heidelberg. https://doi.org/10.1007/978-3-642-37555-2

Regier, M.C., Taylor, J.D., Borcyk, T., Yang, Y., Pannier, A.K., 2012. Fabrication and characterization of DNA-loaded zein nanospheres. J. Nanobiotechnology 10, 44. https://doi.org/10.1186/1477-3155-10-44

Ren, Q., Kwan, A.H., Sunde, M., 2013. Two forms and two faces, multiple states and multiple uses: Properties

and applications of the self-assembling fungal hydrophobins. Pept. Sci. 100, 601–612. https://doi.org/10.1002/bip.22259

Rodríguez-Hernández, J., Lecommandoux, S., 2005. Reversible Inside−Out Micellization of pH-responsive and Water-Soluble Vesicles Based on Polypeptide Diblock Copolymers. J. Am. Chem. Soc. 127, 2026–2027. https://doi.org/10.1021/ja043920g

Rodriguez-Nogales, A., Algieri, F., De Matteis, L., Lozano-Perez, A.A., Garrido-Mesa, J., Vezza, T., de la Fuente, J.M., Cenis, J.L., Gálvez, J., Rodriguez-Cabezas, M.E., 2016. Intestinal anti-inflammatory effects of RGD-functionalized silk fibroin nanoparticles in trinitrobenzenesulfonic acid-induced experimental colitis in rats. Int. J. Nanomedicine 11, 5945–5958. https://doi.org/10.2147/IJN.S116479

Sahoo, N., Sahoo, R.K., Biswas, N., Guha, A., Kuotsu, K., 2015. Recent advancement of gelatin nanoparticles in drug and vaccine delivery. Int. J. Biol. Macromol. 81, 317–331. https://doi.org/10.1016/j.ijbiomac.2015.08.006

Sanchez-Gaytan, B.L., Fay, F., Lobatto, M.E., Tang, J., Ouimet, M., Kim, Y., Van Der Staay, S.E.M., Van Rijs, S.M., Priem, B., Zhang, L., Fisher, E.A., Moore, K.J., Langer, R., Fayad, Z.A., Mulder, W.J.M., 2015. HDL-Mimetic PLGA Nanoparticle To Target Atherosclerosis Plaque Macrophages. Bioconjug. Chem. 26, 443–451. https://doi.org/10.1021/bc500517k

Sarangthem, V., Kim, Y., Singh, T.D., Seo, B.Y., Cheon, S.H., Lee, Y.J., Lee, B.H., Park, R.W., 2016. Multivalent targeting based delivery of therapeutic peptide using AP1-ELP carrier for effective cancer therapy. Theranostics 6, 2235–2249. https://doi.org/10.7150/thno.16425

Sarparanta, M.P., Bimbo, L.M., Mäkilä, E.M., Salonen, J.J., Laaksonen, P.H., Helariutta, K.A.M., Linder, M.B., Hirvonen, J.T., Laaksonen, T.J., Santos, H.A., Airaksinen, A.J., 2012. The mucoadhesive and gastroretentive properties of hydrophobin-coated porous silicon nanoparticle oral drug delivery systems. Biomaterials 33, 3353–3362. https://doi.org/10.1016/j.biomaterials.2012.01.029

Schaal, J.L., Li, X., Mastria, E., Bhattacharyya, J., Zalutsky, M.R., Chilkoti, A., Liu, W., 2016. Injectable polypeptide micelles that form radiation crosslinked hydrogels in situ for intratumoral radiotherapy. J. Control. Release 228, 58–66. https://doi.org/10.1016/j.jconrel.2016.02.040

Seib, F.P., Jones, G.T., Rnjak-Kovacina, J., Lin, Y., Kaplan, D.L., 2013. pH-Dependent Anticancer Drug Release from Silk Nanoparticles. Adv. Healthc. Mater. 2, 1606–1611. https://doi.org/10.1002/adhm.201300034

Seib, F.P., Kaplan, D.L., 2013. Silk for drug delivery applications: Opportunities and challenges. Isr. J. Chem. 53, 756–766. https://doi.org/10.1002/ijch.201300083

Shah, M., Edman, M.C., Janga, S.R., Shi, P., Dhandhukia, J., Liu, S., Louie, S.G., Rodgers, K., MacKay, J.A., Hamm-Alvarez, S.F., 2013. A rapamycin-binding protein polymer nanoparticle shows potent therapeutic activity in suppressing autoimmune dacryoadenitis in a mouse model of Sjögren's syndrome. J. Control. Release 171, 269–279. https://doi.org/10.1016/j.jconrel.2013.07.016

Shahzad, M.M.K., Mangala, L.S., Han, H.D., Lu, C., Bottsford-Miller, J., Nishimura, M., Mora, E.M., Lee, J.-W., Stone, R.L., Pecot, C. V., Thanapprapasr, D., Roh, J.-W., Gaur, P., Nair, M.P., Park, Y.-Y., Sabnis, N., Deavers, M.T., Lee, J.-S., Ellis, L.M., Lopez-Berestein, G., McConathy, W.J., Prokai, L., Lacko, A.G., Sood, A.K., 2011. Targeted Delivery of Small Interfering RNA Using Reconstituted High-Density Lipoprotein Nanoparticles. Neoplasia 13, 309-IN8. https://doi.org/10.1593/neo.101372

Shi, C., Yu, H., Sun, D., Ma, L., Tang, Z., Xiao, Q., Chen, X., 2015. Cisplatin-loaded polymeric nanoparticles: Characterization and potential exploitation for the treatment of non-small cell lung carcinoma. Acta Biomater. 18, 68–76. https://doi.org/10.1016/j.actbio.2015.02.009

Shi, P., Aluri, S., Lin, Y.A., Shah, M., Edman, M., Dhandhukia, J., Cui, H., MacKay, J.A., 2013. Elastin-based protein polymer nanoparticles carrying drug at both corona and core suppress tumor growth in vivo. J. Control. Release 171, 330–338. https://doi.org/10.1016/j.jconrel.2013.05.013

Shirasu, T., Koyama, H., Miura, Y., Hoshina, K., Kataoka, K., Watanabe, T., 2016. Nanoparticles effectively target rapamycin delivery to sites of experimental aortic aneurysm in rats. PLoS One 11, 1–21. https://doi.org/10.1371/journal.pone.0157813

Shirbaghaee, Z., Bolhassani, A., 2016. Different applications of virus-like particles in biology and medicine: Vaccination and delivery systems. Biopolymers 105, 113–132. https://doi.org/10.1002/bip.22759

Shutava, T.G., Balkundi, S.S., Vangala, P., Steffan, J.J., Bigelow, R.L., Cardelli, J.A., O'Neal, D.P., Lvov, Y.M., 2009. Layer-by-layer-coated gelatin nanoparticles as a vehicle for delivery of natural polyphenols. ACS Nano 3, 1877–1885. https://doi.org/10.1021/nn900451a

Simnick, A.J., Amiram, M., Liu, W., Hanna, G., Dewhirst, M.W., Kontos, C.D., Chilkoti, A., 2011. In vivo tumor targeting by a NGR-decorated micelle of a recombinant diblock copolypeptide, in: Journal of Controlled Release. pp. 144–151. https://doi.org/10.1016/j.jconrel.2011.06.044

Smith, M.A., Mohammad, R.A., 2014. Vedolizumab: An α4β7 Integrin Inhibitor for Inflammatory Bowel

Diseases. Ann. Pharmacother. 48, 1629–1635. https://doi.org/10.1177/1060028014549799
Smits, F.C.M., Buddingh, B.C., Van Eldijk, M.B., Van Hest, J.C.M., 2015. Elastin-like polypeptide based nanoparticles: Design rationale toward nanomedicine. Macromol. Biosci. 15, 36–51.
Song, B., Song, J., Zhang, S., Anderson, M.A., Ao, Y., Yang, C.Y., Deming, T.J., Sofroniew, M. V., 2012. Sustained local delivery of bioactive nerve growth factor in the central nervous system via tunable diblock copolypeptide hydrogel depots. Biomaterials 33, 9105–9116. https://doi.org/10.1016/j.biomaterials.2012.08.060
Song, W., Tang, Z., Zhang, D., Zhang, Y., Yu, H., Li, M., Lv, S., Sun, H., Deng, M., Chen, X., 2014. Anti-tumor efficacy of c(RGDfK)-decorated polypeptide-based micelles co-loaded with docetaxel and cisplatin. Biomaterials 35, 3005–3014. https://doi.org/10.1016/j.biomaterials.2013.12.018
Song, Z., Han, Z., Lv, S., Chen, C., Chen, L., Yin, L., Cheng, J., 2017. Synthetic polypeptides: From polymer design to supramolecular assembly and biomedical application. Chem. Soc. Rev. 46, 6570–6599. https://doi.org/10.1039/c7cs00460e
Spohn, G., Schori, C., Keller, I., Sladko, K., Sina, C., Guler, R., Schwarz, K., Johansen, P., Jennings, G.T., Bachmann, M.F., 2014. Preclinical efficacy and safety of an anti-IL-1β vaccine for the treatment of type 2 diabetes. Mol. Ther. - Methods Clin. Dev. 1, 14048. https://doi.org/10.1038/mtm.2014.48
Sudheesh, M.S., Vyas, S.P., Kohli, D. V., 2011. Nanoparticle-based immunopotentiation via tetanus toxoid-loaded gelatin and aminated gelatin nanoparticles. Drug Deliv. 18, 320–330. https://doi.org/10.3109/10717544.2010.549525
Sueyoshi, D., Anraku, Y., Komatsu, T., Urano, Y., Kataoka, K., 2017. Enzyme-Loaded Polyion Complex Vesicles as in Vivo Nanoreactors Working Sustainably under the Blood Circulation: Characterization and Functional Evaluation. Biomacromolecules 18, 1189–1196. https://doi.org/10.1021/acs.biomac.6b01870
Suma, T., Miyata, K., Anraku, Y., Watanabe, S., Christie, R.J., Takemoto, H., Shioyama, M., Gouda, N., Ishii, T., Nishiyama, N., Kataoka, K., 2012a. Smart multilayered assembly for biocompatible siRNA delivery featuring dissolvable silica, endosome-disrupting polycation, and detachable PEG. ACS Nano 6, 6693–6705. https://doi.org/10.1021/nn301164a
Suma, T., Miyata, K., Ishii, T., Uchida, S., Uchida, H., Itaka, K., Nishiyama, N., Kataoka, K., 2012b. Enhanced stability and gene silencing ability of siRNA-loaded polyion complexes formulated from polyaspartamide derivatives with a repetitive array of amino groups in the side chain. Biomaterials 33, 2770–2779. https://doi.org/10.1016/j.biomaterials.2011.12.022
Takeda, K.M., Yamasaki, Y., Dirisala, A., Ikeda, S., Tockary, T.A., Toh, K., Osada, K., Kataoka, K., 2017. Effect of shear stress on structure and function of polyplex micelles from poly(ethylene glycol)-poly(l -lysine) block copolymers as systemic gene delivery carrier. Biomaterials 126, 31–38. https://doi.org/10.1016/j.biomaterials.2017.02.012
Tarhini, M., Greige-Gerges, H., Elaissari, A., 2017. Protein-based nanoparticles: From preparation to encapsulation of active molecules. Int. J. Pharm. 522, 172–197. https://doi.org/10.1016/j.ijpharm.2017.01.067
Thambi, T., Park, J.H., Lee, D.S., 2016. Stimuli-responsive polymersomes for cancer therapy. Biomater. Sci. 4, 55–69. https://doi.org/10.1039/C5BM00268K
Thirupathi Kumara Raja, S., Prakash, T., Gnanamani, A., 2017. Redox responsive albumin autogenic nanoparticles for the delivery of cancer drugs. Colloids Surfaces B Biointerfaces 152, 393–405. https://doi.org/10.1016/j.colsurfb.2017.01.044
Tian, H., Guo, Z., Lin, L., Jiao, Z., Chen, J., Gao, S., Zhu, X., Chen, X., 2014. PH-responsive zwitterionic copolypeptides as charge conversional shielding system for gene carriers. J. Control. Release 174, 117–125. https://doi.org/10.1016/j.jconrel.2013.11.008
Tian, H., Lin, L., Jiao, Z., Guo, Z., Chen, J., Gao, S., Zhu, X., Chen, X., 2013. Polylysine-modified polyethylenimine inducing tumor apoptosis as an efficient gene carrier. J. Control. Release 172, 410–418. https://doi.org/10.1016/j.jconrel.2013.06.026
Tokareva, O., Michalczechen-Lacerda, V.A., Rech, E.L., Kaplan, D.L., 2013. Recombinant DNA production of spider silk proteins. Microb. Biotechnol. 6, 651–63. https://doi.org/10.1111/1751-7915.12081
Totten, J.D., Wongpinyochit, T., Seib, F.P., 2017. Silk nanoparticles: proof of lysosomotropic anticancer drug delivery at single-cell resolution. J. Drug Target. 25, 865–872. https://doi.org/10.1080/1061186X.2017.1363212
Tseng, C.-L., Chen, K.-H., Su, W.-Y., Lee, Y.-H., Wu, C.-C., Lin, F.-H., 2013. Cationic gelatin nanoparticles for drug delivery to the ocular surface: in vitro and in vivo evaluation. J. Nanomater. 2013, 1–11. https://doi.org/10.1155/2013/238351
Tseng, C.L., Wu, S.Y.H., Wang, W.H., Peng, C.L., Lin, F.H., Lin, C.C., Young, T.H., Shieh, M.J., 2008. Targeting

efficiency and biodistribution of biotinylated-EGF-conjugated gelatin nanoparticles administered via aerosol delivery in nude mice with lung cancer. Biomaterials 29, 3014–3022. https://doi.org/10.1016/j.biomaterials.2008.03.033

Turabee, M.H., Thambi, T., Lym, J.S., Lee, D.S., 2017. Bioresorbable polypeptide-based comb-polymers efficiently improves the stability and pharmacokinetics of proteins in vivo. Biomater. Sci. 5, 837–848. https://doi.org/10.1039/C7BM00128B

Uesugi, Y., Kawata, H., Jo, J.I., Saito, Y., Tabata, Y., 2010. An ultrasound-responsive nano delivery system of tissue-type plasminogen activator for thrombolytic therapy. J. Control. Release 147, 269–277. https://doi.org/10.1016/j.jconrel.2010.07.127

Uesugi, Y., Kawata, H., Saito, Y., Tabata, Y., 2012. Ultrasound-responsive thrombus treatment with zinc-stabilized gelatin nano-complexes of tissue-type plasminogen activator. J. Drug Target. 20, 224–234. https://doi.org/10.3109/1061186X.2011.633259

Uno, Y., Piao, W., Miyata, K., Nishina, K., Mizusawa, H., Yokota, T., 2011. High-Density Lipoprotein Facilitates *In Vivo* Delivery of α-Tocopherol–Conjugated Short-Interfering RNA to the Brain. Hum. Gene Ther. 22, 711–719. https://doi.org/10.1089/hum.2010.083

Upadhyay, K.K., Bhatt, A.N., Mishra, A.K., Dwarakanath, B.S., Jain, S., Schatz, C., Le Meins, J.F., Farooque, A., Chandraiah, G., Jain, A.K., Misra, A., Lecommandoux, S., 2010. The intracellular drug delivery and anti tumor activity of doxorubicin loaded poly(γ-benzyl l-glutamate)-b-hyaluronan polymersomes. Biomaterials 31, 2882–2892. https://doi.org/10.1016/j.biomaterials.2009.12.043

Upadhyay, K.K., Mishra, A.K., Chuttani, K., Kaul, A., Schatz, C., Le Meins, J.F., Misra, A., Lecommandoux, S., 2012. The in vivo behavior and antitumor activity of doxorubicin-loaded poly(γ-benzyl l-glutamate)-block-hyaluronan polymersomes in Ehrlich ascites tumor-bearing BalB/c mice. Nanomedicine Nanotechnology, Biol. Med. 8, 71–80. https://doi.org/10.1016/j.nano.2011.05.008

Urry, D.W., Luan, C.H., Parker, T.M., Gowda, D.C., Prasad, K.U., Reid, M.C., Safavy, A., 1991. Temperature of Polypeptide Inverse Temperature Transition Depends on Mean Residue Hydrophobicity. J. Am. Chem. Soc. 113, 4346–4348. https://doi.org/10.1021/ja00011a057

Van Eldijk, M.B., Smits, F.C.M., Vermue, N., Debets, M.F., Schoffelen, S., Van Hest, J.C.M., 2014. Synthesis and self-assembly of well-defined elastin-like polypeptide-poly(ethylene glycol) conjugates. Biomacromolecules 15, 2751–2759. https://doi.org/10.1021/bm5006195

van Hest, J.C.M., Tirrell, D.A., 2001. Protein-based materials, toward a new level of structural control. Chem. Commun. 19, 1897–1904. https://doi.org/10.1039/b105185g

Verma, D., Gulati, N., Kaul, S., Mukherjee, S., Nagaich, U., 2018. Protein Based Nanostructures for Drug Delivery. J. Pharm. 2018, 1–18. https://doi.org/10.1155/2018/9285854

Wang, L., Qin, G., Geng, S., Dai, Y., Wang, J.Y., 2013. Preparation of zein conjugated quantum dots and their in vivo transdermal delivery capacity through nude mouse skin. J. Biomed. Nanotechnol. 9, 367–376. https://doi.org/10.1166/jbn.2013.1557

Wang, M., Miura, Y., Tsuchihashi, K., Miyano, K., Nagano, O., Yoshikawa, M., Tanabe, A., Makino, J., Mochida, Y., Nishiyama, N., Saya, H., Cabral, H., Kataoka, K., 2016. Eradication of CD44-variant positive population in head and neck tumors through controlled intracellular navigation of cisplatin-loaded nanomedicines. J. Control. Release 230, 26–33. https://doi.org/10.1016/j.jconrel.2016.03.038

Wolfrum, C., Shi, S., Jayaprakash, K.N., Jayaraman, M., Wang, G., Pandey, R.K., Rajeev, K.G., Nakayama, T., Charrise, K., Ndungo, E.M., Zimmermann, T., Koteliansky, V., Manoharan, M., Stoffel, M., 2007. Mechanisms and optimization of in vivo delivery of lipophilic siRNAs. Nat. Biotechnol. 25, 1149–1157. https://doi.org/10.1038/nbt1339

Wong, L.R., Ho, P.C., 2018. Role of serum albumin as a nanoparticulate carrier for nose-to-brain delivery of R-flurbiprofen: implications for the treatment of Alzheimer's disease. J. Pharm. Pharmacol. 70, 59–69. https://doi.org/10.1111/jphp.12836

Wongpinyochit, T., Uhlmann, P., Urquhart, A.J., Seib, F.P., 2015. PEGylated Silk Nanoparticles for Anticancer Drug Delivery. Biomacromolecules 16, 3712–3722. https://doi.org/10.1021/acs.biomac.5b01003

Wu, L., Fang, S., Shi, S., Deng, J., Liu, B., Cai, L., 2013. Hybrid Polypeptide Micelles Loading Indocyanine Green for Tumor Imaging and Photothermal Effect Study. Biomacromolecules 14, 3027–3033. https://doi.org/10.1021/bm400839b

Wu, P., Liu, Q., Li, R., Wang, J., Zhen, X., Yue, G., Wang, H., Cui, F., Wu, F., Yang, M., Qian, X., Yu, L., Jiang, X., Liu, B., 2013. Facile preparation of paclitaxel loaded silk fibroin nanoparticles for enhanced antitumor efficacy by locoregional drug delivery. ACS Appl. Mater. Interfaces 5, 12638–12645. https://doi.org/10.1021/am403992b

Xia, X.X., Wang, M., Lin, Y., Xu, Q., Kaplan, D.L., 2014. Hydrophobic drug-triggered self-assembly of

nanoparticles from silk-elastin-like protein polymers for drug delivery. Biomacromolecules 15, 908–914.
Xie, J., Chiang, L., Contreras, J., Wu, K., Garner, J.A., Medina-Kauwe, L., Hamm-Alvarez, S.F., 2006. Novel Fiber-Dependent Entry Mechanism for Adenovirus Serotype 5 in Lacrimal Acini. J. Virol. 80, 11833–11851. https://doi.org/10.1128/JVI.00857-06
Xu, H.-T., Fan, B.-L., Yu, S.-Y., Huang, Y.-H., Zhao, Z.-H., Lian, Z.-X., Dai, Y.-P., Wang, L.-L., Liu, Z.-L., Fei, J., Li, N., 2007. Construct Synthetic Gene Encoding Artificial Spider Dragline Silk Protein and its Expression in Milk of Transgenic Mice. Anim. Biotechnol. 18, 1–12. https://doi.org/10.1080/10495390601091024
Xu, H., Yang, D., Cai, C., Gou, J., Zhang, Y., Wang, L., Zhong, H., Tang, X., 2015. Dual-responsive mPEG-PLGA-PGlu hybrid-core nanoparticles with a high drug loading to reverse the multidrug resistance of breast cancer: An in vitro and in vivo evaluation. Acta Biomater. 16, 156–168. https://doi.org/10.1016/j.actbio.2015.01.039
Yang, S., Damiano, M.G., Zhang, H., Tripathy, S., Luthi, A.J., Rink, J.S., Ugolkov, A. V., T. K. Singh, A., Dave, S.S., Gordon, L.I., Thaxton, C.S., 2013. Biomimetic, synthetic HDL nanostructures for lymphoma. Proc. Natl. Acad. Sci. 110, 2511–2516. https://doi.org/10.1073/pnas.1213657110
Yingchoncharoen, P., Kalinowski, D.S., Richardson, D.R., 2016. Lipid-Based Drug Delivery Systems in Cancer Therapy: What Is Available and What Is Yet to Come. Pharmacol. Rev. 68, 701–787. https://doi.org/10.1124/pr.115.012070
Yokoyama, M., Inoue, S., Kataoka, K., Yui, N., Okano, T., Sakurai, Y., 1989. Molecular design for missile drug: Synthesis of adriamycin conjugated with immunoglobulin G using poly(ethylene glycol)-block-poly(aspartic acid) as intermediate carrier. Die Makromol. Chemie 190, 2041–2054. https://doi.org/10.1002/macp.1989.021900904
Yokoyama, M., Miyauchi, M., Yamada, N., Okano, T., Sakurai, Y., Kataoka, K., 1990. Characterization and Anticancer Activity of the Micelle-forming Polymeric Anticancer Drug Adriamycin-conjugated Poly (ethylene glycol) -Poly (aspartic acid) Block Copolymer Characterization. Cancer Res. 15, 1693–1700. https://doi.org/10.1016/j.ijpharm.2008.08.011
Yoo, J., Sanoj Rejinold, N., Lee, D.Y., Jon, S., Kim, Y.C., 2017. Protease-activatable cell-penetrating peptide possessing ROS-triggered phase transition for enhanced cancer therapy. J. Control. Release 264, 89–101. https://doi.org/10.1016/j.jconrel.2017.08.026
Yu, H., Tang, Z., Li, M., Song, W., Zhang, D., Zhang, Y., Yang, Y., Sun, H., Deng, M., Chen, X., 2016. Cisplatin loaded poly(L-glutamic acid)-g-methoxy poly(ethylene glycol) complex nanoparticles for potential cancer therapy: Preparation, in vitro and in vivo evaluation. J. Biomed. Nanotechnol. 12, 69–78. https://doi.org/10.1166/jbn.2016.2152
Yu, H., Tang, Z., Zhang, D., Song, W., Zhang, Y., Yang, Y., Ahmad, Z., Chen, X., 2015. Pharmacokinetics, biodistribution and in vivo efficacy of cisplatin loaded poly(l-glutamic acid)-g-methoxy poly(ethylene glycol) complex nanoparticles for tumor therapy. J. Control. Release 205, 89–97. https://doi.org/10.1016/j.jconrel.2014.12.022
Yu, S., Zhang, D., He, C., Sun, W., Cao, R., Cui, S., Deng, M., Gu, Z., Chen, X., 2017. Injectable Thermosensitive Polypeptide-Based CDDP-Complexed Hydrogel for Improving Localized Antitumor Efficacy. Biomacromolecules 18, 4341–4348. https://doi.org/10.1021/acs.biomac.7b01374
Yu, Z., Yu, M., Zhang, Z., Hong, G., Xiong, Q., 2014. Bovine serum albumin nanoparticles as controlled release carrier for local drug delivery to the inner ear. Nanoscale Res. Lett. 9, 1–7. https://doi.org/10.1186/1556-276X-9-343
Zhang, B., Luo, Y., Wang, Q., 2010. Development of silver-zein composites as a promising antimicrobial agent. Biomacromolecules 11, 2366–2375. https://doi.org/10.1021/bm100488x
Zhang, S., Anderson, M.A., Ao, Y., Khakh, B.S., Fan, J., Deming, T.J., Sofroniew, M. V., 2014. Tunable diblock copolypeptide hydrogel depots for local delivery of hydrophobic molecules in healthy and injured central nervous system. Biomaterials 35, 1989–2000. https://doi.org/10.1016/j.biomaterials.2013.11.005
Zhang, W., He, H., Liu, J., Wang, J., Zhang, S., Zhang, S., Wu, Z., 2013. Pharmacokinetics and atherosclerotic lesions targeting effects of tanshinone IIA discoidal and spherical biomimetic high density lipoproteins. Biomaterials 34, 306–319. https://doi.org/10.1016/j.biomaterials.2012.09.058
Zhang, Y., Cui, L., Li, F., Shi, N., Li, C., Yu, X., Chen, Y., Kong, W., 2016. Design, fabrication and biomedical applications of zein-based nano/micro-carrier systems. Int. J. Pharm. 513, 191–210. https://doi.org/10.1016/j.ijpharm.2016.09.023
Zhang, Y., Xiao, C., Ding, J., Li, M., Chen, X., Tang, Z., Zhuang, X., Chen, X., 2016. A comparative study of linear, Y-shaped and linear-dendritic methoxy poly(ethylene glycol)-block-polyamidoamine-block-poly(L-glutamic acid) block copolymers for doxorubicin delivery in vitro and in vivo. Acta Biomater. 40, 243–253. https://doi.org/10.1016/j.actbio.2016.04.007

Zhang, Y., Yang, Z., Tan, X., Tang, X., Yang, Z., 2017. Development of a More Efficient Albumin-Based Delivery System for Gambogic Acid with Low Toxicity for Lung Cancer Therapy. AAPS PharmSciTech 18, 1987–1997. https://doi.org/10.1208/s12249-016-0670-4

Zhao, D., Zhao, X., Zu, Y., Li, J., Zhang, Y., Jiang, R., Zhang, Z., 2010. Preparation, characterization, and in vitro targeted delivery of folate-decorated paclitaxel-loaded bovine serum albumin nanoparticles. Int. J. Nanomedicine 5, 669–677. https://doi.org/10.2147/IJN.S12918

Zhao, L., Li, N., Wang, K., Shi, C., Zhang, L., Luan, Y., 2014. A review of polypeptide-based polymersomes. Biomaterials 35, 1284–1301. https://doi.org/10.1016/j.biomaterials.2013.10.063

Zhao, L., Xu, H., Li, Y., Song, D., Wang, X., Qiao, M., Gong, M., 2016. Novel application of hydrophobin in medical science: A drug carrier for improving serum stability. Sci. Rep. 6, 1–9. https://doi.org/10.1038/srep26461

Zhao, P., Atanackovic, D., Dong, S., Yagita, H., He, X., Chen, M., 2017. An Anti-Programmed Death-1 Antibody (αPD-1) Fusion Protein That Self-Assembles into a Multivalent and Functional αPD-1 Nanoparticle. Mol. Pharm. 14, 1494–1500. https://doi.org/10.1021/acs.molpharmaceut.6b01021

Zhao, P., Dong, S., Bhattacharyya, J., Chen, M., 2014. ITEP nanoparticle-delivered salinomycin displays an enhanced toxicity to cancer stem cells in orthotopic breast tumors. Mol. Pharm. 11, 2703–2712. https://doi.org/10.1021/mp5002312

Zhao, P., Xia, G., Dong, S., Jiang, Z.X., Chen, M., 2016. An iTEP-salinomycin nanoparticle that specifically and effectively inhibits metastases of 4T1 orthotopic breast tumors. Biomaterials 93, 1–9. https://doi.org/10.1016/j.biomaterials.2016.03.032

Zhao, Z., Li, Y., Xie, M.-B., 2015. Silk Fibroin-Based Nanoparticles for Drug Delivery. Int. J. Mol. Sci. 16, 4880–4903. https://doi.org/10.3390/ijms16034880

Zheng, C., Zheng, M., Gong, P., Deng, J., Yi, H., Zhang, P., Zhang, Y., Liu, P., Ma, Y., Cai, L., 2013. Polypeptide cationic micelles mediated co-delivery of docetaxel and siRNA for synergistic tumor therapy. Biomaterials 34, 3431–3438. https://doi.org/10.1016/j.biomaterials.2013.01.053

Zhu, B., Wang, H., Leow, W.R., Cai, Y., Loh, X.J., Han, M.-Y., Chen, X., 2016. Silk Fibroin for Flexible Electronic Devices. Adv. Mater. 28, 4250–4265. https://doi.org/10.1002/adma.201504276

Zhu, H., Dong, C., Dong, H., Ren, T., Wen, X., Su, J., Li, Y., 2014. Cleavable PEGylation and hydrophobic histidylation of polylysine for siRNA delivery and tumor gene therapy. ACS Appl. Mater. Interfaces 6, 10393–10407. https://doi.org/10.1021/am501928p

Zochowska, M., Piguet, A.C., Jemielity, J., Kowalska, J., Szolajska, E., Dufour, J.F., Chroboczek, J., 2015. Virus-like particle-mediated intracellular delivery of mRNA cap analog with in vivo activity against hepatocellular carcinoma. Nanomedicine Nanotechnology, Biol. Med. 11, 67–76. https://doi.org/10.1016/j.nano.2014.07.009

Zou, T., Gu, L., 2013. TPGS emulsified zein nanoparticles enhanced oral bioavailability of daidzin: In vitro characteristics and in vivo performance. Mol. Pharm. 10, 2062–2070. https://doi.org/10.1021/mp400086n